THE EFFECTS OF CRACKS ON THE SEISMIC ANALYSIS OF
REINFORCED CONCRETE NUCLEAR CONTAINMENT VESSELS

by

Jay K. Smith
Research Assistant

Peter Gergely and Richard N. White
Project Co-Directors

April 1977   Report No. 368

An Interim Report to the National Science Foundation

Department of Structural Engineering

Cornell University

Ithaca, New York

BIBLIOGRAPHIC DATA SHEET	1. Report No. NSF/RA-770118	2.	3. Recipient's Accession No.
4. Title and Subtitle Effects of Cracks on the Seismic Analysis of Reinforced Concrete Nuclear Containment Vessels (Interim Report)			5. Report Date April 1977
			6.
7. Author(s) J. K. Smith			8. Performing Organization Rept. No. 368
9. Performing Organization Name and Address Cornell University Department of Structural Engineering Ithaca, NY 14850			10. Project/Task/Work Unit No.
			11. Contract/Grant No. ATA7303178
12. Sponsoring Organization Name and Address Research Applied to National Needs (RANN) National Science Foundation Washington, D.C. 20550			13. Type of Report & Period Covered Interim
			14.

15. Supplementary Notes

16. Abstracts

This investigation studies the feasibility of the proposal for eliminating or reducing inclined steel in concrete containment vessels. The plausibility of this alternative design which utilizes the combination of dowel action of the longitudinal reinforcement and the shear transfer capacity of the horizontal cracks is studied. The results of tests performed to investigate the shear transfer characteristics of cracks are shown and discussed. The test results are used as input to a finite element model which is used to study the shear stress distribution of cracks. A computer program is developed which incorporates these experimental and analytical results into the seismic analysis of a cracked reinforced concrete containment vessel. A linear seismic analysis which yields results giving a least squares fit to the non-linear results for the synthetic earthquake is also developed.

17. Key Words and Document Analysis.   17a. Descriptors
Reinforced concrete
Radiation hazards
Nuclear reactors
Nuclear energy
Nuclear reactor accidents
Nuclear reactor containment
Containment
Earthquakes
Earthquake resistant construction
Cracks
Cracking (fracturing)

17b. Identifiers/Open-Ended Terms

Nuclear containment vessels
Seismic analysis

17c. COSATI Field/Group

18. Availability Statement NTIS	19. Security Class (This Report) UNCLASSIFIED	21. No. of Pages 175
	20. Security Class (This Page) UNCLASSIFIED	22. Price A08-A01

FORM NTIS-35 (REV. 10-73)   ENDORSED BY ANSI AND UNESCO.   THIS FORM MAY BE REPRODUCED   USCOMM-DC 8265-P74

i.

CAPITAL SYSTEMS GROUP, INC.
6110 EXECUTIVE BOULEVARD
SUITE 250
ROCKVILLE, MARYLAND 20852

ABSTRACT OF REPORT

Reinforced concrete nuclear containment vessels would be cracked in both the horizontal and vertical directions by an internal pressurization caused by a loss of coolant accident in the reactor and steam supply system of a nuclear power plant. If an earthquake occurs simultaneously with the loss of coolant accident some means must be found to transfer the shear forces developed by the earthquake across the cracks. Current design codes imply that inclined reinforcement needs to be used in highly seismic areas to transfer these forces across the cracks. The inclined steel is expensive to form and decreases the quality of the concrete because of the congestion of steel reinforcing bars. The plausibility of an alternative design which utilizes the combination of dowel action of the longitudinal reinforcement and the shear transfer capacity of the horizontal cracks is studied in this report. The effects of the vertical cracks are not considered.

The results of tests performed to investigate the shear transfer characteristics of cracks are shown and discussed. These test results are used as input to a finite element model which was used to study the shear stress distribution at cracks.

A computer program was developed which incorporated these experimental and analytical results into the seismic analysis of a cracked reinforced concrete containment vessel. Since the shear transfer mechanism of the cracks was found to be nonlinear this program is a nonlinear seismic analysis program. Soil-structure interaction is included in the analysis. A synthetic earthquake generated from response spectra given in NRC 1.60 was used as the base acceleration in all the computer runs. The effects of not including the horizontal cracks and changing the stiffness of the

underlying soil are studied.

A linear seismic analysis which yields results giving a least squares fit to the nonlinear results for the synthetic earthquake was also developed.

It is felt that the shear transfer capabilities of the combination of cracked concrete and reinforcement orthogonal to the cracks can adequately resist the shear forces developed by design earthquakes normally used in containment vessel design. Hence, it should be possible to eliminate or greatly reduce the inclined reinforcing steel currently used in most containments to carry seismic shear forces. A final recommendation on this important design question can be made after suitable experiments are conducted on reinforced concrete specimens subjected to combined biaxial tension and cyclic shear.

ib

ACKNOWLEDGEMENT

TABLE OF CONTENTS

ie

Chapter 1

INTRODUCTION

1.1   Nuclear Containment Vessels

The heart of a nuclear power station is the nuclear reactor and its
steam supply system.   Of equal importance, for reasons of safety, is the
containment vessel which houses the reactor along with its steam supply
system components (see Figure 1.1).   The purposes of the containment are
to prevent leakage of radioactive substances to the outside environment
and to support the structures and equipment connected to it.   The vessel
shown in Figure 1.1 is typical of the large reinforced concrete contain-
ment vessels now used in pressurized water reactors.   It consists of a
large cylindrical shell (4 1/2 feet thick) with a hemispherical head,
resting on a circular foundation.   The containment vessel volume must be
able to dissipate the energy released during a loss of coolant accident
in the reactor.   This accident creates an internal pressure which stresses
the containment vessel.   The containment vessel shell must be able to
transmit these and all other forces down to the foundation mat.   In
concrete containment vessels a 1/4 to 3/8 inch steel liner is attached
to the inner surface of the shell to prevent leakage.   This liner per-
forms no load carrying function but must be able to undergo the strains
which are imposed on it by the concrete shell wall.

Since the containment vessel is of great importance to nuclear safety, it must be able to maintain its structural integrity during an earthquake. This means that a material failure which could cause radioactive leakage should not occur in the steel liner. One of the design conditions for the containment combines the internal pressure from a loss of coolant accident acting simultaneously with the dead weight of the containment vessel and the Safe Shutdown Earthquake (SSE). The Safe Shutdown Earthquake, as defined by the Nuclear Regulatory Commission (NRC), is considered to be the "earthquake which produces the vibratory ground motion for which structures, systems and components important to safety are designed to remain functional." The horizontal design response spectra, given in the NRC Regulatory Figure Guide 1.60 as "the spectra representing the effects of the vibratory motion of the SSE," is shown in Figure 1.3.

Because concrete has little tensile strength, the internal pressurization will cause cracks in the containment in both the horizontal and vertical (principal) directions (see Figure 1.2). Both prestressed steel tendons and normal reinforcing steel are being used in concrete containment vessels. There is little or no cracking in prestressed vessels. However, the construction of these prestressed vessels is expensive because of the difficulty of prestressing in the circumferential direction. Only reinforced concrete containments will be discussed in this investigation. Presently most reinforced concrete vessel walls have steel not only in the two principal directions but also in directions inclined ± 45° from these principal directions. This inclined steel is designed to transfer the SSE inertial shearing forces across the cracks in the vessel wall. In a cylindrical wall, inclined bars will form a

series of helixes. These continuously curved bars are very expensive
to form and cause congestion problems during construction. If a design
could be developed which eliminates these inclined bars, lower construc-
tion costs and improved concrete quality (because of reduced congestion
of reinforcing bars) would result. If the orthogonal steel in the prin-
cipal directions were assumed to carry shear across the cracks by dowel
action and if the cracks themselves have shear transfer capability then
a design could be formulated that does not rely on inclined steel. The
earthquake shearing forces would then be carried to the foundation by
a combination of dowel action of the vertical reinforcing bars and by
the shear transfer capacity of the horizontal cracks.

1.2 Scope of this Investigation

The central purpose of this investigation is to study the feasi-
bility of the above proposal for eliminating or reducing inclined steel
in concrete containment vessels. Chapter 2 deals with the phenomenon
of shear transfer across cracks in concrete. The results of tests
which give the load-displacement behavior of the shear transfer mechanism
of cracked concrete blocks (with internal reinforcing bars to include
dowel action) are shown and discussed. The distribution of shear
stresses at horizontal cracks is studied through use of a finite element
model. The maximum shear stress is an important design parameter because
a high shear stress could cause a diagonal tension failure or dowel
splitting in the containment vessel wall.

In Chapter 3 a lumped mass model of the containment vessel shown in

Figure 1.1 is developed for linear seismic analysis. The effects of including rotational degrees of freedom in the analysis are discussed. A computer program which performs linear seismic analysis (modal analysis) is developed. Soil-Structure Interaction is added to the model in Chapter 4. In Chapter 5, the cracks caused by internal pressurization are included in the seismic analysis of the containment vessel. Since the load-displacement behavior of these cracks is nonlinear (as shown in Chapter 2) the seismic analysis becomes nonlinear. The modeling of the crack stiffness is discussed along with the analytical tools which are required to perform the nonlinear analysis. The computer program developed to perform nonlinear analysis is then used with the lumped mass model of the containment vessel shown in Figure 1.1 for a time history of ground accelerations corresponding to the NRC response spectrum of Figure 1.3. Soil-Structure Interaction is included in this model. Three different runs which correspond to three different stiffnesses of the underlying soil are made. The modal analysis program of Chapter 3 is input with the same ground accelerations and the results of the linear and nonlinear analyses are compared. System identification is used to obtain a linear model which produces results which "best fit" the results of the nonlinear analysis. Chapter 6 states the main conclusions of this investigation and proposes future work which relates to this topic.

1.3 Design Philosophy

The design of reinforced concrete containment vessels is governed

by Section III Division 2 of the ASME Boiler and Pressure Vessel Code [14].
The load combination of interest is the extreme environmental load. This
load combination is

$$1.0 \ D + 1.0 \ L + 1.0 \ T_o + 1.0 \ E_{ss} + 1.0 \ P_v \qquad\qquad (1.1)$$

where D, L, T_o, E_{ss} and P_v are the dead, live, temperature, SSE and
external pressure loads, respectively. For the containment the only
live load is the internal pressure due to the loss of coolant accident
(LOCA). P_v and T_o are not included here because they are unknown.

The allowable membrane compression stress in the concrete is .60 f'_c
where f'_c is the compressive strength of the concrete (normally $f'_c \cong$ 4 Ksi
for containment vessels). Concrete tensile strength is neglected. The
allowable tangential shear stress is dependent upon ρ, the reinforcement
ratio:

$$v_c = 12,000 \ \rho \qquad\qquad \rho \leq .01 \qquad\qquad (1.2a)$$

$$v_c = 93 + 2,700 \ \rho \qquad\qquad .01 \leq \rho \leq .025. \qquad\qquad (1.2b)$$

v_c is the maximum tangential shear stress (in psi) which may be carried
by the concrete. v_c may not exceed 160 psi. ρ is taken as the lesser of
the reinforcement ratios in the meridional and circumferential directions.

The design yield strength of the steel reinforcement cannot exceed
60,000 psi. The average tension and compression stresses must not
exceed .9 f_y, where f_y is the tensile yield strength of the reinforcing
bars.

According the ASME Section III [14], if v_u (the nominal design shear stress) is greater than v_c, then the following reinforcement shall be provided:

(1) The meridional and circumferential reinforcement shall be designed to resist 1.5 times the shear force corresponding to v_c in addition to the membrane forces which result from the LOCA.

(2) The excess shear force corresponding to $(v_u - v_c)$ shall be resisted by inclined reinforcement.

The steel liner is designed on the basis of allowable tensile and compressive strains. The ASME code states that for extreme environmental loads $\varepsilon_{sc} = .002$ and $\varepsilon_{st} = .001$ where ε_{sc} is the allowable liner compressive strain and ε_{st} is the allowable liner tensile strain. The anchors which attach the liner to the concrete containment are spaced at about 20 inches. The allowable relative displacement between the anchors that is commonly used in design is .1 inch.

Chapter 2

SHEAR TRANSFER IN NUCLEAR CONTAINMENT VESSELS

2.1 Cracks in Nuclear Containment Vessels

Current design criteria specify that the nuclear containment vessel must be able to withstand the simultaneous occurrence of a design basis accident which would give rise to internal pressurization and a strong motion (SSE) earthquake. The internal pressure creates tension forces in both the longitudinal and circumferential directions while the earthquake causes inertial forces which in turn cause shearing forces and bending moments in the vessel. These forces and moments must be transferred across the horizontal and vertical cracks in the reinforced concrete caused by pressurization. Clearly the crack patterns, crack widths and spacings are important. Crack widths (caused by internal pressurization) vary from .01 to .015 inches. Horizontal cracks with regular spacings throughout the vessel will be assumed. The possible effects of vertical cracks will be discussed later in this chapter and in Chapter 5. It has been found from tests at Cornell University [1,2] and elsewhere that a mechanism exists which makes it possible to transfer shear force across cracks in concrete. This mechanism is called interface shear transfer (IST) or aggregate interlock. The effect of the shearing stiffness of these cracks on the shear stress distribution in

the vessel is studied in this chapter. The maximum shear stresses may then be found once the shear forces acting at each section are known.

2.2 Interface Shear Transfer

Several types of tests have been conducted at Cornell to determine the behavior of IST in concrete [1]. Some of these tests were used solely to investigate IST, with no reinforcing bars crossing the crack plane. Other test specimens had internally embedded reinforcing bars and had a greased plate inserted at the crack plane so that the only shear stiffness was produced by dowel action. Still other specimens had internal bars crossing the crack plane and thus included the effects of both dowel action and IST. The early tests which included both IST and dowel action were done on the testing setup shown in Figure 2.1. This "beam-type" specimen was loaded by two beams, one above and one below the concrete specimen. When the positive (+) rollers were used the shear diagram is as shown. The shear loading direction could be reversed by use of the negative (-) rollers. All beam specimens had a single #14 bar located in the middle of the 15 in. x 15 in. specimen. This longitudinal bar was stressed until a crack occurred in the specimen at mid-length of the specimen. Unfortunately, there were variations in the width of this crack due to the self-weight of the beam and the axial tensioning system. With the tension held constant, fully reversing shear loads were applied. The 15th cycle load-slip curve for the beam specimen with the most uniform initial crack width is shown in Figure 2.2 (curve F). The load history was: cycles 1 - 15 at ± 100 psi shear,

cycles 16 - 25 at ± 125 psi and cycles 26 - 30 at ± 150 psi. Curve F is
for an initial crack width (ICW) of .03 inches and an axial tension at
28 ksi. The tension in the bars was maintained through the test to model
the stress which occurs in the longitudinal bars of a containment due to
internal pressurization. By this time the shearing stiffness for small
slippage has decreased from the early cycle stiffness because of the
degradation of the contact surface due to the 15 load cycles. When the
slip increases in the 15th cycle the stiffness increases also. This is
caused by an increased overriding action at the crack plane. This over-
riding increases the axial force in the reinforcing bar which in turn
increases frictional resistance. Thus each load increment must overcome
greater frictional resistance and the load-slip curves are upward
curving after the low initial stiffness. The seating against the concrete
of the reinforcing bar also increases the stiffness with increasing slip.
Curve F will be used as the input for IST + dowel stiffness for the
remainder of this chapter.

2.3 Shear Stress Distributions

The shearing stiffness of the cracks (due to the IST mechanism) may
affect the shear stress distribution in the containment vessel. A con-
tainment vessel after internal pressurization is shown in Figure 2.3. If
no cracks were present and the concrete was assumed to remain elastic
the sinusoidal shear stress distribution shown in Figure 2.5 is found.
The presence of the cracks may change the shear stress distribution as
shown by the dashed line in Figure 2.6. The increase in shear stress

(over the elastic distribution) near $\phi = 0°$ is due to the behavior shown in the Figure 2.2. Curve F shows that the crack stiffness increases with increasing slip. Since the greatest slip occurs at $\phi = 0°$ the stiffness is greatest here. A large stiffness concentration for low values of ϕ could cause higher shear stresses to occur for these values of ϕ than would be predicted by Figure 2.5.

The shear stress distribution in a section of the cracked cylinder will be found using the linear analysis program SAP IV [3]. It will be assumed that the stiffness of all of the cracks in the vessel can be characterized by curve F in Figure 2.2. While the initial crack width, axial stress and reinforcing percentage may be different in the actual vessel it is felt that the ratio of the high stiffness to the initial low stiffness of these curves will not change drastically with variations in these parameters. This ratio is the most important influence of the cracks on shear stress distribution. The bilinear idealization of curve F is shown in Figure 2.4.

The SAP IV model of the cracked cylindrical section is shown in Figure 2.7. Only the horizontal cracks are included in this model. The effects of the vertical cracks will be discussed later. Three horizontal cracks occur in the cylindrical section and these are modeled by the truss elements 1 - 27. It was felt that at least three crack layers were required to significantly affect the sinusoidal shear stress distribution. The horizontal crack spacing used in this model is 10 feet. This spacing was used to achieve nearly square flat shell finite elements (see next paragraph). This improves the results obtained from these elements. The stiffness of truss elements 1 - 27 will be the slope of either lines 1 or 2 in Figure 2.4. The length of each truss element (L_t)

is

$$L_t = \sqrt{(2 \times \sin 5° \times 720)^2 + (.03)^2} = 125.5''. \tag{2.1}$$

The cross-sectional area (A_t) of elements 1 - 27 is taken as $1/9 \times$ the total cross-sectional area of the quarter cylinder

$$A_t = \frac{1}{9} \times \left(\frac{\pi (720)(48)}{2}\right) = 6032 \text{ in}^2. \tag{2.2}$$

Two different Young's moduli, E_1 and E_2 are chosen to model the slopes 1 and 2 in the following manner:

$$\text{Slope 1} = \frac{20 \times A_t}{.01} = \frac{E_1 A_t}{L_t}$$

$$E_1 = 251 \text{ ksi}$$

$$\text{Slope 2} = \frac{(125 - 20)}{(.016 - .01)} \frac{A_t}{} = \frac{E_2 A_t}{L_t}$$

$$E_2 = 220 \text{ ksi}. \tag{2.3}$$

A series of flat shell finite elements developed by Clough and Felippa [4] which combine plate bending and plane stress behavior are used to model the quarter shell. This element uses four compatible triangles which each use the constant strain triangle and the LCCT9 element to represent the membrane and bending behavior, respectively. The LCCT9 element is based on a cubic displacement formulation for the transverse displacement which gives linearly varying moment fields (thus the name Linear Curvature Compatible Triangles with 3 degrees of freedom

at each node). These four triangles are combined to form a rectangle with a central node along with the four corner nodes. The six degrees of freedom associated with this central node are condensed out at the element formulation level. The resulting quadrilateral element has twenty-four degrees of freedom, i.e., six degrees of freedom per node in the global coordinate system. The thin shell elements model elastic uncracked concrete and have the appropriate Young's modulus (3640 ksi) and Poisson's ratio (.17).

Since only one-quarter of the shell is being modeled, certain boundary conditions must be used to adequately model the behavior of the full cross-section. The shear force V is assumed to act in the direction of the global Z-axis (see Figure 2.7). This means that the Z-axis must be a line of symmetry. To insure this, the X displacement and rotations about the Y and Z axes are deleted for nodes 1 - 8. For kinematic stability the Z displacement at node 8 is also deleted. The support reactions that were developed due to this deletion were negligible so that shear stress distribution in the cylinder was not affected. The vertical displacements in the direction of the global Y-axis were deleted for nodes 73 - 80. This nodal line represents the neutral axis of the cylindrical cantilever beam so no vertical displacements should exist along this line if bending only is considered.

The SAP IV model was loaded incrementally by imposing nodal loads at the top nodes 73, 65, 57, 49, 41, 33, 25, 17, 9, 1. Equal but opposite loads were imposed on nodes 80, 72, 64, 56, 48, 40, 32, 24, 16, 8. The idea was to examine the shear stress distribution at the central crack (elements 10 - 18) to see what changes from the original distribution had occurred due to the top two cracks. The original shear stress

distribution at the top nodes was assumed to be the elastic distribution for a beam of cylindrical cross-section. This distribution is shown in Figure 2.6 with τ_{max} = 1.0 psi. The shear area is A/2, where A is the cross-sectional area. The nodal loads are arrived at by computing work equivalent forces which correspond to this elastic shear stress. Since the displacements which correspond to the shear stress are linear, the work equivalent forces at node i are computed according to the following equation:

$$P_{zi} = t \int_{\phi_i - 5°}^{\phi_i + 5°} \tau(\phi) \cos\phi \, R_c \, d\phi$$

$$P_{xi} = t \int_{\phi_i - 5°}^{\phi_i + 5°} \tau(\phi) \sin\phi \, R_c \, d\phi \quad (i = 1, 9, 17, 25, 33, \\ 41, 49, 57, 65, 73)$$

$$\tau(\phi) = \tau_{max} \cos\phi$$

$$\tau_{max} = \frac{V}{\text{Shear Area}} = \frac{2V}{A}. \tag{2.4}$$

The incremental loading procedure used will be described by reviewing some of the typical load steps that were used and the stiffness changes which occurred after each of the load steps. The result of the first load step is shown in Figure 2.8. Since all of the cracked elements (truss elements 1 - 27) had Young's modulus E_1 the cylinder acted as in the usual uncracked elastic manner with the SAP IV results being almost exactly the same as the elastic ($\tau = 1 \cos\phi$) distribution. Note that the maximum stress (which occurs in bars 1, 10 and 19 which correspond to $\phi = 5°$) is 20 psi. This means that the actual SAP IV results, which

were based on a maximum shear stress (τ_{max}) loading of 1 psi, have been scaled up by a factor of 20 so that the most highly stressed bars (1, 10, 19) will be at the break point in the shear-slip curve (Figure 2.5). Since the expected elastic shear stress distribution was obtained in the SAP IV model the boundary conditions discussed above would seem to be verified. In the second load step (Figure 2.9) bars 1, 10 and 19 had the high E_2 Young's modulus while the rest of the bars remained at E_1. The loading corresponding to 1 cosϕ distribution will stress bars 2, 11 and 20 to .6 psi (see Figure 2.9). Adding this to the 19.4 psi in these bars from the first load step produces a total of 20 psi which now puts these bars at the stiffness break point. For the next load step bars 1, 2, 10, 11, 19 and 20 will have the high modulus E_2. The load increments continue in this manner, with each successive bar along the crack being loaded until it reaches the stiffness break point. From there on this bar will have the modulus E_2. The remaining load steps (shown in Table 2.1) continue in this manner. Total stresses are obtained by simple addition of the results from each load step. The shear stress distributions from each load step are shown in Figures 2.8 - 2.16.

The stiffness change from the last stiff bar to the first flexible bar always causes a stress concentration at the last stiff bar. The magnitude of this stress concentration varies for the different load steps but the distortion from the elastic distribution is quite evident except for the run with bars 1 - 7 stiff, which is to be expected. The maximum stress ratio (maximum inelastic stress to maximum elastic stress) is approximately 1.7 and occurs with bars 1 and 2 stiff. While there are large stress concentrations in the individual load steps, these concentrations cancel each other out when total stresses after each load

step are computed. This can be seen from Figure 2.17 where the deviations

from the elastic distribution of total stresses is very small. The

reason for this is that the load steps with the highest stress concen-

trations (steps 2 - 6) are very small load steps with the maximum deviation

from the elastic distribution being only 3 psi in step 6 (Figure 2.13).

Therefore, the maximum shear stress distribution does not change appre-

ciably from the elastic distribution shown in Figure 2.6 when the non-

linear action of IST is included. The elastic shear area of A/2 may

then be used at the cracks.

During an earthquake the overturning moment caused by inertial

forces may cause the crack width to change. If the crack were to close

completely over some portion of its circumference then this would be

the source of a large stiffness concentration which may alter the shear

stress distribution. In section 5.5 it is shown that for a total

unbonded length at the crack of 2.5 inches the change in crack width is

small compared to the initial crack width. Therefore the shear stress

distribution is not significantly altered from the sinusoidal distribu-

tion. The unbonded length of 2.5 inches was observed in tests at Cornell.

A much larger unbonded length, such as 15 inches, may cause a significant

alteration in the shear stress distribution because the crack may then

close completely. However, this (the closing of the crack) would only

occur for an extremely brief period of time and the assumption of an

unbonded length of 15 inches at the crack is far fetched.

Figure 2.3 shows that vertical cracks also exist in the containment.

These cracks may effectively decrease the flexural and shear stiffness

of the containment vessel. It is not yet known how much this stiffness

decrease might be. The effects on seismic analysis of this stiffness

decrease will be discussed in Chapter 5.

Chapter 3

LINEAR SEISMIC ANALYSIS OF A CONTAINMENT VESSEL

3.1 Idealization of the Containment Shell Vessel

A seismic analysis of the containment shell must be performed to obtain the forces and deformations caused by the SSE which are required in design. The current practice is to use a linear model for seismic analysis which does not take into account the cracks in the vessel wall. The dynamic structural model which is used in seismic analysis attempts to model the real structure (in this case the containment vessel of a nuclear power plant) with a finite number of discrete node points. The number of nodes used in a dynamic analysis is normally much less than would be used in a static analysis of the same structure. The best rationalization for the inexactness of the dynamic model is that the earthquake loading itself is a totally random occurrence with characteristics which cannot be accurately predicted. Clearly there is no point in developing a highly refined dynamic model when the loadings are uncertain because of the random nature of earthquakes.

In this chapter a linear dynamic model of the containment shown in Figure 1.1 will be developed. The results from this model will be compared with the results of the nonlinear model (which includes the effects of cracking) developed in Chapter 5.

The equations of motion for a structure undergoing ground accelerations are

$$[M] \{\ddot{u}\} + [C] \{\dot{u}\} + [K] \{u\} = - [M] \{\ddot{x}_g\} \qquad (3.1)$$

where $\ddot{u}$, $\dot{u}$, u and x_g are the relative acceleration, relative velocity, relative displacement and ground acceleration, respectively. These quantities are shown in Figure 3.1 where

$$\lfloor u \rfloor = \lfloor u_1 \ \theta_1 \ u_2 \ \theta_2 \ u_3 \ \theta_3 \ u_4 \ \theta_4 \ u_5 \ \theta_5 \rfloor . \qquad (3.2)$$

The relative displacements u_i are related to the total displacements x_i by

$$u_i = x_i - x_g \qquad\qquad i = 1 \ldots 5 \qquad (3.3)$$

where x_g is the ground displacement. The rotational degrees of freedom $\theta_1 \ldots \theta_5$ will be included in this analysis so $[M]$, $[C]$ and $[K]$ in (3.1) will be 10×10 matrices. Later in this chapter the effects of dropping the rotational degrees of freedom will be studied.

In Figure 3.2 the actual containment vessel and the dynamic model are shown. The lumped mass method is used to model the containment. The 120 ft. cylinder is broken up into four equal segments with mass of M_c and mass moment of inertia of I_{mc}. The density of the concrete is .150 k/ft^3.

$$M_c = \frac{2\pi \times 69.75 \times 4.5 \times 120 \times .15}{4 \times 386.4} = 22.967 \text{ k-sec}^2/\text{in} \qquad (3.3a)$$

$$I_{mc} = M_c \left[\frac{R_c^2}{2} + \frac{1}{3} \left(\frac{L_c}{4} \right)^2 \right] = 8.293 \times 10^6 \text{ k-sec}^2\text{-in} \qquad (3.3b)$$

M_c and I_{mc} are the values of the lumped masses at nodes 2 - 5 in Figure 3.2. The hemispherical head is modeled by node 1. Node 1 is located at the center of gravity of the head ($R_s/2$ above the bottom of the head). The mass (M_s) and mass moment of inertia (I_{ms} taken about the CG) of the spherical head are

$$M_s = \frac{2\pi \times 68.75^2 \times 2.5 \times .15}{386} = 28.822 \text{ k-sec}^2/\text{in} \qquad (3.4a)$$

$$I_{ms} = \frac{2}{3} M_s R_s^2 - M_s \left(\frac{R_s}{2} \right)^2 = 8.174 \times 10^6 \text{ k-sec}^2\text{-in} \qquad (3.4b)$$

The mass matrix [M] for a lumped mass representation is always a diagonal matrix. The diagonal members of [M] for the model shown in Figure 3.2 are

$$\begin{bmatrix} M \end{bmatrix} = \begin{bmatrix} M_s & & & & & & \\ & I_{ms} & & & & & \\ & & M_c & & & & \\ & & & I_{mc} & & & \\ & & & & \ddots & & \\ & & & & & M_c & \\ & & & & & & I_{mc} \end{bmatrix} \qquad (3.5)$$

The stiffness matrix [K] in equation (3.1) is based on the shear beam element stiffness matrix (see Figure 3.3 and Table 3.1). This reflects the assumption that the containment vessel acts as a vertical

cantilever beam with a thin walled cylindrical cross-section. The validity of this assumption is discussed in [8]. For concrete typical values of Young's modulus and the shear modulus are E = 3640 ksi and G = 1540 ksi. I and A_s are the moment of inertia and shear area of the beam. For the cylindrical beam segments $I = \pi R_c^3 t_c$ and $A_s = \pi R_c t_c$. The shear area is one-half the cross-sectional area, since the concrete is assumed to behave elastically. For the beam segment which models the hemispherical head average values of A_s and I are computed in the following manner:

$$A_{s1} = \pi R_s t_s \times \frac{412.5}{592.5} + \pi R_c t_c \times \frac{180}{592.5}$$

$$A_{s1} = 97270 \text{ in}^2 \tag{3.6a}$$

$$I_1 = \pi R_s^3 t_s \frac{\int_0^{\pi/6} \cos^2\phi \, d\phi}{\int_0^{\pi/6} d\phi} \times \frac{412.5}{592.5} + \pi R_c^3 t_c \frac{180}{592.5}$$

$$I_1 = 6.7064 \times 10^{10} \text{ in}^4 \tag{3.6b}$$

The global stiffness matrix [K] (see Table 3.2) is formed directly by simple addition of terms which correspond to the same degree of freedom.

The damping matrix [C] is the most difficult part of the model to define. In this analysis [C] will be based on the ratio of critical damping which occurs in each mode of vibration. This will be explained further in the next section on modal analysis.

3.2 Modal Analysis

In modal analysis the first step taken is the calculation of the natural frequencies and mode shapes of the idealized model. This corresponds to the solution of the undamped free vibration problem, which may be stated as

$$[M] \{\ddot{u}\} + [K] \{u\} = \{0\}. \tag{3.7}$$

We now assume a harmonic solution for the displacement $\{u\}$ in the form

$$\{u\} = \{\phi\} \sin\omega t$$

$$\lfloor \phi \rfloor = \lfloor \phi_1 \ \phi_2 \ \cdots\cdots \ \phi_{10} \rfloor. \tag{3.8}$$

Substituting (3.8) into (3.7) we find that there are ten possible values of the frequency ω and ten associated eigenvectors $\lfloor \phi \rfloor$ which satisfy (3.7). The modal matrix $[A]$ is made up of these ten eigenvectors.

$$[A] = [\{\phi\}_1 \ \{\phi\}_2 \ \cdots\cdots \ \{\phi\}_{10}]. \tag{3.9}$$

It may be shown [11] that the following relationships are true:

$$[A]^T [M] [A] = [I] = [\tilde{M}] \tag{3.10a}$$

$$[A]^T [C] [A] = [\bar{C}] \tag{3.10b}$$

$$[A]^T [K] [A] = [E] \tag{3.10c}$$

where [I] is the identity matrix and [E] is a diagonal matrix containing $\omega_1^2 \ldots \omega_{10}^2$ on the diagonal. In this formulation the eigenvectors have been orthonormalized with respect to the mass matrix. [$\bar{C}$] is a diagonal matrix only if [C] is proportional to the stiffness and/or the mass matrix:

$$[C] = \alpha_1 [M] + \alpha_2 [K]. \tag{3.11}$$

Equation (3.1) may now be written as ten uncoupled equations:

$$\ddot{q}_k + (\alpha_1 + \alpha_2 \omega_k^2) \dot{q}_k + \omega_k^2 q_k = \bar{F}_k \qquad (k = 1 \ldots 10) \tag{3.12a}$$

$$\{q\} = [A] \{u\} \tag{3.12b}$$

$$\{\bar{F}\} = - [A]^T \{\ddot{x}_g\}. \tag{3.12c}$$

Equation (3.12a) represents the contribution of the kth mode to the motion of the 10 dof system and is completely uncoupled as far as (3.11) holds. The coefficients α_1 and α_2 can be used to get only two different values of modal damping. In this treatment a constant damping ratio will be used for all modes. For nuclear containment vessels, the commonly used value is about 5%.

$$\beta_k = \frac{\bar{C}_{kk}}{2\bar{M}_{kk}\omega_k} = .05 \qquad \text{(for all k).} \tag{3.13}$$

Equation (3.12a) now becomes

$$\ddot{q}_k + 2\beta_k \omega_k \dot{q}_k + \omega_k^2 q_k = \bar{F}_k \qquad (3.14)$$

The computer program MODAL (source listing in Appendix A) has been developed to do modal analysis. The Jacobi method [11] is used to find frequencies and mode shapes. The Newmark β method [11] is used to integrate the uncoupled equations of motion (3.14).

3.3 Rotational Degrees of Freedom

The linear dynamic analysis program MODAL was tested and verified through use of the dynamic capabilities of SAP IV [3]. The test earthquake (ground accelerations $\ddot{x}_g$) is shown in Figure 3.4. The idealized structural model used is that shown in Figure 3.2. The results from both SAP IV and MODAL for the displacement of the top mass (defined as u_1) are given by curve 1 in Figure 3.5, the small differences between the two analyses not being discernible with the scale used.

It is standard procedure in dynamic analysis to eliminate rotational degrees of freedom. This can be done by using any one of a number of condensation methods or by dropping all terms in the stiffness and mass matrices which are associated with rotational degrees of freedom. Condensation procedures require that a matrix be inverted each time the stiffness matrix is set up. It would be expensive to use one of these condensation methods in a nonlinear analysis since it would require finding the inverse of a 5 × 5 matrix every time a stiffness change was encountered. A much simpler method would be to drop out rotational degrees of freedom from the model and subject this new model to the test

earthquake. Curve 2 in Figure 3.5 shows the effects of dropping the rotational degrees of freedom. Clearly the model is significantly stiffer than the model corresponding to curve 1. This can be seen quite clearly in Table 3.3. The first column shows the natural frequencies obtained when the rotational degrees of freedom are included.

Column 2 gives the frequencies obtained by dropping the rotational degrees of freedom. A comparison of the fundamental frequencies shows that the 5 DOF model has a fundamental frequency which is 25% higher than the 10 DOF model. Curve 2 shows that this increase in stiffness affects the motion of the top mass significantly for the base motion shown in Figure 3.4. However, it must be noted that this base motion is of extremely short duration (.25 seconds) and means nothing as far as design requirements go. The NRC response spectra shown in Figure 1.3 is the basis of seismic design of containment vessels (see Introduction). This figure shows that the frequencies of 6.0 cps and 7.5 cps occur in a flat region of the graph for the spectral acceleration. For a maximum base acceleration of 1.0 g both frequencies correspond to a spectral acceleration of about 3.5 g (for 5% critical damping). The maximum displacements for 6.0 cps and 7.5 cps are 1.0 inches and .5 inches, respectively. This would seem to indicate that dropping the rotational degrees of freedom will give forces and moments which are acceptable but will underestimate the maximum displacements by about 50%. This is borne out by the results of the test case since the maximum base shears were fairly close for the two models (.139 ksi for the 5 DOF model and .159 ksi for the 10 DOF model). Since the time history of displacements is of great importance it is concluded that rotational degrees of freedom should be included in the seismic analysis of a containment vessel. Rotational

degrees of freedom will be included in the rest of this study.

Chapter 4

SOIL-STRUCTURE INTERACTION

4.1 Introduction

If a seismograph were placed in an area in which no buildings were

located the time history of the ground movements obtained would be the

"free field" accelerations. Normally, the flexible multistory buildings

built in this country do not have sufficient stiffness and mass to affect

these free field accelerations. If a seismic analysis were to be per-

formed on one of these buildings it would usually be sufficient to use

the free field accelerations as the base accelerations defined as $\ddot{x}_g$ in

the previous chapter. However, a nuclear containment vessel is much

stiffer than most multistory buildings. If the containment vessel is

at least as stiff as the underlying soil then the inertial forces developed

during an earthquake will cause local deformations in the soil in the

area of the foundation. These local soil deformations may alter the

free field motion considerably. The degree of alteration depends on the

relative stiffness and mass ratios between the structure and the soil.

Naturally if the structure is much stiffer than the soil the local foun-

dation base motion may be quite different from the free field motion.

This change in motion at the soil-structure interface is called soil-

structure interaction. Soil-structure interaction should be differentiated

from soil amplification.

Soil amplification is the effect of local soil conditions on the seismic waves produced by an earthquake. The effect may be one of amplification, attenuation or filtering of the underlying "base rock" motions. In Figure 4.1 the base rock motion is shown as $\ddot{x}_1$, the free field motions (which occur a large distance from the containment) are $\ddot{x}_2$ and ground accelerations at the base of the foundation (taking into account soil amplification and soil-structure interaction) are $\ddot{x}_3$.

4.2 Brief Summary of Seismic Waves

The underlying causes of earthquakes are not yet well known. The most widely accepted theory at this time is the elastic rebound theory developed by H. F. Reid following the San Francisco earthquake of 1906. Reid's study of the large shear displacements along the San Andreas fault led him to conclude that the vibrational energy of earthquakes originates from the release of accumulated strain in the earth's crust. These strains are caused by the movement of large crustal plates. In the case of the San Andreas fault this movement is a counterclockwise rotation of the Pacific basin crustal plates relative to the North Averican continental land mass [11]. The strain release is a sudden shearing fracture.

The wave systems which result from this fracture are what actually cause the surface vibratory motion. It can be shown [5] by using the three dimensional wave equations that in an unbounded isotropic solid on two types of elastic wave may be propagated. These waves are called

the irrotational (P-waves) and equivoluminal (S-waves) waves. The velocities of the P-waves (C_1) and S-waves (C_2) are

$$C_1 = \sqrt{(\lambda_L + 2G)/\rho_s}$$

$$C_2 = \sqrt{G/\rho_s}. \tag{4.1}$$

λ_L is Lame's constant, G is the shear modulus and ρ_s is the density of the medium through which the waves travel. Clearly the P-waves travel faster than the S-waves through all media. When there is a bounding surface, surface waves also occur. It can be shown that these surface waves (one type is Rayleigh waves) decay rapidly with depth of the medium but show much less amplitude decay than P-waves or S-waves at the surface boundary. The surface motion contains both vertical and horizontal (parallel to wave direction) components. They travel with a velocity (C_R) slightly less than that of the S-waves. For μ (Poisson's ratio) = .25, C_R = .9194 C_1.

Seismographic records show that earthquakes may be broken down into two stages. These are the preliminary tremor and main shock. The preliminary tremor consists of two phases, which correspond to the arrival of first the P-waves and then the S-waves through the interior body of the earth. The main shock may be broken down into three phases. In the first two phases the movement is horizontal and transverse to the direction of wave propagation. In the third phase the horizontal movement is in the propagation direction. The movements in the main shock are much larger than in the preliminary tremor. Originally it was felt that the main shock was caused by Rayleigh waves travelling over the surface

of the earth from the initial disturbance. However, the vertical compo-
nent of motion is larger than the horizontal component at the surface for
Rayleigh waves. Also the horizontal motion in Rayleigh waves is in the
wave propagation direction. Thus Rayleigh waves don't explain the motion
in the first two phases of the main tremor.

Love [6] proposed that the transverse movements in the main shock
are caused by waves which travel through an outer crust of the earth
which differs in material properties from the interior. These waves,
calles Love waves, do not penetrate deeply into the interior of the earth
and because of this create large amplitude motions at large distances
from the initial disturbance. For Love waves to be confined to this
outer crust, the S-wave velocity C_2 for this outer layer must be less
than C_2 for the next lower layer. Love waves will not occur unless this
is true. The Love wave travels with a velocity somewhere between C_2 for
the outer crust and C_2 for the next lower layer. The transverse motion
in the first two phases of the main shock is then caused by Love waves.
The longitudinal motion in the third phase must then be caused by Rayleigh
waves, which travel at a speed less than C_2.

4.3 Modeling of the Soil

The stiffness and damping effect of the soil will be modeled using
equivalent springs and dashpots. The values for these springs and dashpots
are found from the problem of a rigid circular footing which oscillates
on an elastic half-space. For ground motion in the horizontal direction,
·e need spring constants which correspond to the u_f and ϕ_f degrees of

freedom shown in Figure 4.2. These springs are actually functions of the load frequency, but it has been found [7] that the following frequency independent expressions are adequate.

$$K_u = \frac{32(1 - \mu)Gr_o}{7 - 8\mu}$$

$$K_\phi = \frac{8Gr_o^3}{3(1 - \mu)} . \tag{4.2}$$

G and μ are the shear modulus and Poisson's ratio for the soil and K_u and K_ϕ are the translational and rotational spring constants shown in Figure 4.3. Poisson's ratio varies from about .35 to .5 in soils, depending upon the degree of saturation. A value of .4 will be used in this investigation. From various in-situ tests, typical values of the shear wave velocity C_2 may vary from about 500 fps (weak soils) to 2000 fps (rock). G is directly related to C_2 by (4.1). Table 4.1 gives values of K_u and K_ϕ for shear velocities of 500 fps, 1200 fps and 2000 fps with $\mu = .4$ in all cases.

In an ideal elastic half-space only geometrical damping exists. Geometrical damping is caused by the loss of energy which occurs when the elastic waves travel from the footing out to infinity. Calling the translational and rotational geometric damping ratios D_{uG} and $D_{\phi G}$, we have from [7] that

$$D_{uG} = \frac{.288}{(B_u)^{1/2}} \qquad\qquad B_u = \frac{(7 - 8\mu)m_f}{32(1 - \mu)\rho_s r_o^3}$$

$$D_{\phi G} = \frac{.15}{(1 + B_\phi)(B_\phi)^{1/2}} \qquad\qquad B_\phi = \frac{3(1 - \mu)I_f}{8\rho_s r_o^5} \tag{4.3}$$

m_f and I_f are the mass and mass moment of inertia (calculated at the top of the foundation) of the circular foundation. ρ_s is the density of the underlying soil.

$$m_f = \frac{\pi r_o^2 t_f \gamma_c}{g} = 61.74 \text{ k-sec}^2/\text{in}$$

$$I_f = \frac{1}{4} M_f r_o^2 + \frac{1}{3} M_f t_f^2 = 12.742 \times 10^6 \text{ k-sec}^2\text{-in}$$

$$\gamma_c = \text{Unit weight of concrete} = .15 \text{ K/ft}^3$$

$$t_f = \text{Foundation thickness} = 9 \text{ ft}$$

$$r_o = \text{Foundation radius} = 75 \text{ ft}$$

B_u and B_ϕ are the modified mass ratios. They essentially describe the relationship between the mass of the foundation which undergoes either translational or rocking motion and and effective mass of the underlying soil. It is felt that equations (4.3) give soil damping percentages which are too high [8].

In real soils hysteretic damping is also important. Hysteresis occurs when loading and unloading follow different paths on the stress-strain diagram (see Figure 4.4). In each complete loading cycle an amount of energy equivalent to the area inside the hysteresis loop is dissipated. Hysteresis in soils is caused by slippage between particles and clearly is dependent upon the magnitude of maximum strain in the soil. For SSE earthquakes (peak ground acceleration greater that .1 g) this damping is usually taken as about 5%. The total damping ratios D_u and D_ϕ

are then the sum of geometric and hysteretic damping.

$$D_u = D_{uG} + .05$$

$$D_\phi = D_{\phi G} + .05 \qquad (4.4)$$

If the above value of m_f and I_f are substituted into the equations for geometric damping (4.3) estremely high values of D_{uG} and $D_{\phi G}$ result (for $\mu = .4$, $D_{uG} = .56$ and $D_{\phi G} = .14$). Since the validity of equation (4.3) is in doubt, the values of $D_u = .25$ and $D_\phi = .05$ will be used in all subsequent analysis. These values are recommended in [9].

The necessary additions to the global stiffness matrix are shown in Table 4.2. The first ten rows and columns are exactly the same as in Table 3.2. The element stiffness matrix $[K_{ff}]$ contains the stiffness contributions of the translational and rotational soil springs.

4.4 Mass and Damping Matrices for SSI

Certain changes and additions must be made in the mass, stiffness and damping matrices described in Chapter 3 to implement the soil-structure interaction model shown in Figure 4.3. The degrees of freedom to be included in this analysis are

$$\lfloor u \rfloor = \lfloor u_1 \ \theta_1 \ u_2 \ \theta_2 \ u_3 \ \theta_3 \ u_4 \ \theta_4 \ u_5 \ \theta_5 \ u_f \ \theta_f \rfloor . \qquad (4.5)$$

In (4.5) $u_1 \ldots u_5$ and u_f are displacements relative to the ground.

$\theta_1 \ldots \theta_5$ and ϕ_f are total rotations. Positive sign conventions for u

are shown in Figures 3.1 and 4.2. The mass matrix [M] is now

$$[M] = \begin{bmatrix} 28.822 & & & & & & & & & \\ & 8.174 \times 10^6 & & & & & & & & \\ & & 22.967 & & & & & & & \\ & & & 8.293 \times 10^6 & & & & & & \\ & & & & 22.967 & & & & & \\ & & & & & 8.293 \times 10^6 & & & & \\ & & & & & & 22.967 & & & \\ & & & & & & & 8.293 \times 10^6 & & \\ & & & & & & & & 22.967 & \\ & & & & & & & & & 8.293 \times 10^6 \\ & & & & & & & & & & m_f \\ & & & & & & & & & & & \sum_{i=1}^{5} I_i + I_f \end{bmatrix} \qquad (4.6)$$

Since the lumped mass model of the containment vessel remains the same

the first 10 members of the main diagonal of [M] are the same as the

lumped masses shown in Figure 3.2. m_f and I_f were calculated in the

previous section.

The normal method of assigning percentages of critical damping to

each mode in order to develop a damping matrix (see Chapter 3) is no

longer longer valid when the effects of soil are included in the analysis

since the soil has much more damping (normally more than 10% of critical)

than the containment vessel. The subregioned energy proportion method [10]

for calculating modal damping values will be used to incorporate the dif-

ferent critical damping ratios for the soil and structure into one effec-

tive critical damping ratio for each mode. In this method, the modal

damping ratio D_m is the weighted average of dissipated strain energy:

$$D_m = \frac{\sum\limits_{i=1}^{nm} E_{im} d_i}{E_m} \tag{4.7}$$

D_m = modal damping factor at m^{th} mode

d_i = fraction of damping factor of ith mass

E_m = total energy in m^{th} mode

E_{im} = energy in i^{th} mass in m^{th} mode

nm = number of masses in analysis

$$E_{im} = \frac{1}{2} \phi_{\ell m} \, k_{\ell j}^{(i)} \, \phi_{jm} \qquad \ell = 1 \ldots nm \qquad j = i \ldots nm \qquad \text{no sum on m}$$

$$E_m = \sum\limits_{i=1}^{nm} E_{im}$$

ϕ_{ij} = modal displacement of ith mass for j^{th} mode

$k_{\ell j}^{(i)}$ = element stiffness of ith member connecting nodes ℓ and j (see

Table 3.1). The modal damping ratios thus calculated may then be used in

the program MODAL as described in Chapter 3 and the Appendix. If direct

numerical integration of the equations of motion is to be performed (as

will be done in the next chapter), then the fully populated damping matrix

[C] may be found:

$$[C] = [A^T] \, [D] \, [A]^{-1} \tag{4.8}$$

[D] is a diagonal matrix which contains the modal damping factors obtained

from (4.7).

Soil-structure interaction is included in all of the seismic analyses

discussed in the next chapter. The effects of changing the stiffness of

the underlying soil will be studied in particular.

Chapter 5

SEISMIC ANALYSIS INCLUDING CRACKS

5.1 Introduction

In this chapter the effect of including cracks in seismic analysis
will be studied. First, new IST test results are described. The ideali-
zation of these cracks for use in the nonlinear computer program SAC is
shown. The numerical integration techniques used in SAC are described.
A synthetic time history is used as input to SAC in a parameter study
designed to study the effects of including cracks in seismic analysis and
to show the significance of varying the values of the soil springs described
in Chapter 4. Finally system identification is used to find a linear
model which can best approximate the results obtained from SAC.

5.2 Modeling of the Cracks

The circumferential (horizontal) and longitudinal (vertical) cracks
in the vessel may have a significant effect on the dynamic response of the
vessel due to the SSE. The effect of cracks on seismic analysis has been
studied previously at Cornell [15]. The important design parameters (as
described in the Introduction) which may be affected are the liner distor-

tion and the maximum shear stress in the concrete containment vessel. For the seismic analysis, recent IST test results [2] are used. In the beam tests described in Chapter 2 the dead weight of the specimen and the axial loading system made it difficult to achieve a uniform crack width at the shear plane before the initiation of the cyclic shear test. In the more recent tests, the loading setup shown in Figure 5.1 was used. An independent frame was used to tension the internal reinforcing bars. The crack at mid-height of the block was formed by initially tensioning the reinforcing bars. The location of the crack was set by use of a crack-iniating groove which was formed into the specimen during casting. The shear loading was applied at the vertical beams, which could be moved up or down to reverse the loading direction. This setup resulted in less tilting at the crack plane and a more uniform crack width. After the desired initial crack width was obtained by stressing the reinforcing bars, the cyclic shear stress tests were begun.

In one of the test specimens two #14 reinforcing bars were cast into the specimen in a plane perpendicular to the direction of loading. The reinforcement ratio (steel area/cross-sectional area) for the block was .0178. The reinforcement ratio for the longitudinal steel in a typical containment vessel is .0185 (two #18's spaced at 8 inches) which is reasonably close to this test case. Presently, no tests have been done using #18 bars but the effects of increasing the bar diameter may be significant. The initial crack width was .02 inches with a bar tension of 31 ksi.

The cyclic loading schedule was: 9 cycles at 110 psi on the gross concrete area, 6 cycles at 125 psi, 11 cycles at 202 psi, 13 cycles at 260 psi and 4 cycles more at 260 psi with the bar tension increased to

41 ksi. Each loading cycle was composed of a complete reversal of the maximum stresses listed above. Cycles 1, 15 and 25 were loaded incrementally so that detailed measurements of horizontal slip, increase in crack width and bar strains could be taken. The specimen failed during the 42nd cycle at a stress of 230 psi. The mode of failure was a sudden brittle splitting fracture which was due to the dowel forces in the reinforcing bars. Figure 5.2 shows the shear stress versus horizontal slip measurements for the 1st, 15th and 25th cycle. The loading portion of the 1st cycle is almost linear, while the 15th and 25th cycles show the same hardening effects as was observed in the beam tests. After the 1st cycle the shape and slope of the hysteresis loops were essentially the same with only the maximum slip changing with each cycle. The maximum slip increased at a nearly constant rate in these tests. The crack width remained nearly constant at .02 inches until just before failure.

In the seismic analysis only the horizontal cracks will be included. As was mentioned previously in Chapter 2, the vertical cracks may significantly affect the shear and flexural stiffness of the containment vessel. Since only uniaxial tests have been performed at this time it is difficult to quantitatively assess the effects of horizontal cracks. It is felt that a decrease in the flexural stiffness of the containment is not a significant factor. Tests using the program MODAL have shown that if the flexural stiffness of the containment vessel is reduced by one-third the fundamental frequency changes by less than 1%. However, a large change in the shear stiffness of the vessel would produce significant changes in the seismic analysis. Current tests under way at Cornell include cracks in both the horizontal and vertical directions. These tests should give quantitative results on how much the vertical cracks affect the shear stiffness of the

containment vessel.

The stiffness of the horizontal cracks is found from the test results shown in Figure 5.2. To simplify the analysis these curves are idealized in the manner shown in Figure 5.3. In this figure the data from the 25th loading cycle and the idealization are shown. The idealization consists of six straight lines which were drawn to model as best as possible the slope of the hysteresis curves and the area inside the curves (energy loss/cycle). Note that in Figure 5.3 the shear-slip curve is nonsymmetric about the y-axis. It was felt that this was due to eccentricity in the axial loading system and the entire hysteresis loop is moved to the left in Figure 5.4 so that the loop is anti-symmetric about the y-axis.

In this same figure four assumptions which have not yet been experimentally verified are shown. Unloading from point A on line 1-2 is done along line A-B which is parallel to line 2-3. This assumption should be correct since the unloading stiffness remained almost constant for all cycles, including the early cycles which only went up to 110 psi maximum shear stress. The second assumption is that reloading from point C on line 2-3 goes along line C-D which is parallel to line 1-2. The reasoning behind this is that the higher loading stiffness (the slope of line 1-2) is activated when loading occurs at a shearing stress greater than the stress at point 1 (30 psi in this case). The last assumption is also based on this. Line E-F shows unloading from a stress greater than that at point 2 (202 psi). Reloading occurs along line F-G (parallel to line 1-2) since the stress at point F is greater than the stress at point 1. These three assumptions all hold true for the shear-displacement curves in the third quadrant. The arrows in Figure 5.4 show the possible load directions along each of the six lines. Along line 1-2 only loading occurs. Only

unloading occurs along (or parallel to) line 2-3. Slip may occur in both directions along lines 3-4 and 1-6. Loading in the negative direction occurs along line 4-5 and unloading along (or parallel to) line 5-6. Only unloading occurs along 3-H and 6-I. As mentioned above, loading starts in a direction parallel to line 2-3 from both these lines.

The hysteresis loops change with load cycling in the manner shown in Figure 5.2. The idealization of this phenomenon is shown in Figure 5.6. The first cycle of loading is assumed to be linear (for both loading and unloading). The hysteretic behavior first appears in the second cycle and continues through the rest of the load cycles. The slope of each of the six line segments that compose the hysteresis loop remains the same for all cycles. The stiffness break point is 30 psi (for loading) for all cycles. The manner in which one cycle of loading or unloading is defined is described in the next section.

The flexibility of the cracks must be included in the global stiffness matrix [K]. This is done by considering the cracked cantilever beam shown in Figure 5.7. For purposes of illustration, the element stiffness matrix will be developed for the case of one crack in the beam, but this formulation may easily be generalized to the case of N cracks in a beam. First the deflection u_1 and rotation due to the loads P_1 and M_1 are calculated. At the crack plane the bond between the reinforcing bars and concrete is deatroyed for a certain length. In the tests described previously the unbonded length was about 2 inches. Since these tests were perforned on #14 bars the unbonded length (L_u) was scaled up to $18/14 \times 2 = 2.5$ inches for use in this analysis. The linear scale factor was used because unbonded length is a function of the bar force/bond force ratio. The bar force and the bonding force (per unit length) are proportional to the

reinforcing bar area and circumference, respectively. Over the unbonded length a conservative assumption would be that the moment of inertia is provided only by the longitudinal reinforcement. This moment of inertia over the unbonded length at the crack plane will be called I_c. Including this in a moment area analysis of the cracked shear beam we find that

$$
\begin{Bmatrix} u_1 \\ \theta_1 \end{Bmatrix} = \begin{bmatrix} \left(\dfrac{L^3}{3EI} + \dfrac{L}{GA_s} + \dfrac{1}{K_c} + A\right) & \left(\dfrac{L^2}{2EI} + B\right) \\ \left(\dfrac{L^2}{2EI} + B\right) & \left(\dfrac{L}{EI} + C\right) \end{bmatrix} \begin{Bmatrix} P_1 \\ M_1 \end{Bmatrix}
$$

$$
A = \frac{L^2 L_u}{4E} \frac{1}{I_c} - \frac{1}{I} \qquad B = \frac{L L_u}{2E} \frac{1}{I_c} - \frac{1}{I} \qquad C = \frac{L_u}{E} \frac{1}{I_c} - \frac{1}{I} \qquad (5.2)
$$

where K_c is the crack stiffness.

This equation is inverted to obtain

$$
\begin{Bmatrix} P_1 \\ M_1 \end{Bmatrix} = \frac{1}{\det} \begin{bmatrix} \dfrac{L}{EI} + C & -\dfrac{L^2}{2EI} + B \\ -\dfrac{L^2}{2EI} + B & \dfrac{L^3}{3EI} + \dfrac{L}{GA_s} + \dfrac{1}{K_c} + A \end{bmatrix} \begin{Bmatrix} u_1 \\ \theta_1 \end{Bmatrix}
$$

$$
\det = \frac{L^4}{12E^2 I^2} + \frac{L}{EI}\left(\frac{L}{GA_s} + \frac{1}{K_c}\right) + \frac{AL}{EI} + C\left(\frac{L^3}{3EI} + \frac{L}{GA_s} + \frac{1}{K_c} + A\right)
$$

$$
- B\left(\frac{L^2}{2EI} + B\right) \qquad (5.3)
$$

$$
\begin{Bmatrix} P_1 \\ M_1 \end{Bmatrix} = \begin{bmatrix} K_{11} \end{bmatrix} \begin{Bmatrix} u_1 \\ \theta_1 \end{Bmatrix}
$$

$$
(5.4)
$$

From equilibrium

$$\begin{Bmatrix} P_2 \\ M_2 \end{Bmatrix} = \begin{bmatrix} -1 & 0 \\ -L & -1 \end{bmatrix} \begin{Bmatrix} P_1 \\ M_1 \end{Bmatrix} \tag{5.5}$$

$$\begin{Bmatrix} P_2 \\ M_2 \end{Bmatrix} = \begin{bmatrix} K_{21} \end{bmatrix} \begin{Bmatrix} u_1 \\ \theta_1 \end{Bmatrix} \tag{5.6}$$

$$\begin{bmatrix} K_{21} \end{bmatrix} = \frac{1}{\det} \begin{bmatrix} -\left(\dfrac{L}{EI} + C\right) & \dfrac{L^2}{2EI} + B \\ B - \dfrac{L^2}{2EI} - LC & \dfrac{L^3}{6EI} + BL - \dfrac{L}{GA_s} - \dfrac{1}{K_c} - A \end{bmatrix} \tag{5.7}$$

If the cracked beam element is fixed at node 1 ($u_1 = 0$, $\theta_1 = 0$) and free at node 2, then u_2 and θ_2 for the loads P_2 and M_2 are

$$\begin{Bmatrix} u_2 \\ \theta_2 \end{Bmatrix} = \begin{bmatrix} \dfrac{L^3}{3EI} + \dfrac{L}{GA_s} + \dfrac{1}{K_c} + A & -\left(\dfrac{L^2}{2EI} + B\right) \\ -\left(\dfrac{L^2}{2EI} + B\right) & \dfrac{L}{EI} + C \end{bmatrix} \begin{Bmatrix} P_2 \\ M_2 \end{Bmatrix} \tag{5.8}$$

After inversion (5.8) becomes

$$\begin{Bmatrix} P_2 \\ M_2 \end{Bmatrix} = \frac{1}{\det} \begin{bmatrix} \dfrac{L}{EI} + C & \dfrac{L^2}{2EI} + B \\ \dfrac{L^2}{2EI} + B & \dfrac{L^3}{3EI} + \dfrac{L}{GA_s} + \dfrac{1}{K_c} + A \end{bmatrix} \begin{Bmatrix} u_2 \\ \theta_2 \end{Bmatrix} \tag{5.9}$$

$$\begin{Bmatrix} P_2 \\ M_2 \end{Bmatrix} = \begin{bmatrix} K_{22} \end{bmatrix} \begin{Bmatrix} u_2 \\ \theta_2 \end{Bmatrix} \qquad (5.10)$$

$$\begin{Bmatrix} P_1 \\ M_1 \end{Bmatrix} = \begin{bmatrix} K_{12} \end{bmatrix} \begin{Bmatrix} u_2 \\ \theta_2 \end{Bmatrix} \qquad (5.11)$$

From the reciprocal law we have that

$$\begin{bmatrix} K_{12} \end{bmatrix} = \begin{bmatrix} K_{21} \end{bmatrix}^T \qquad (5.12)$$

The complete cracked beam element stiffness matrix for N equally spaced cracks is given in Table 5.1. Formulas for A, B, C and det are also given for N equally spaced cracks in the beam element.

The crack stiffness K_c is obtained from the hysteresis loops in Figure 5.6. The slopes of these lines are in units of ksi/in. The values must be multiplied by the shear area of A/2 (as was concluded in Chapter 2) to obtain the crack stiffness K_c. The factor of N/K_c (in Table 5.1) will be changing during the seismic analysis as the shear stress at the cracks traverses the hysteresis loops. Some method must be devised of keeping track of where each crack is on its respective loop. This is discussed in the following section.

5.3 Nonlinear Seismic Analysis

A program has been written to perform seismic analysis incorporating the effects of circumferential cracking. This program, which is named

SAC (Seismic Analysis including Cracks, see Appendix) uses numerical integration rather than the method of normal modes used by MODAL. Since the cracks are to be included the overall stiffness of the vessel is no longer constant but is a function of the shearing stresses in the vessel. Because of this direct numerical integration of the equations of motion (3.1) is performed. The mass [M] and damping [C] matrices have been described in Chapter 4. The element stiffness matrix shown in Table 5.1 is used in the manner shown in Table 4.2 to obtain the global stiffness [K]. Equations (3.1) are solved iteratively using the Newmark β method. The convergence criterion for ending the iterations is

$$(\Delta u_{t_{i+1}} - \Delta u_{t_i})/\Delta u_{t_i} \leq TOL \qquad (5.13)$$

with Δu_{t_i} being the change in relative displacement from time t to time $(t + \Delta t)$ for the ith iteration and $\Delta u_{t_{i+1}}$ the same quantity for the i + 1 iteration. TOL is the convergence criterion which should be .001 or less for reasonable accuracy. The size of the time step, Δt, is critical as far as obtaining accuracy and rapid iteration convergence. It was found during test runs that did not include crack flexibilities that the maximum time step where convergence could be achieved was .0025 seconds. This time step will be used throughout this chapter also.

Stiffness changes will occur during some time steps. This is obvious when one sees the nonlinear stiffness idealization of the cracks shown in Figure 5.4. The SAC subroutine INHYST keeps track of where each crack is on the hysteresis loops of Figure 5.6 and makes changes in the crack stiffness when necessary. A time step is repeated only when the stiffness change from line 2-3 to line 3-4 or from line 5-6 to line 6-1 occurs (see

Figure 5.5). This is because the high velocities which occur during the unloading from lines 2-3 and 5-6 can cause the crack slip to go far below the specified slips at points 3 and 6, which causes the loop to grow much wider than originally specified. The iteration scheme designed to prevent this is shown in Figure 5.5. At time t, one of the cracks is at the position marked on line 2-3 of the hysteresis loop. At time $(t + \Delta t)$, point 3 has been missed by a significant amount. The program SAC goes back to time t, refines the time step Δt to $\Delta t'$ (according to simple linear interpolation) and computes the shear stress and crack displacement at $(t + \Delta t')$. If the shear stress is not within a specified limit $(\pm .05$ shear$_3)$ of shear$_3$, then another iteration using a smaller time step $\Delta t''$ is performed. This process continues until the specified limits are met. The same procedure is used for the stiffness change between lines 5-6 (and all lines parallel to it) and for the change between lines parallel to 2-3 and 3-4.

The changing of hysteresis loops due to cycling is shown in Figure 5.6. All cracks start on the cycle 1 line. Once the shear stress of 30 psi is exceeded and unloading starts the unloading proceeds along a line parallel to line 2-3 (as shown by dashed line A-B). The 2nd cycle loop is reached when A-B intersects line 3-4. From there on the cycles are defined in the following manner: a cycle occurs when the shear stress across a crack unloads from a stress of at least $\pm$ 100 psi to a stress of less than $\pm$ 50 psi.

The lines which make up all the hysteresis loops have the same slopes. The only difference between these loops is that the points 1 and 4 move further away from the origin at a uniform rate as cycling proceeds. This is confirmed by the test data described previously which showed that the

maximum slip in each cycle increased at a fairly uniform rate (.0001 in/ cycle). The method of changing from the 2nd cycle loop to the 3rd cycle loop is shown in Figure 5.8. The shear at a crack on the 2nd cycle loop has increased to above 100 psi. Unloading occurs along the dashed line and goes below 50 psi. Since this means that the 3rd cycle has now been reached the unloading continues along line 3'-4' of the 3rd cycle loop instead of 3-4 of the 2nd loop. These unloading paths have not yet been verified completely by testing but they seem to be a rational way of explaining a complex phenomenon and are the most convenient manner of including the effects of cycling in the program.

5.4 Input to Linear and Nonlinear Analyses

The earthquake to be used as ground motion is specified as a time history of ground accelerations which correspond to the horizontal design response spectrum from NRC provision 1.60 shown in Figure 1.3. A deterministic method described in [12] used a "spectrum-suppressing" technique to develop a ground motion time history which corresponds to this spectrum. This method is used to generate a base motion time history which has a maximum ground acceleration of .4 g (typical for an SSE) and a duration of 11.5 seconds.

Computer Run 1 makes use of the linear model described in Chapter 3. The member properties and lumped masses are given in Figure 3.2. The element and global stiffness matrices are given in Tables 3.1 and 4.1. The mass matrix is given in Table 5.6. The soil springs used are those given for the medium stiffness soils shown in Table 4.2. The damping

matrix is found using the method described in Chapter 4 with the critical damping percentages recommended there. Note that no cracks at all are assumed in the containment vessel and that the concrete is assumed to remain elastic throughout the earthquake. The linear seismic analysis program MODAL is used to perform the analysis.

Runs 2 - 4, made with the SAC nonlinear analysis program, included the effects of the cracks shown in Figure 1.2. This figure shows the cracking pattern of a containment vessel which has been internally pressurized for test purposes. Large horizontal cracks (about .015 inches wide) occurred at the construction joints, which were spaced at 5'-6" in this vessel. Between these joints smaller cracks occurred which did not run completely around the vessel. At the construction joints the moment of inertia is I_c, as was described in section 5.3. In between the joints small cracks do exist so it would be incorrect to use the moment of inertia of the full section there. Since the cracks do not extend to the neutral axis the fully cracked moment of inertia is also not correct. The moment of inertia I will then be taken as the average of the full section moment and the cracked section moment. The member properties for these three runs are given in Table 5.4. The element and global stiffness matrices are given in Tables 5.1 and 4.2, respectively. The mass and damping matrices are the same as for Run 1. The crack spacing is the 5'-6" shown in Figure 1.2. The only parameters to be varied in Runs 2 - 4 are the soil spring stiffnesses. Run 2 uses the K_u and K_ϕ given for medium stiffness soils in Table 4.2. Run 3 corresponds to soft soils and Run 4 uses the hard soil values. The medium soil stiffness of Run 2 is the most likely soil to be encountered in practice so the results of this run have the most importance for design considerations. Table 5.5 summarizes the

soil types and crack spacings used for each computer run.

5.5 Discussion of Results

The displacement time histories for the top (mass 1) and bottom masses (mass 5) are shown for Runs 1 - 4 in Figures 5.9 - 5.12. Figures 5.9 and 5.10 show the results for the uncracked containment founded on a soil of medium stiffness (Run 1) and for the cracked containment vessel founded on a medium soil (Run 2), respectively. These figures show the effects of including the cracks in the seismic analysis of a containment vessel. The maximum response for both runs occurs in the interval between t = 10.15 and t = 10.5. The most obvious difference is that both the maximum positive and negative displacement peaks are greater for Run 2. This is to be expected since the inclusion of the cracks creates a more flexible model. The difference in maximum peaks is not great; the ratio of peaks for Run 1 to Run 2 being about .85. This increase in flexibility is also apparent in the period of oscillation. In both runs a positive peak occurred at t = 10.15. For Run 1 the next positive peak occurs at t = 10.46 for a period of .31 seconds. For Run 2 the next positive peak occurs at t = 10.53 for a period of .38 seconds. These periods are about the same for both runs for the large oscillations which occur between t = 8.9 and t = 9.3. This lengthening of period can once again be explained by the inclusion of crack flexibility. The maximum values for displacement (of mass 1, the top mass) shear and crack slip are given in Table 5.2 for Runs 1 - 4. The difference in maximum shear stress is negligible for Runs 1 and 2. However, Table 5.2 points out that the linear analysis

gives no values for crack slip, an important design parameter which will be discussed later in this section.

Figures 5.9 and 5.10 show that significant differences exist in the displacement time histories for the uncracked and cracked seismic analyses. The displacement or acceleration time histories are of particular importance in seismic analysis of equipment which is supported by the containment vessel. Normally this equipment is not included in the analysis of the containment. If the equipment were included the results would probably be unreliable because of the large difference in mass between the containment and the equipment. Because of this the containment and the equipment are analyzed separately and the results from the containment analysis are used as input for seismic analysis of the equipment. In Figure 1.1 it is shown that a crane is supported by a concrete floor which frames into the containment wall. Certainly the motion of the top of this crane would be of importance in design. Because of the differences in maximum response and oscillation period, it may be necessary to use the results of the nonlinear analyses as input for seismic analysis of equipment. Figures 5.11 and 5.12 show the displacement time histories for Run 3 (cracked vessel with soft underlying soil) and Run 4 (cracked vessel with hard underlying soil), respectively. Figure 5.11 shows that soft underlying soil increases the maximum displacement by a factor of 2.565/1.543 = 1.67 and increases the period of oscillation over the maximum response interval from .38 to .55 seconds. Figure 5.12 shows that a hard underlying soil decreases the maximum displacement by a factor of 1.2/1.543 = .78. The oscillation period decreases from .38 to .32. The softening and hardening of the soils therefore produces the expected changes in response. This is also borne out by the maximum values given in Table 5.2. While the

hardening of the soil in Run 4 produced only a small increase in shear stress (which would be expected in a stiffer system) the softening of the soil produces an extremely large decrease in maximum shear stress of 54%. The maximum crack slip increases with maximum shear stress, as expected.

The maximum number of cycles (using the cycle definition of section 5.3) naturally increases with increasing soil stiffness. It should be noted that the number of cycles obtained is not equal to the duration of the earthquake divided by the oscillation period. A different cycle definition may have caused this to come about. Certainly the higher the number of cycles and maximum shear stress the greater is the chance of concrete failure by dowel splitting. In section 5.2 it was stated that the IST test specimen failed by dowel splitting during the 42nd cycle of loading. However, the loading schedule was more severe than could be expected during an SSE design earthquake. Most of these cycles were complete reversal cycles from shear stresses of greater than 200 psi to less than -200 psi. Certainly this is much more severe than the criterion of a decrease from at least 100 psi to less than 50 psi. The maximum shear stress of 280 psi was reached only once during the earthquake. Because of this it is felt that dowel splitting will probably not occur. The only reservation comes from the fact that the tests were performed on #14 bars instead of the #18 bars normally used in containment vessels. #18 bars unquestionably would pose a more critical dowel splitting problem, but how severe this problem is cannot be estimated without further testing.

Figures 5.13 - 5.15 show hysteresis loops for the bottom beam segment which models the bottom 180 inches of the containment (see Figure 4.3) for Runs 2 - 4. These loops were drawn for the period where the maximum shear stress for each run was obtained. These figures show that some error

exists in making the stiffness change from lines 6-1 and 3-4 to lines 1-2 and 4-5. In Figure 5.13 the loop shown is for the 15th cycle. This means that the crack slip at the stiffness break point should be $(15 - 2) \times .0001 + 2.67 \times 10^{-3} = 3.97 \times 10^{-3}$ inches. The shear stress at this stiffness break should always be 30 psi. At time $t = 10.42$ the shear stress is 38 psi and the crack slip is 5.5×10^{-3} inches. It would be possible to reduce these errors by repeating the previous time step with a smaller step size but it was not felt that these errors were critical enough to justify this procedure. The main effect of these errors may be to increase the maximum crack slip of 13.6×10^{-3} inches slightly from the value that would be obtained if the time step were repeated. However, the difference is likely to be very small and also would be on the conservative side.

Figure 5.13 also shows one of the main effects of cycling, which is the narrowing of the hysteresis loop at low slips. The line followed by the cracks from $t = 10.61$ to $t = 10.63$ slightly higher up and parallel to the line followed from $t = 10.17$ to $t = 10.22$. This is the same behavior as shown in Figure 5.6. Figure 5.14 shows an example of somewhat surprising behavior. Unloading occurred from $t = 10.36$ to $t = 10.43$ along the 7th cycle hysteresis loop. However, reloading occurred at $t = 10.43$ before the expected 6-1 line (dashed line) for the 7th cycle was reached. Reloading occurred along a line parallel to 6-1 because the shear stress was less than 30 psi. The effect of this was to cause a stiffness change at $t = 10.58$ at a crack slip of 5.25×10^{-3} inches rather than 3.17×10^{-3} inches. Since test results did not look into a change of loading like this it is hard to say if this is an inadequacy of the model. Clearly this may cause crack slips to be larger than they should be, but since the maximum slips in Table 5.2 are not unexpectedly large this is probably not

a critical problem.

Table 5.3 shows the maximum seismic bending stresses which occurred in Runs 1 - 4. The concrete stress occurs in the concrete between the construction joints. The moment of inertia for the concrete is I (see Table 5.4). The maximum concrete seismic bending stress is .696 ksi in Run 4. The steel stress shown in Table 5.3 occurs in the reinforcing bars at the horizontal cracks located at the construction joints. The moment of inertia here is I_c (see Table 5.4). The longitudinal tensile stresses due to an internal pressurization of 50 psi are $pR_c/2t_c$ = .388 ksi. Including dead weight (.165 ksi) but not including the effects of vertical ground accelerations, the maximum total concrete compression stress in the longitudinal direction is .696 - .388 + .165 = .473 ksi, which is less than the concrete allowable of .6 f_c (see section 1.3). The maximum longitudinal tensile stress is .696 + .388 - .165 = .919 ksi. The tensile stress in the circumferential direction is pR_c/t_c = .776 ksi. The maximum seismic shear stress is .280 ksi.

The seismic shear stress may cause additional cracking in the vessel. At ϕ = -45° (Figure 2.7) the longitudinal stresses are tensile. The principal tensile stress at ϕ = -45° is .95 ksi inclined at 40° from the horizontal. This means that new crack planes inclined at 40° from the vertical may be created by the earthquake. It should be noted that this angle of inclination will change around the circumference of the vessel as the shear stress and longitudinal bending stress change. These new cracks may have some effect on the seismic response of the vessel but at this time it is not known how significant this effect may be.

Using ρ = .0185 (the typical longitudinal reinforcement ratio for concrete containment vessels) equation (1.2b) gives v_c = .140 ksi.

According to the ASME code [14] the excess shear stress of .140 ksi (.280 - .140) must be carried by inclined steel. As explained previously in this section, it is felt that the recent IST tests performed at Cornell [2] show that the combination of IST plus dowel action can effectively transfer .280 ksi across the cracks without including inclined reinforcement.

If two layers of #18 reinforcing bars are spaced at 8 inches (1.0 $in^2/$ in) around the circumference of the vessel then the stress in each rebar due to internal pressurization would be

$$\frac{\pi R_c^2 p}{2\pi R_c} = \frac{pR_c}{2} = 20.9 \text{ ksi.}$$

Adding this to the maximum siesmic bending stress of 29.2 ksi and subtracting 8.9 ksi (dead weight) the total rebar stress is 41.2 ksi. Since 60 ksi steel is normally used in containments this is less than .9 f_y. However, if the shear and bending stresses in the rebar due to dowel action are included, the yield point may be reached. Presently it is not possible to estimate what these additional stresses are. This yielding would only occur over the unbonded length of the rebar.

The changes in crack width (shown in Table 5.3) due to the seismic bending stresses are all small compared to the initial crack width of .015 inches. These changes were computed over the unbonded bar length of 2.5 inches. If the change of crack width had been at least half as large as the initial crack width, then it could have been argued that the crack stiffness changes during the seismic analysis, since it has been shown that crack stiffness is a function of crack width. However, this was not the case so the change in crack width does not affect the analysis.

In the Introduction it was stated that the steel liner and its anchors

must be able to withstand the deformations imposed upon it by the concrete. The maximum deformation imposed on the liner is the sum of the maximum crack slip shown in Table 5.2 and the elastic shear deformation in the concrete between the construction joints. The maximum crack slip is .0143 inches in Run 4. The maximum shear stress of 280 psi also occurs in this run. The elastic shear strain in the concrete is approximately

$$\frac{.280}{1540} = .000182.$$

If the anchors are spaced at 20 inches, the elastic shear deformation over this distance is

$$.000182 \times 20 = .00364 \text{ inches.}$$

The maximum relative displacement which occurs between the anchors is then

$$.0143 + .00364 = .01794 \text{ inches.}$$

This value is far below the allowable .1 inch used as a design requirement. Since the liner is attached to the concrete the liner strain is assumed to be compatible with the concrete strain. If the liner steel modulus is 29000 ksi then

$$\varepsilon_c = .473/29000 = 1.63 \times 10^{-5} < .002$$

$$\varepsilon_t = (.388 + .696 - .165)/29000 = 3.17 \times 10^{-5} < .001$$

where ε_c and ε_t are the maximum compressive and tensile strains in the liner. These values are far below the ASME allowables of .002 and .001 (see Introduction).

From the stresses shown in Tables 5.2 and 5.3 it would appear that flexible soils are the optimum soils for the foundation of nuclear containment vessels. This would be an incorrect conclusion. Besides the much larger displacements that occur, it would be doubtful that a soft soil such as clay or silty clays with sand could undergo the stresses imposed upon it by the foundation and a soil failure would be likely. However, the strength of the underlying soils undergoing dynamic stresses and strains is an extremely difficult problem which will not be studied here.

5.6 System Identification

The dynamic response of a single degree of freedom structural system can be described by the following single degree of freedom system:

$$\ddot{x} + a_1 x + a_2 \dot{x} = p(t). \tag{5.14}$$

Here x is the displacement of the single degree of freedom and p(t) is the forcing function. The coefficients a_1 and a_2 represent the stiffness and damping properties of the system. The system identification problem is normally concerned with determining these properties so that the above mathematical model will yield results which are in best possible agreement with experimental data derived from the testing of a prototype structural system. Formulated in this manner, the identification problem reduces to

a best-fit problem. Here the parameters a_1 and a_2 will be determined so that (5.14) will yield results that give the best possible agreement with the results from the nonlinear analyses discussed in the previous section. This can be done by using the direct method [13] of system identification. In this method it is assumed that $x(t)$, $\dot{x}(t)$ and $\ddot{x}(t)$ are known from the nonlinear analysis at N discrete points over the time interval $t = 0$ to $t = T$. To obtain the "best fit" values for a_1 and a_2, the quadratic functional

$$J(a) = \sum_{i=1}^{N} (\ddot{x}_i + a_1 x_i + a_2 \dot{x}_i - p_i)^2 \tag{5.15}$$

is minimized. Clearly (5.15) corresponds to a least squares curve fit. p_i is the inertial force due to the base accelerations of the earthquake. Minimizing (5.15) gives the following:

$$\frac{\partial J(a)}{\partial a_1} = 2x_i \ddot{x}_i + 2a_1 x_i^2 + 2a_2 x_i \dot{x}_i - 2x_i p_i = 0 \tag{5.16a}$$

$$\frac{\partial J(a)}{\partial a_2} = 2\dot{x}_i \ddot{x}_i + 2a_1 x_i \dot{x}_i + 2a_2 \dot{x}_i^2 - 2\dot{x}_i p_i = 0. \tag{5.16b}$$

Summing (5.16a) and (5.16b) over the N time points gives

$$a_1 \sum_{i=1}^{N} x_i^2 + a_2 \sum_{i=1}^{N} x_i \dot{x}_i = \sum_{i=1}^{N} (x_i p_i - x_i \ddot{x}_i) \tag{5.17a}$$

$$a_1 \sum_{i=1}^{N} x_i \dot{x}_i + a_2 \sum_{i=1}^{N} \dot{x}_i^2 = \sum_{i=1}^{N} (\dot{x}_i p_i - \dot{x}_i \ddot{x}_i). \tag{5.17b}$$

Using Cramer's rule,

$$a_1 = \frac{1}{det} \ (D1 \times C22 - D2 \times C12) \tag{5.18a}$$

$$a_2 = \frac{1}{det} \ (C11 \times D2 - D1 \times C12) \tag{5.18b}$$

$$C11 = \sum_{i=1}^{N} x_i^2 \qquad\qquad D1 = \sum_{i=1}^{N} (x_i p_i - x_i \ddot{x}_i)$$

$$C12 = \sum_{i=1}^{N} x_i \dot{x}_i \qquad\qquad D2 = \sum_{i=1}^{N} (\dot{x}_i p_i - \dot{x}_i \ddot{x}_i)$$

$$C22 = \sum_{i=1}^{N} \dot{x}_i^2 \qquad\qquad det = C11 \times C22 - C12^2$$

Therefore for a single degree of freedom system there exists a closed form solution (5.18) for the parameters a_1 and a_2. In the nonlinear analysis performed in this chapter there are a total of 12 degrees of freedom. Modal analysis will be used to uncouple the 12 simultaneous equations of dynamic equilibrium. Then separate values of a_1 and a_2 may be computed for each mode, with each modal equation (3.14) corresponding to (5.14). If the displacements, velocities and accelerations for each time step from the nonlinear analysis are stored in the vectors $\lfloor u \rfloor$, $\lfloor \dot{u} \rfloor$ and $\lfloor \ddot{u} \rfloor$, the transformation to the generalized coordinate $\lfloor q \rfloor$ is accomplished in the following manner (see [3.12b]):

$$\{q\} = [A]^{-1} \{u\} \tag{5.19a}$$

$$\{\dot{q}\} = [A]^{-1} \{\dot{u}\} \tag{5.19b}$$

$$\{\ddot{q}\} = [A]^{-1} \{\ddot{u}\} \tag{5.19c}$$

Comparing (3.4) and (5.4),

$$a_{1K} = \omega_K^{\ 2} \qquad\qquad (5.20a)$$

$$a_{2K} = 2 \beta_K \omega_K \qquad\qquad (5.20b)$$

for the Kth mode.

The above procedure for determining the parameters a_1 and a_2 was carried out during Run 2 (medium soil stiffness). This particular run was chosen because the values used for the two soil springs represent the soil stiffness most likely to be encountered at power plant sites. The values obtained for a_1 and a_2 for the first three modes are shown in Table 5.7. These values were then used as input for MODAL. The results for the displacement of the top mass using only the first mode are shown by the dashed line in Figure 5.10. The results obtained using the first two modes were almost the same. However, when three modes were included in the analysis, the displacements became extremely large. This is probably because the third mode participates very little in the motion of the model and because of this the system identification method computes a stiffness parameter a_1 which is very low. It would be expected that a_1 for the third mode would be significantly higher than a_1 for the two lower modes, but Table 5.5 shows otherwise. Because of this low stiffness in mode three the corresponding modal equation makes bogus contributions which yield ridiculously large displacements. It appears then that using the first mode only is the most effective way of using this particular application of system identification. As shown in Figure 5.10, the displacement time history yielded by the first mode gives a very good approximation to

the nonlinear analysis. The maximum shear stress (282 psi) is also reasonably close to the value obtained by the nonlinear analysis (272 psi). It is therefore concluded that the system identification using the first mode only gives satisfactory results for both displacement time histories and maximum stresses and displacements. If a_1 and a_2 for the first mode are divided by ω_1^2 and $2\beta_1\omega_1$ it is found that

$$\overline{a}_1 = a_1/\omega_1^2 = .667 \tag{5.21a}$$

$$\overline{a}_2 = a_2/2\beta_1\omega_1 = 1.493. \tag{5.21b}$$

$\overline{a}_1$ shows the effect of including the cracks in the analysis. For an uncracked vessel $\overline{a}_1 = 1.0$. Clearly $\overline{a}_1 = 1.0$ shows that the cracks increase the flexibility of the model. In the same way $\overline{a}_2$ takes into account the effects of the hysteretic behavior of the cracks by increasing the viscous damping coefficient. With no hysteretic behavior $\overline{a}_2 = 1.0$. It would probably be incorrect to generalize these results for all base acceleration time histories. By this it is meant that a different synthetic earthquake may very well produce different values for $\overline{a}_1$ and $\overline{a}_2$. Further work must be done using different base acceleration histories and different soil stiffness before (5.21a) and (5.21b) could be recommended for use in design.

Chapter 6

CONCLUSIONS

The main conclusions of this study are:

1. The presence of cracks in the concrete does not significantly affect the shear stress distribution in a reinforced concrete containment vessel during and earthquake. The distribution is essentially the same sinusoidal distribution which exists in elastic thin-walled cylinders. Because of this, the shear area of A/2 normally associated with elastic uncracked analysis is used in the nonlinear analysis in stiffness formulations and for determining maximum shear stress.

2. In linear seismic analysis rotational degrees of freedom must be included to obtain accurate displacement time histories. This must also be true for nonlinear analysis. Therefore, rotational degrees of freedom were included in all analyses.

3. There is a significant difference in the displacement time histories obtained by linear (uncracked) and nonlinear (cracked) siesmic analysis. The maximum shear stresses obtained by the two methods are quite close. The effect of soil-structure interaction can be quite substantial. As the soils which underly the containment become softer the maximum stresses in the vessel will decrease significantly but maximum displacement increase by a large degree.

4. The system identification method provides a good linear approxi-

mation to the nonlinear analysis. The resultant displacement time history gives sufficiently accurate results to be used as input for seismic analysis of equipment. However, some important design parameters such as maximum crack slip connot be provided by a linear analysis.

5. The liner distortions and strains which result from the nonlinear analysis are within allowable values. The stresses in the concrete containment are either less than the allowables given by ASME or are less than the stresses which caused failure in the IST tests. The biaxial tension field which exists in the containment vessel may give dowel splitting failures at lower shear stresses than in the uniaxial IST tests that were described here. However, the combined mechanism of IST and dowel action appears capable of replacing the inclined bars presently used to transfer shearing forces down to the foundation mat.

It is felt that adequate analytical tools exist for seismic analysis of cracked containment vessels. More experimental work is needed to investigate the combined behavior of IST and dowel action, particularly for the larger #18 bars used in containment vessel construction. It would also be interesting to see the effects of cycling at low stresses in the range of 50 psi rather than the 200 psi actually used in the tests so far. During an earthquake shear as high as 200 psi occur very rarely while 50 psi is quite common. The loading schedule used in past IST tests has been too regular. The results of seismic analyses show that shear stress loadings in the containment are very irregular and may change directions at unexpected places in the hysteresis loop which represents the load-slip behavior of the cracks. Current IST tests underway include specimens with cracks which run in both the horizontal and vertical directions and are pretensioned in both directions to simulate biaxial tension. Input from

these tests could be used in the nonlinear analysis program developed in this study to give an improved model of the containment vessel.

REFERENCES

1.   White, R. N., Gergely, P., Laible, J. P., and Fajardo, O. A., "Seismic Shear Transfer Across Cracks in Concrete Nuclear Reactor Containment Vessels," Proc. Fifth World Conf. On Earthquake Engineering, Rome, 1973.

2.   Jimenez, R., Perdikaris, P., Gergely, P. and White, R. N., "Interface Shear Transfer and Dowel Action in Cracked Reinforced Concrete Subject to Cyclic Shear," Methods of Structural Analysis, V. 1, pps. 457-475, Proc. of the National Structural Engineering Conf., ASCE, University of Wisconsin, 1976.

3.   Bathe, K., Wilson, E. L., and Peterson, F. E., "SAP IV - A Structural Analysis Program for Static and Dynamic Response of Linear Systems," Dept. of Civil Engineering, University of California, Berkeley, 1974.

4.   Clough, R. W. and Felippa, C. A., "A Refined Quadrilateral Element for Analysis of Plate Bending," Proc. of the Second Conf. on Matrix Methods in Structural Mechanics, Wright-Patterson Air Force Base, Ohio, October, 1968.

5.   Kolsky, H., Stress Waves In Solids, Dover Publications, New York, 1963.

6.   Love, A. E. H., <u>Some Problems of Geodynamics</u>, University Press, Cambridge, 1911.

7.   Richart, F. E., Hall, J. P. and Woods, R. P., <u>Vibrations of Soils and Foundations</u>, Prentice Hall Inc., Englewood Cliffs, New Jersey, 1970.

8.   Hansen, R. J., <u>Seismic Design for Nuclear Power Plants</u>, M.I.T. Press, Cambridge, Mass., 1970.

9.   Whitman, R. V., Christian, J. T. and Bigg, J., "Parametric Analysis of Soil - Structure Interaction for a Reactor Building," <u>Proc. of the First Int. Conf. of Structural Mech. in Reactor Technology</u>, V. 5, pps. 257-259, Berlin, 1971.

10.   Chiu, K. D. and Kuo, H. J., "Modal Damping in Dynamic Analysis of Structures," <u>Structural Design of Nuclear Plant Facilities</u>, V. 2, pps. 499-514, ASCE, New York, 1973.

11.   Clough, R. W. and Penzien, J., <u>Dynamics of Structures</u>, McGraw-Hill, New York, 1975.

12.   Tsai, N., "Spectrum-Compatible Motions for Design Purposes," pps. 345-355, <u>Journal of the Engineering Mechanics Division</u>, ASCE, EM2, April, 1972.

13.   DiStefano, N. and Rath, L., "Modeling and Identification in

Nonlinear Structural Dynamics - 1. One Degree of Freedom Models,"
EERC, Univ. of California, Berkeley, 1974.

14.   ASME Boiler and Pressure Vessel Code, Section III, Division 2,
ACI 359-74, ASME Boiler and Pressure Vessel Committee, ASME, New York,
1975.

15.   Laible, J. P. and Gergeley, P., "Nonlinear Dynamic Analysis of
Cracked Reinforced Concrete Nuclear Containment Structures," Nuclear
Design and Engineering, 30, September, 1974.

LIST OF SYMBOLS

A   Cross-sectional area

A_s Shear area

[A]   Matrix containing the eigenvectors

[C]   Damping matrix

D_u Translational critical soil damping ratio

D_ϕ Rotational critical soil damping ratio

E   Young's modulus

f_c' Compressive strength of concrete

f_y Yield strength of reinforcing bars

G   Shear modulus

I   Moment of inertia

I_c Cracked moment of inertia

K_c Crack stiffness

K_u Translational soil spring

K_ϕ Rotational soil spring

[K]   Global stiffness matrix

L   Length of beam segment

[M]   Lumped mass matrix

p   Internal pressure caused by loss of coolant accident

q_i Generalized coordinate for i^{th} mode

R_c Radius of the containment vessel cylinder

SSE   Safe Shutdown Earthquake

t   Time during seismic analysis

t_c Thickness of containment vessel cylindrical wall

$\lfloor u \rfloor^T$ Vector of relative displacements

$\lfloor \dot{u} \rfloor^T$ Vector of relative velocities

$\lfloor \ddot{u} \rfloor^T$ Vector of relative accelerations

v_c Maximum tangential shear stress which may be carried by concret according to existing codes

v_u Design tangential shear stress

V Total shear force at a cross-section

β_i Critical damping ratio for the ith mode

ρ Steel reinforcement ratio

ϕ Angle that meridional plane makes with x-axis in a cylinder (see Figure 2.7)

ω_i Natural frequency for the ith mode

Δ Crack slip

τ Shear stress

μ Poisson's ratio

λ Shear flexibility factor

λ_L Lame's constant

APPENDIX A

1. Description of the Computer Program MODAL

This program computes the response of a linear structure subjected to base accelerations which model an earthquake. The structure is idealized as a vertical cantilever shear beam with the mass lumped at the node points (lumped mass model). Soil-structure interaction may be included. When soil-structure interaction is included effective damping ratios for each mode are calculated using the subregioned energy proportion method. The natural frequencies and mode shapes are calculated using the Jacobi method. The uncoupled modal equations are integrated using the linear acceleration method.

2. Input to MODAL

The input for a sample problem will be given. The model to be input is the model of the reinforced concrete containment vessel shown in Figure 4.3. Soil-structure interaction will be included. The soil springs K_u and K_ϕ have the values 100,000 K/in and 10×10^{10} k-in, respectively. The shear area and moment of inertia for all beam segments are 150,000 in^2 and 9×10^{10} in, respectively. The shear area is taken as A/2, where A is the cross-sectional area. The lumped masses are $m_1 = 30$ K-sec^2/in, $m_2 = m_3 = m_4 = m_5 = 25$ K-sec^2/in and $m_f = 60$ K-sec^2/in. The lumped mass moments of inertia are $I_1 = I_2 = I_3 = I_4 = I_5 = 8 \times 10^6$ K-sec^2-in and $I_f = 13 \times 10^6$ K-sec^2-in. The material properties are G (shear modulus) = 1500 ksi and E (Young's modulus) = 3000 ksi. The modal damping ratio for

all modes of vibration of the concrete containment is .05. The modal damping ratios for the soil in the translational and rotational directions are .25 and .05, respectively. The test earthquake shown in Figure 3.4 will be used as the base accelerations. The IBM cards (with FORTRAM format) to be input after the *DATA card follow. The units are kips, inches and seconds. The maximum number of degrees of freedom is 12.

CARD 1   (5I5, F10.0)

      cols 1-5:   12 (total number of degrees of freedom)

      cols 6-10:   3 (number of modes to be included in the analysis)

      cols 11-15: 12 (number of time steps in the analysis)

      cols 16-20: 10 (number of base acceleration time points)

      cols 21-25: 3 (number of Jacobi iterations, the suggested

                   number is 3)

      cols 26-35: .01 (recommended length of time step in seconds)

CARD 2   (8F10.0)

      cols 1-10:   30. (m_1)

      cols 11-20: 8.0E06 (I_1)

      cols 21-30: 25. (m_2)

      cols 31-40: 8.0E06 (I_2)

      cols 41-50: 25. (m_3)

      cols 51-60: 8.0E06 (I_3)

      cols 61-70: 25. (m_4)

      cols 71-80: 8.0E06 (I_4)

CARD 3   (4F10.0)

    cols 1-10:   25. (m_5)

    cols 11-20: 8.0E06 (I_5)

    cols 21-30: 60. (m_f)

    cols 31-40: 13.0E06 (I_f)

CARD 4   (2F10.0, I5, 2F10.0)

    cols 1-10:   1500. (G)

    cols 11-20: 3000. (E)

    cols 21-25: 1 (1 = soil-structure interaction is to be

                  included, 0 = no soil-structure interaction)

    cols 26-35: 10.0E10 (K_ϕ)

    cols 36-45: 100000. (K_u)

CARD 5   (5F10.0)

    cols 1-10:   592.5 (length of top beam segment, see Figure 4.3)

    cols 11-20: 360. (length of 2nd beam segment)

    cols 21-30: 360. (length of 3rd beam segment)

    cols 31-40: 360. (length of 4th beam segment)

    cols 41-50: 180. (length of 5th beam segment)

CARD 6   (5F10.0)

    cols 1-10:   9.0E10 (moment of inertia of top beam segment)

    cols 11-20: 9.0E10 (moment of inertia of 2nd beam segment)

    cols 21-30: 9.0E10 (moment of inertia of 3rd beam segment)

    cols 31-40: 9.0E10 (moment of inertia of 4th beam segment)

    cols 41-50: 9.0E10 (moment of inertia of 5th beam segment)

CARD 7   (5F10.0)

      cols 1-10:   150000. (shear area of top beam segment)

      cols 11-20:   150000. (shear area of 2nd beam segment)

      cols 21-30:   150000. (shear area of 3rd beam segment)

      cols 31-40:   150000. (shear area of 4th beam segment)

      cols 41-50:   150000. (shear area of 5th beam segment)

CARD 8   (3F10.0)

      cols 1-10:   .05 (critical damping ratio for concrete contain-
                            ment vessel)

      cols 11-20:   .25 (critical damping ratio for translational
                            motion in underlying soil; D_u in Figure 4.3)

      cols 21-30:   .05 (critical damping ratio for rotational motion
                            in underlying soil; D_ϕ in Figure 4.3)

CARD 9   (2F10.0)

      cols 1-10:   0. (time in seconds of base acceleration)

      cols 11-20:   .084 (base acceleration, fraction of g acceleration
                            of gravity)

CARD 10   (2F10.0)

      cols 1-10:   .023 (time in seconds of base acceleration)

      cols 11-20:   .158 (base acceleration, fraction of g acceleration
                            of gravity)

CARD 11   (2F10.0)

      cols 1-10:   .058 (time of base acceleration)

cols 11-20:   .271 (base acceleration)

CARD 12   (2F10.0)

cols 1-10:   .083 (time of base acceleration)

cols 11-20:   .349 (base acceleration, fraction of g acceleration

of gravity)

CARD 13   (2F10.0)

cols 1-10:   .113 (time of base acceleration)

cols 11-20:   .446 (base acceleration)

CARD 14   (2F10.0)

cols 1-10:   .149 (time of base acceleration)

cols 11-20:   .509 (base acceleration)

CARD 15   (2F10.0)

cols 1-10:   .186 (time of base acceleration)

cols 11-20:   .382 (base acceleration)

CARD 16   (2F10.0)

cols 1-10:   .23 (time of base acceleration)

cols 11-20:   .191 (base acceleration)

CARD 17   (2F10.0)

cols 1-10:   .256 (time of base acceleration)

cols 11-20:   .058 (base acceleration)

CARD 18   (2F10.0)

    cols 1-10:   .3 (time of base acceleration)

    cols 11-20: 0. (base acceleration)

3.   Output from MODAL

For each time step, the relative translational displacement and inertial force associated with each mass is printed out. The shear stress in each beam segment is also printed out. Previous to this the global stiffness matrix, natural undamped frequencies and eigenvectors are printed.

```
                              *** MODAL ***
C
C
C
C
C       THIS PROGRAM COMPUTES THE EARTHQUAKE RESPONSE OF A LIN
C          EAR
C       STRUCTURE THROUGH THE USE OF THE NORMAL MODES TECHNIQU
C          E.
C       THE MAIN BODY OF THE PROGRAM (WHICH FOLLOWS DIRECTLY)
C       READS IN DATA AND CALLS ALL THE SUBROUTINES. THE SUBRO
C          UTINES
C       ARE NAMED STIFF,JACOBY,RATIO,INQUAK AND LINACC. STIFF
C          SETS UP THE
C       STIFFNESS MATRIX AND JACOBY COMPUTES THE NATURAL FREQU
C          ENCIES
C       AND EIGENVECTORS OF THIS MATRIX. RATIO COMPUTES THE EF
C          FECTIVE
C       CRITICAL DAMPING RATIOS FOR EACH MODE TAKING SOIL-STRU
C          CTURE
C       INTERACTION INTO ACCOUNT.
C       INQUAK READS IN THE EARTHQUAKE ACCELERATION DATA AND C
C          OMPUTES
C       THE CORRESPONDING GENERALIZED FORCE. LINACC NUMERICALL
C          Y
C       INTEGRATES THE EQUATIONS OF MOTION USING THE LINEAR
C       ACCELERATION ASSUMPTION. A MORE IN DEPTH DESCRIPTION I
C          S
C       GIVEN IN THE SUBROUTINES THEMSELVES.
C
        COMMON /DYN/GSTIFF(3),GMASS(3),DAMP(3),EQFOR(12),GFORC
      C E(3),
      1DISP(12),RKFOR(12)
        COMMON /EIG/GLOK(12,12),OMEGA(12),A(12,12),PMASS(12),A
      C TR(12,12)
        COMMON /PROP/AS(5),RIZ(5),SL(5),SIZ(5)
        DIMENSION D(5)
        DIMENSION BETA(5)
        DIMENSION A1(3),A2(3)
C
C
C       N IS THE NUMBER OF DEGREES OF FREEDOM. NM IS THE NUMBE
C          R
C       OF MODES TO BE SUPERIMPOSED. H IS THE TIME STEP AND NH
C          IS THE
C       TOTAL NUMBER OF TIME STEPS IN THE ANALYSIS. NTP IS THE
C       NUMBER OF GROUND ACCELERATION POINTS READ IN SUBROUTIN
C          E
C       INQUAK. RMASS IS THE LUMPED MASS VECTOR,G IS THE SHEAR
C          MODULUS
C       ,AS IS THE SHEAR AREA AND SL IS THE LENGTH OF EACH SHE
C          AR
C       BEAM SEGMENT. IF IROT=1 SOIL STRUCTURE INTERACTION IS
C       INCLUDED. ROTK IS THE ROTATIONAL SOIL SPRING AND TRANS
C          K
C       IS THE TRANSLATIONAL SOIL SPRING. K IS THE NUMBER OF
C       JACOBY ITERATIONS AND BETA IS THE CRITICAL DAMPING RAT
```

```
C          IO.
C      T=TIME OF ANALYSIS.
C
       READ(5,10) N,NM,NH,NTP,K,H
       READ(5,11) (RMASS(I),I=1,8)
       READ(5,11) (RMASS(I),I=9,12)
       READ(5,12) G,E,IROT,ROTK,TRANSK
       READ (5,14) (SL(I),I=1,5)
       READ(5,14) (RIZ(I),I=1,5)
       READ(5,14) (AS(I),I=1,5)
       READ(5,14) BETA,CTRANS,CROT
       NTHETA=1
       T=0.
       ICOUNT=0
       JCOUNT=0
       IFLAG=0
       NS=N
       IF (IROT.EQ.0) GO TO 20
       NS=N-2
   20 CONTINUE
       DO 21 I=1,NM
   21 D(I)=BETA
       CALL STIFF(NS,IROT,ROTK,TRANSK,G,NTHETA,E)
       CALL JACOBY(N,K)
       IF (IROT.EQ.0) GO TO 99
       CALL RATIO(N,BETA,CTRANS,CROT,TRANSK,ROTK)
   99 CONTINUE
       DO 2 I=1,NM
       DAMP(I)=2.*D(I)*OMEGA(I)
       GSTIFF(I)=OMEGA(I)**2
    2 GMASS(I)=1.0D0
       WRITE(6,48) (GSTIFF(I),I=1,NM)
       WRITE(6,48) (DAMP(I),I=1,NM)
   48 FORMAT(/10X,5E14.7)
       DO 4 I=1,NH
       CALL INQUAK(N,T,NTP,ICOUNT,NTHETA,NM,IROT)
       CALL LINACC(N,NM,H,T,JCOUNT)
       T=T+H
    4 CONTINUE
   10 FORMAT(5I5,3F10.0)
   11 FORMAT(8F10.0)
   12 FORMAT(2F10.0,I5,2F10.0)
   13 FORMAT(I5)
   14 FORMAT(5F10.0)
       STOP
       END
       SUBROUTINE INQUAK(N,T,NTP,ICOUNT,NTHETA,NM,IROT)
       COMMON /DYN/GSTIFF(3),GMASS(3),DAMP(3),EQFOR(12),GFORC
     C  E(3),
      1DISP(12),RKFOR(12)
       COMMON /EIG/GLOK(12,12),OMEGA(12),A(12,12),RMASS(12),A
     C  TR(12,12)
       DIMENSION GRACC(20),TIME(20)
C
```

```
C        THIS SUBROUTINE INITIALLY READS IN THE GROUND ACCELERA
C           TION
C        HISTORY AND KEEPS TRACK OF THE CURRENT VALUE. THE GENE
C           RALIZED
C        FORCE WHICH APPEARS ON THE RHS OF THE UNCOUPLED MODAL
C        EQUATIONS IS THE VECTOR GFORCE WHICH IS COMPUTED HERE.
C        GFORCE=-ATR*RMASS*GRACC,WHERE ATR IS THE TRANSPOSE OF
C           THE
C        MODAL MATRIX AND RMASS IS THE LUMPED MASS VECTOR.
C
         IF (ICOUNT.EQ.1) GO TO 3
         ICOUNT=1
         DO 1 I=1,NTP
         READ(5,11) TIME(I),GRACC(I)
       1 CONTINUE
         DO 2 I=1,NTP
         GRACC(I)=386.4*GRACC(I)
       2 CONTINUE
C
C        NOW FIND THE CURRENT VALUE (FOR TIME=T) OF THE GROUND
C        ACCELERATION X.
C
       3 IF (T.GT.TIME(NTP)) GO TO 7
         I=1
       4 I=I+1
         IF (T.GT.TIME(I)) GO TO 4
         IF (T.LT.TIME(I-1)) GO TO 4
         SLOPE=(GRACC(I)-GRACC(I-1))/(TIME(I)-TIME(I-1))
         X=GRACC(I-1)+(T-TIME(I-1))*SLOPE
         N1=N-1
         DO 8 I=1,N1,2
         EQFOR(I)=-RMASS(I)*X
         EQFOR(I+1)=0.
       8 CONTINUE
     101 DO 6 I=1,NM
         GFORCE(I)=0.
         DO 6 J=1,N
         GFORCE(I)=ATR(I,J)*EQFOR(J)+GFORCE(I)
       6 CONTINUE
       7 RETURN
      11 FORMAT(2F10.0)
         END
         SUBROUTINE LINACC(N,NM,H,T,JCOUNT)
         IMPLICIT REAL*4 (M)
         COMMON /DYN/GSTIFF(3),GMASS(3),DAMP(3),EQFOR(12),GFORC
        C E(3),
        1DISP(12),RKFOR(12)
         COMMON /EIG/GLOK(12,12),OMEGA(12),A(12,12),RMASS(12),A
        C TR(12,12)
         COMMON /PROP/AS(5),RIZ(5),SL(5),SIZ(5)
         DIMENSION CFORCE(12),RINFOR(12),DELDSP(3),DELVEL(3),DE
        C LACC(3),
        1MDISP(3),MVEL(3),MACC(3),B(12,12),C(12,12),ACC(12),VEL
        C (12)
```

```
C
C       THIS SUBROUTINE USES THE ASSUMPTION THAT THE ACCELERAT
C          ION
C       VARIES LINEARLY IN EACH TIME STEP TO COMPUTE THE CHANG
C          ES
C       IN VELOCITY AND DISPLACEMENT FOR EACH UNCOUPLED MODAL
C       EQUATION.RMASS AND GLOK ARE THE ACTUAL STRUCTURAL LUMP
C          ED
C       MASS VECTOR AND GLOBAL STIFFNESS MATRIX.THE GENERALIZE
C          D
C       MASS,STIFFNESS AND DAMPING ARE THE GMASS,GSTIFF AND DA
C          MP VECTORS.
C       THE RELATIVE DISPLACEMENTS AT TIME T ARE CONTAINED IN
C          THE
C       DISP VECTOR.
C       MDISP,MVEL AND MACC ARE VECTORS CONTAINING THE DISPLAC
C          EMENTS
C       ,VELOCITY AND ACCELERATION AT TIME T FOR EACH MODAL EQ
C          UATION.
C       RKFOR IS THE VECTOR OF SHEAR FORCES IN EACH STORY.DELD
C          SP,
C       DELVEL AND DELACC ARE VECTORS WHICH CONTAIN THE CHANGE
C           IN
C       DISPLACEMENT,VELOCITY AND ACCELERATION FOR EACH MODE.
C       CFORCE AND RINFOR CONTAIN THE TOTAL DAMPING AND INERTI
C          AL FORCES
C       AT TIME T.EQFOR IS THE INERTIAL FORCE DUE TO THE EARTH
C          QUAKE
C       AND GFORCE IS THIS FORCE GENERALIZED IN THE UNCOUPLED
C       EQUATIONS.
C
C       AT TIME T=0 INITIALIZE DISPLACEMENTS,VELOCITIES AND AC
C          CELERATIONS.
C
        IF (JCOUNT.GT.0) GO TO 300
        JCOUNT=1
        DO 1 I=1,N
        DISP(I)=0.
        RKFOR(I)=0.
        RINFOR(I)=0.
      1 CONTINUE
        DO 71 I=1,NM
        MDISP(I)=0.
        MVEL(I)=0.
        MACC(I)=GFORCE(I)/GMASS(I)
        DELDSP(I)=0.
        DELVEL(I)=0.
        DELACC(I)=0.
     71 CONTINUE
        GO TO 400
C
C       FOR EACH TIME STEP SOLVE FOR DELACC. THEN, USING THE L
C          INEAR
C       ACCELERATION ASSUMPTION, COMPUTE DELVEL AND DELDSP.
```

```
C
300 DO 2 I=1,NM
    DELACC(I)=(GFORCE(I)-MACC(I)-DAMP(I)*(MVEL(I)+H*MACC(I
   C  ))-
   1GSTIFF(I)*(MDISP(I)+MVEL(I)*H+MACC(I)*(H**2/2.0E0)))/(
   C  1.0E0+
   2DAMP(I)*H/2.0E0+GSTIFF(I)*(H**2/6.0E0))
    DELDSP(I)=MVEL(I)*H+(H**2/6.0E0)*(3.0E0*MACC(I)+DELACC
   C  (I))
    DELVEL(I)=(H/2.0E0)*(2.0E0*MACC(I)+DELACC(I))
    MDISP(I)=MDISP(I)+DELDSP(I)
    MVEL(I)=MVEL(I)+DELVEL(I)
    MACC(I)=MACC(I)+DELACC(I)
  2 CONTINUE
C
C    NOW COMPUTE THE TOTAL RELATIVE DISPLACEMENTS (DISP),
C    TOTAL INERTIAL FORCES (RINFOR) AND TOTAL SHEAR FORCES
C    (RKFOR) AND PRINT THESE QUANTITIES OUT.
C    DISP=A*MDISP
C    RINFOR=RMASS*A*OMEGA*MDISP.RKFOR (SHEAR FORCE) IS THE
C    SUM OF ALL INERTIAL FORCES (RINFOR) ABOVE AND INCLUDIN
C     G
C    MASS I.
C
    DO 3 I=1,N
    DISP(I)=0.
    DO 3 J=1,NM
    DISP(I)=A(I,J)*MDISP(J)+DISP(I)
  3 CONTINUE
    DO 4 I=1,N
    DO 4 J=1,NM
    B(I,J)=RMASS(I)*A(I,J)
  4 CONTINUE
    DO 5 I=1,N
    DO 5 J=1,NM
    C(I,J)=B(I,J)*OMEGA(J)**2
  5 CONTINUE
    DO 9 I=1,N
    RINFOR(I)=0.
    DO 9 J=1,NM
    RINFOR(I)=C(I,J)*MDISP(J)+RINFOR(I)
  9 CONTINUE
    DO 6 I=1,5
    RKFOR(I)=0.
    L=2*I-1
    DO 6 J=1,L,2
    RKFOR(I)=RINFOR(J)+RKFOR(I)
  6 CONTINUE
    DO 68 I=1,5
    RKFOR(I)=RKFOR(I)/AS(I)
 68 CONTINUE
400 WRITE(6,10) T
    DO 8 I=1,5
    L=2*I-1
```

```
      WRITE(6,11) DISP(L),RINFOR(L),RKFOR(I)
    8 CONTINUE
   10 FORMAT(/10X,'TIME=',F7.2,' SECONDS',5X,'DISPLACEMENT',
     18X,'INERTIAL FORCE',6X,'SHEAR STRESS'/)
   11 FORMAT(35X,E10.3,10X,E10.3,10X,E10.3)
      RETURN
      END
      SUBROUTINE STIFF(N,IROT,ROTK,TRANSK,G,NTHETA,E)
C
C     THIS SUBROUTINE COMPUTES THE GLOBAL STIFFNESS MATRIX,G
C        LOK.
C     SHEAR AREA AND ROTATIONAL DEGREES OF FREEDOM ARE INCLU
C        DED
C     IN THE VERTICAL CANTILEVER BEAM MODEL.
C
      COMMON /EIG/GLOK(12,12),OMEGA(12),D(12,12),RMASS(12),A
     C TR(12,12)
      COMMON /PROP/AS(5),RIZ(5),SL(5),SIZ(5)
      DIMENSION TK(10),ELK(4,4),VK(12)
      DO 88 I=1,5
      TK(I)=SL(I)/(G*AS(I))
      TK(I)=1./TK(I)
   88 CONTINUE
      NN=N
      N1=N-1
      NN=N
      IF (IROT.EQ.0) GO TO 14
      NN=N+2
   14 DO 13 I=1,NN
      DO 13 J=1,NN
      GLOK(I,J)=0.
   13 CONTINUE
      DO 10 I=1,N1,2
C
C     SET UP THE BEAM ELEMENT STIFFNESS MATRIX,ELK(4,4)
C
      SH=(3.*E*RIZ((I+1)/2)/SL((I+1)/2)**3)/TK((I+1)/2)
      ELK(1,1)=12.*E*RIZ((I+1)/2)/SL((I+1)/2)**3
      ELK(1,2)=-6.*E*RIZ((I+1)/2)/SL((I+1)/2)**2
      ELK(1,3)=-ELK(1,1)
      ELK(1,4)=ELK(1,2)
      ELK(2,2)=4.*E*RIZ((I+1)/2)/SL((I+1)/2)
      ELK(2,2)=ELK(2,2)*(1.+SH)
      ELK(2,3)=-ELK(1,2)
      ELK(2,4)=2.*E*RIZ((I+1)/2)/SL((I+1)/2)
      ELK(2,4)=ELK(2,4)*(1.-2.*SH)
      ELK(3,3)=ELK(1,1)
      ELK(3,4)=-ELK(1,2)
      ELK(4,4)=ELK(2,2)
      DO 3 K=1,4
      DO 3 J=1,K
      ELK(J,K)=ELK(J,K)/(1.+4.*SH)
    3 ELK(K,J)=ELK(J,K)
      GLOK(I,I)=ELK(1,1)+GLOK(I,I)
```

```
      GLOK(I+1,I+1)=ELK(2,2)+GLOK(I+1,I+1)
      GLOK(I+1,I)=ELK(2,1)+GLOK(I+1,I)
      GLOK(I+2,I)=ELK(3,1)
      GLOK(I+3,I)=ELK(4,1)
      GLOK(I+2,I+1)=ELK(3,2)
      GLOK(I+3,I+1)=ELK(4,2)
      GLOK(I+2,I+2)=ELK(3,3)
      GLOK(I+3,I+2)=ELK(4,3)
      GLOK(I+3,I+3)=ELK(4,4)
   10 CONTINUE
      DO 11 I=1,NN
      DO 11 J=1,NN
   11 GLOK(I,J)=GLOK(J,I)
      IF (IROT.EQ.0) GO TO 45
C
C
C     IF IROT=1 THEN SOIL STRUCTURE INTERACTION IS TO BE INC
C        LUDED.
C
      GLOK(NN-1,NN-1)=GLOK(NN-1,NN-1)+TRANSK
      GLOK(NN,NN)=GLOK(NN,NN)+ROTK
   45 RETURN
      END
      SUBROUTINE RATIO(N3,BETA2,CTRANS,CROT,TRANSK,ROTK)
      COMMON /DYN/GSTIFF(3),GMASS(3),DAMP(3),EQFOR(12),GFORC
     C  E(3),
     1DISP(12),RKFOR(12)
      COMMON /EIG/GLOK(12,12),OMEGA(12),A(12,12),RMASS(12),A
     C  TR(12,12)
      COMMON /PROP/ AS(5),RIZ(5),SL(5),SIZ(5)
      DIMENSION V(5),RMOM(5)
      DIMENSION EN(12,12),ET(12),B(12)
C
C
C     THIS SUBROUTINE IS CALLED ONLY IF SOIL STRUCTURE INTER
C        ACTION
C     IS TO BE INCLUDED IN THE ANALYSIS. SINCE THE CRITICAL
C        DAMPING
C     RATIOS IN THE STRUCTURAL AND SOIL DEGREES OF FREEDOM U
C        SUALLY
C     DIFFER BY A LARGE AMOUNT SOME COMMON MODAL DAMPING VAL
C        UES
C     ARE REQUIRED. THE SUBREGIONED ENERGY PROPORTION METHOD
C     IS USED TO DO THIS. THE STEPS INVOLVED IN THE METHOD A
C        RE
C     EXPLAINED BELOW.
C
C     FIRST SET UP THE VECTOR B WHICH CONTAINS THE CRITICAL
C        DAMPING
C     RATIO FOR EACH MASS. THE DAMPING RATIO FOR ALL THE STR
C        UCTURAL
C     MASSES IS BETA2. THE TRANSLATIONAL SOIL DAMPING RATIO
C        IS CTRANS
C     AND THE ROTATIONAL SOIL DAMPING RATIO IS CROT.
C
      NM=12
```

```
      N=N3-2
      N2=N/2
      DO 100 I=1,N
      B(I)=BETA2
  100 CONTINUE
      B(N+1)=CTRANS
      B(N+2)=CROT
C
C
C     NOW COMPUTE THE STRAIN ENERGY IN THE ITH MASS. THE STR
C        AIN
C     ENERGY FOR EACH LUMPED MASS FOR EACH MODE IS STORED IN
C     THE MATRIX EN.THE INTERNAL MODAL STRAIN ENERGY IS ONE
C     HALF THE PRODUCT OF THE AVERAGE INTERNAL FORCES AT THE
C     LUMPED MASS AND THE MODAL DISPLACEMENT.
C
      DO 1 J=1,NM
      DO 2 I=1,N2
      SK=SL(I)/(G*AS(I))
      XF=0.
      EI=E*RIZ(I)
      S=0.
      T=0.
      C=0.
      AA=0.
      BB=0.
      DET=SL(I)**4/(12.*EI**2)+SL(I)*SK/EI+S*SL(I)/EI+C*
     1(SL(I)**3/EI+SK+S)-T*SL(I)**2/EI-T**2
      RMOM(I)=((A(2*I+1,J)-A(2*I-1,J))*(SL(I)**2/EI+T)+A(2*I
     C  ,J)*
     1(SL(I)**3/EI+SK+S)+A(2*I+2,J)*(SL(I)**3/EI+T*SL(I)
     2-SK-S))/DET
      V(I)=((A(2*I-1,J)-A(2*I+1,J))*(SL(I)/EI+C)-A(2*I,J)*(S
     C  L(I)**2
     1/(2.*EI)+T)+A(2*I+2,J)*(T-SL(I)**2/(2.*EI)-SL(I)*C))/D
     C  ET
      EN(2*I-1,J)=V(I)**2*SK/2.
      EN(2*I,J)=(1./(2.*E*RIZ(I)))*(RMOM(I)**2*SL(I)+RMOM(I)
     C  *V(I)
     1*SL(I)**2+V(I)**2*SL(I)**3/3.)
      EN(2*I,J)=EN(2*I,J)+RMOM(I)**2*UL*XF/2.+RMOM(I)*V(I)*B
     C  B+
     1V(I)**2*AA
    2 CONTINUE
      EN(N+1,J)=TRANSK*A(N+1,J)**2*.5
      EN(N+2,J)=ROTK*A(N+2,J)**2*.5
    1 CONTINUE
C
C
C     COMPUTE THE TOTAL ENERGY IN EACH MODE AND STORE IN VEC
C        TOR
C     ET.
C
      DO 7 I=1,NM
      ET(I)=0.
      DO 7 J=1,NM
```

```
      ET(I)=EN(J,I)+ET(I)
    7 CONTINUE
C
C     NOW COMPUTE THE MODAL DAMPING RATIOS (STORED IN VECTOR
C        D).
C
      DO  8  I=1,NM
      D(I)=0.
      DO 8 J=1,NM
      D(I)=EN(J,I)*B(J)+D(I)
    8 CONTINUE
      DO 13 I=1,NM
      D(I)=D(I)/ET(I)
   13 CONTINUE
      DO 9 I=1,NM
      WRITE(6,12) I,D(I)
    9 CONTINUE
   12 FORMAT(/10X,'MODAL DAMPING FOR MODE',I1,'=',E10.3)
      RETURN
      END
      SUBROUTINE JACOBY(N,K)
      COMMON /DYN/GSTIFF(3),GMASS(3),DAMP(3),EQFOR(12),GFORC
     C  E(3),
     1DISP(12),RKFOR(12)
      COMMON /EIG/GLOK(12,12),OMEGA(12),A(12,12),RMASS(12),A
     C  TR(12,12)
      DIMENSION EM(12),STB(12,12),T(12,12),TT(12,12),B(12,12
     C  ),
     1ST(12,12),A1(12,12)
      DIMENSION C(12,12)
C
C     THIS SUBROUTINE CALCULATES EIGENVECTORS AND EIGENVALUE
C        S
C     FROM A GIVEN STIFFNESS MATRIX AND MASS VECTOR. N IS TH
C        E
C     NUMBER OF STRUCTURAL DEGREES OF FREEDOM IN THE SYSTEM,
C     EM IS THE MASS VECTOR AND ST IS THE STRUCTURAL STIFFNE
C        SS MATRIX.
C     ONLY THE STRUCTURAL PORTION OF THE GLOBAL STIFFNESS MA
C        TRIX
C     IS DIAGONALIZED SO THE FREQUENCIES AND MODE SHAPES ARE
C        FOR
C     A FIXED BASE STRUCTURE.
C
      DO 75 I=1,N
      DO 75 J=1,N
      ST(I,J)=GLOK(I,J)
   75 CONTINUE
      DO 76 I=1,N
      EM(I)=RMASS(I)
   76 CONTINUE
      CALL PRINT5(ST,N)
      CALL UNIT(A1,N)
C
```

```
C        STB=(1/SQRT(EM))*(ST)*(1/SQRT(EM)). THE STIFFNESS MATR
C          IX
C        ST IS TRANSFORMED INTO A FORM IN WHICH THE JACOBI METH
C          OD
C        CAN BE APPLIED.
C
         DO 10 I=1,N
      10 EM(I)=SQRT(EM(I))
         DO 12 I=1,N
         DO 12 J=1,N
      12 STB(I,J)=ST(I,J)/(EM(J)*EM(I))
         DO 20 KK=1,K
         DO 15 I=1,N
         DO 15 J=I,N
         IF (I-J) 14,15,14
C
C        T IS A UNIT MATRIX EXCEPT FOR T(I,I),T(J,J),T(I,J),
C        AND T(J,I). BY PRE AND POST MULTIPLYING STB BY T THE
C        ELEMENT STB(I,J) IS SET=0. THIS ACTUALLY A SERIES OF
C        ORTHOGONAL TRANSFORMATIONS TO DIAGONALIZE STB.AFTER ST
C          B
C        IS DIAGONALIZED IT WILL CONTAIN THE EIGENVALUES ON ITS
C        MAIN DIAGONAL.
C
      14 IF (ABS(STB(I,J)).LT.1.0E-10) GO TO 15
         CALL UNIT(T,N)
         DIFF=STB(I,I)-STB(J,J)
         IF (ABS(DIFF)-.00005D0) 30,30,32
      30 TH=.785398E0
         GO TO 33
      32 THC=2.0E0*STB(I,J)/DIFF
         TH=.5E0*ATAN(THC)
      33 T(I,I)=COS(TH)
         T(J,J)=T(I,I)
         T(I,J)=-SIN(TH)
         T(J,I)=-T(I,J)
C
C        CALCULATE THE TRANSPOSE OF T (TT).
C
         CALL TRA(T,TT,N)
C
C        TT*STB*T=STB
C
         CALL PRMULT(STB,TH,I,J,N)
         CALL POMULT(STB,TH,I,J,N)
C
C        A1*T=A1. A1 STORES THE RESULTS OF
C        T1*T2*T3....TK.(THERE ARE K ITERATIONS).A1=SQRT(EM)*A
C        WHERE AIS THE MODAL MATRIX.T1 IS T FOR THE FIRST ITERA
C          TION
C        T2 IS T FOR THE SECOND ITERATION UP TO TK FOR THE KTH
C        ITERATION.
C
         CALL POMULT(A1,TH,I,J,N)
```

```
      15 CONTINUE
C
C        THE MODAL MATRIX A=(1/SQRT(EM))*A1.THE FIRST ROW OF A
C        IS NORMALIZED TO 1
C
         DO 18 J=1,N
         DO 18 I=1,N
      18 A(I,J)=A1(I,J)/EM(I)
      20 CONTINUE
         DO 50 I=1,N
         OMEGA(I)=SQRT(STB(I,I))
      50 CONTINUE
C
C        SORT FREQUENCIES AND EIGENVECTORS STARTING FROM MODE 1
C            (LOWEST)
C        AND GOING UP TO MODE N.
C
         NN=N-1
         DO 80 I=1,NN
         L=I+1
         DO 9 K=L,N
         IF (OMEGA(K).GT.OMEGA(I)) GO TO 9
         WX=OMEGA(I)
         OMEGA(I)=OMEGA(K)
         OMEGA(K)=WX
         DO 300 II=1,N
         AX=A(II,I)
         A(II,I)=A(II,K)
         A(II,K)=AX
     300 CONTINUE
       9 CONTINUE
      80 CONTINUE
C
C        PRINT OUT THE NATURAL FREQUENCIES AND EIGENVECTORS.
C
         DO 11 I=1,N
      11 WRITE(6,122) I,OMEGA(I)
     122 FORMAT(/10X,'FREQUENCY',I5,'=',F10.2)
         CALL PRINT5(A,N)
         CALL TRA(A,ATR,N)
         RETURN
         END
         SUBROUTINE MULT(A,B,C,N)
         DIMENSION A(12,12),B(12,12),C(12,12)
         DO 10 I=1,N
         DO 10 J=1,N
         C(I,J)=0.0E0
         DO 10 L=1,N
      10 C(I,J)=C(I,J)+A(I,L)*B(L,J)
         RETURN
         END
         SUBROUTINE UNIT(A,N)
         DIMENSION A(12,12)
         DO 10 I=1,N
```

```
      DO 8 J=1,N
    8 A(I,J)=0.0E0
   10 A(I,I)=1.0E0
      RETURN
      END
      SUBROUTINE TRA(A,B,N)
      DIMENSION A(12,12),B(12,12)
      DO 10 I=1,N
      DO 10 J=1,N
   10 B(I,J)=A(J,I)
      RETURN
      END
      SUBROUTINE POMULT(STB,TH,I,J,N)
      DIMENSION STB(12,12),C(12,2)
      DO 1 II=1,N
      C(II,1)=STB(II,I)*COS(TH)+STB(II,J)*SIN(TH)
      C(II,2)=STB(II,J)*COS(TH)-STB(II,I)*SIN(TH)
    1 CONTINUE
      DO 2 II=1,N
      STB(II,I)=C(II,1)
      STB(II,J)=C(II,2)
    2 CONTINUE
      RETURN
      END
      SUBROUTINE PRMULT(STB,TH,I,J,N)
      DIMENSION STB(12,12),C(2,12)
      DO 1 JJ=1,N
      C(1,JJ)=STB(I,JJ)*COS(TH)+STB(J,JJ)*SIN(TH)
      C(2,JJ)=STB(J,JJ)*COS(TH)-STB(I,JJ)*SIN(TH)
    1 CONTINUE
      DO 2 JJ=1,N
      STB(I,JJ)=C(1,JJ)
      STB(J,JJ)=C(2,JJ)
    2 CONTINUE
      RETURN
      END
      SUBROUTINE PRINT5(A,N)
      DIMENSION A(12,12)
      WRITE(6,20)
      DO 10 I=1,N
   10 WRITE(6,12) (A(I,J),J=1,N)
   12 FORMAT(10X,10E10.3)
   20 FORMAT(//)
      RETURN
      END
```

APPENDIX B

1.   Description of the Computer Program SAC

This program performs the seismic analysis of cracked nuclear contain-
ment vessels. Only horizontal cracks are taken account of. Because shear

transfer across cracks exhibits stiffness characteristics which change with

the slip at the crack plane, the seismic analysis of cracked containment

vessels is nonlinear. The structure is idealized as a vertical cantilever

shear beam with the cracks contributing additional shear flexibility. The

mass of the vessel is lumped at the node points. Soil-structure inter-

action is included through use of translational and rotational springs

which model the stiffness of the underlying soil. The damping properties

of the structure and soil are included by assigning critical damping ratios

for each mode of vibration. Effective critical damping ratios for each

mode (that include the large soil damping capacity) are calculated through

use of the subregioned energy proportion method. The symmetric fully

populated damping matrix is generated from the critical damping ratios in

the manner shown in section 4.4. Because the model is nonlinear direct

numerical integration of the equations of motion is performed using the

linear acceleration method.

2.   Input to SAC

The same sample problem will be used as in Appendix A. The input is

similar except that the additional information of crack spacing and crack

stiffness will be input. It will be assumed that the horizontal cracks

are spaced at 5'-6". The crack stiffness is input by specifying the six pairs of values for shear stress and crack slip which define the second cycle hysteresis loop (see Figure 5.6). Both cracked and uncracked values for the moment of inertia must be input. The "uncracked" moment of inertia occurs in the concrete between the horizontal cracks (see section 5.4). The cracked moment of inertia is the moment of inertia supplied solely by the longitudinal reinforcing bars which cross the open horizontal cracks. The maximum number of beam segments which may be used is 5. This could be increased by changing the pertinent DIMENSION statements (see source listing of SAC). The units are kips, inches and seconds. The times for which output is printed out may be controlled as described in the next section.

CARD 1   (2F10.0, 2I5)

     cols 1-10:   .0025 (recommended time step size)

     cols 11-20:   .25 (duration of analysis)

     cols 21-25:   5 (number of beam segments)

     cols 26-30:   10 (number of base acceleration time points)

CARD 2   (I5, 2F10.0)

     cols 1-5:   1 (=1 if soil-structure interaction is to be

                  included, = 0 if not)

     cols 6-15:   10.0E10 (K_ϕ)

     cols 16-25:   100000. (K_u)

CARD 3   (3F10.0)

     cols 1-10:   .05 (critical damping ratio for the containment)

cols 11-20: .25 (critical damping ratio for translational

motion in underlying soil)

cols 21-30: .05 (critical damping ratio for rotational motion

in underlying soil)

CARD 4 (3F10.0)

cols 1-10:   1500. (G, shear modulus, ksi)

cols 11-20: 3000. (E, Young's modulus, ksi)

cols 21-30: 837. (R_c, radius of the containment vessel cylinder)

CARD 5 (2I5)

cols 1-5:   9 (number of cracks in top beam segment)

cols 6-10:   6 (number of cracks in 2nd beam segment)

cols 11-15: 6 (number of cracks in 3rd beam segment)

cols 16-20: 6 (number of cracks in 4th beam segment)

cols 21-25: 3 (number of cracks in bottom beam segment)

CARD 6 (4F10.0)

cols 1-10:   150000. (shear area of top beam segment)

cols 11-20: 592.5 (length of top beam segment)

cols 21-30: 9.0E10 (uncracked moment of inertia of top beam

segment)

cols 31-40: 2.0E10 (cracked moment of inertia of top beam

segment)

CARD 7 (4F10.0)

cols 1-10:   150000. (shear area of 2nd beam segment)

cols 11-20: 360. (length of 2nd beam segment)

cols 21-30: 9.0E10 (uncracked moment of inertia of 2nd beam segment)

cols 31-40: 2.0E10 (cracked moment of inertia of 2nd beam segment)

CARD 8   (4F10.0)   (same as CARD 7 for 3rd beam segment)

CARD 9   (4F10.0)   (same as CARD 7 for 4th beam segment)

CARD 10   (4F10.0)

cols 1-10:   150000. (shear area of bottom beam segment)

cols 11-20: 180. (length of bottom beam segment)

cols 21-30: 9.0E10 (uncracked moment of inertia of bottom beam segment)

cols 31-40: 2.0E10 (cracked moment of inertia of bottom beam segment)

CARD 11   (8F10.0)

cols 1-10:   30. (m_1)

cols 11-20: 8.0E06 (I_1)

cols 21-30: 25. (m_2)

cols 31-40: 8.0E06 (I_2)

cols 41-50: 25. (m_3)

cols 51-60: 8.0E06 (I_3)

cols 61-70: 25. (m_4)

cols 71-80: 8.0E06 (I_4)

CARD 12   (4F10.0)

    cols 1-10:   25. (m_5)

    cols 11-20:   8.0E06 (I_5)

    cols 21-30:   60. (m_f)

    cols 31-40:   13.0E06 (I_f)

CARD 13   (2F10.0)

    cols 1-10:   .03 $(\tau_1$ in Figure 5.6)

    cols 11-20:   .0027 $(\Delta_1$ in Figure 5.6)

CARD 14   (2F10.0)

    cols 1-10:   .110 $(\tau_2$ in Figure 5.6)

    cols 11-20:   .005 $(\Delta_2$ in Figure 5.6)

CARD 15   (2F10.0)

    cols 1-10:   -.00053 $(\tau_3$ in Figure 5.6)

    cols 11-20:   .0037 $(\Delta_3$ in Figure 5.6)

CARD 16   (2F10.0)

    cols 1-10:   -.03 $(\tau_4$ in Figure 5.6)

    cols 11-20:   -.0027 $(\Delta_4$ in Figure 5.6)

CARD 17   (2F10.0)

    cols 1-10:   -.110 $(\tau_5$ in Figure 5.6)

    cols 11-20:   -.005 $(\Delta_5$ in Figure 5.6)

CARD 18   (2F10.0)

    cols 1-10:   .00053 (τ_6 in Figure 5.6)

    cols 11-20:   -.0037 (Δ_6 in Figure 5.6)

CARD 19   (I5)

    cols 1-5:   3 (number of printout intervals)

CARD 20   (3F8.0)

    cols 1-8:   .10 (1st printout interval)

    cols 9-16:   .20 (2nd printout interval)

    cols 17-24:   .26 (3rd printout interval)

CARD 21   (3F8.0)

    cols 1-8:   .025 (time between printouts in 1st interval)

    cols 9-16:   .01 (time between printouts in 2nd interval)

    cols 17-24:   .025 (time between printouts in 3rd interval)

CARD 22   (2F10.0)

    cols 1-10:   0. (time in seconds of base acceleration)

    cols 11-20:   .084 (base acceleration, fraction of g, accelera-
                   tion of gravity)

CARD 23   (2F10.0)

    cols 1-10:   .023 (time in seconds of base acceleration)

    cols 11-20:   .158 (base acceleration)

CARD 24   (2F10.0)

cols 1-10:   .058 (time in seconds of base acceleration)

cols 11-20:   .271 (base acceleration)

CARD 25   (2F10.0)

cols 1-10:   .083 (time in seconds of base acceleration)

cols 11-20:   .349 (base acceleration)

CARD 26   (2F10.0)

cols 1-10:   .113 (time in seconds of base acceleration)

cols 11-20:   .446 (base acceleration)

CARD 27   (2F10.0)

cols 1-10:   .149 (time in seconds of base acceleration)

cols 11-20:   .509 (base acceleration)

CARD 28   (2F10.0)

cols 1-10:   .186 (time in seconds of base acceleration)

cols 11-20:   .382 (base acceleration)

CARD 29   (2F10.0)

cols 1-10:   .23 (time in seconds of base acceleration)

cols 11-20:   .191 (base acceleration)

CARD 30   (2F10.0)

cols 1-10:   .256 (time in seconds of base acceleration)

cols 11-20:   .058 (base acceleration)

CARD 31   (2F10.0)

      cols 1-10:   .3 (time in seconds of base acceleration)

      cols 11-20: 0. (base acceleration)

3.   Output from SAC

The times at which output is desired is controlled in the manner shown
by CARDS 19, 20, 21. CARD 19 inputs the number of printout time intervals.
In this case the first printout interval is from t = 0 to t = .10 seconds.
In this interval the time between printouts is .025 seconds so the first
three printouts occur at t = 0, .025, .05. At t = .10 the time between
printouts changes to .01 seconds. Printouts occur at t = .10, .11, .12
.... At t = .20 the time between printouts changes back to .025 seconds
again. The maximum number of different printout time intervals which may
be specified on CARD 19 is 10.

For each printout time the translational displacements, shear stresses
and crack displacements in the containment are printed out. In the dis-
placement column the top number corresponds to the displacement of the top
mass, the second number corresponds to the displacement of the second mass
and so on down. The shear stress and crack slip columns have the values
for the top beam segment in the first row, the second beam segment values
in the second row and so on. After the analysis is completed the maximum
values for shear stress, bending stress, displacements (including rota-
tional and soil degrees of freedom) and crack slip are output. Units are
kips, inches and seconds.

```
C                    ********  SAC  ********
C       THIS PROGRAM,NAMED SAC (SEISMIC ANALYSIS INCLUDING CRA
C          CKS),
C       PERFORMS THE SEISMIC ANALYSIS OF CRACKED NUCLEAR CONTA
C          INMENT
C       VESSELS. THE CONTAINMENT VESSEL IS MODELED BY A VERTIC
C          AL
C       CANTILEVER SHEAR BEAM WITH 5 LUMPED MASSES. AT EACH MA
C          SS
C       POINT 2 DEGREES OF FREEDOM EXIST,ROTATIONAL AND TRANSL
C          ATIONAL.
C       THE SOIL UNDERLYING THE CONTAINMENT VESSEL FOUNDATION
C          IS
C       MODELED BY 2 SPRINGS,TRANSLATIONAL AND ROTATIONAL. IN
C          ALL
C       THERE ARE 12 DEGREES OF FREEDOM.
C
        COMMON /DYN/RMASS(12),DAMP(12,12),CK(6),CFORCE(12),EQF
     C   OR(12),
     1RKFOR(12),OLDFOR(12),RINFOR(12),ACC(12),DISP(12),VEL(1
     C   2),
     2OLDVEL(12),OLDACC(12),SHEAR(12),OLDSHR(12),REL(12),OLD
     C   AMP(12),
     3SHEARK(5),GLOK(12,12),NCR(5),OLDCK(6),NLDIPD(5),OLDREL
     C   (12),RK(8)
     4,TK(6),OLDISP(12)
        COMMON /EIG/OMEGA(12),A(12,12),ATR(12,12),D(12)
        COMMON /B/RLOAD(6),DELTA(6),IPD(5),NCYCLE(5),RLOADN(5,
     C   6),
     1DELTAN(5,6)
        COMMON /PROP/AS(5),RIZ(5),SL(5),E,G,SIZ(5)
C
C       H IS THE TIME STEP SIZE AND ENDTIM IS THE TOTAL DURATI
C          ON
C       OF THE SEISMIC ANALYSIS. NSEG IS THE NUMBER OF BEAM SE
C          GMENTS.
C       NTP IS THE NUMBER OF GROUND ACCELERATION TIME POINTS.
C          NH IS
C       THE TOTAL NUMBER OF TIME STEPS. BETA2 IS THE CONSTANT
C       CRITICAL DAMPING RATIO OF THE CONTAINMENT VESSEL. IF I
C          ROT
C       =1 THEN SOIL-STRUCTURE INTERACTION IS TO BE INCLUDED.
C          ROTK
C       AND TRANSK ARE THE ROTATIONAL AND TRANSLATIONAL SOIL S
C          PRING
C       CONSTANTS. CROT AND CTRANS ARE THE SOIL CRITICAL DAMPI
C          NG RATIOS
C       FOR ROTATIONAL AND TRANSLATIONAL MOTION. G AND E ARE T
C          HE SHEAR
C       AND YOUNG,S MODULII FOR CONCRETE. R IS THE RADIUS OF T
C          HE
C       CONTAINMENT VESSEL WALL. NCR(I) IS THE NUMBER OF HORIZ
C          ONTAL
C       CRACKS IN THE ITH BEAM SEGMENT. AS(I) AND SL(I) ARE TH
```

```
C         E SHEAR
C         AREA AND LENGTH OF THE ITH BEAM SEGMENT. RIZ(I) IS THE
C             MOMENT
C         OF INERTIA OF THE UNCRACKED CONCRETE. SIZ(I) IS THE MO
C             MENT
C         OF INERTIA AT THE HORIZONTAL CRACK OR THE MOMENT OF IN
C             ERTIA
C         PROVIDED BY THE LONGITUDINAL REBARS ONLLY. RMASS CONTA
C             INS THE
C         VALUES OF THE LUMPED MASSES. RLOAD(1...6) AND DELTA(1.
C             ..6)
C         CONTAIN THE SHEAR STRESS AND CRACK SLIP FOR THE 6 POIN
C             TS
C         WHICH DEFINE THE SECOND CYCLE HYSTERESIS LOOP WHICH IN
C             TURN
C         DEFINES THE HORIZONTAL CRACK STIFFNESS. STIFF1 IS THE
C             CRACK
C         STIFFNESS FOR THE FIRST CYCLE. DINC IS THE INCREASE IN
C             DELTA(1)
C         WHICH OCCURS WITH EACH ADDITIONAL LOAD CYCLE.
C
          READ(5,100) H,ENDTIM,NSEG,NTP,NH

          N=2*NSEG
          READ(5,106) IROT,ROTK,TRANSK
          READ(5,101) BETA2,CTRANS,CROT
          IFLAG=0
          JFLAG=0
          KFLAG=0
          ISTIFF=0
          KREF=1
          LFLAG=0
          K=3
          DINC=.0001
          T=0.
          BETA=.1666667
          OH=H
          NM=4
          NDOF=N
          NQUAKE=N
          READ(5,101) G,E,R
          READ(5,110) (NCR(I),I=1,NSEG)
          DO 1 I=1,NSEG
          READ(5,101) AS(I),SL(I),RIZ(I),SIZ(I)
          SHEARK(I)=G*AS(I)/SL(I)
        1 CONTINUE
          IF (IROT.EQ.0) GO TO 60
          NDOF=N+2
          NQUAKE=N+1
       60 CONTINUE
          READ(5,101) (RMASS(I),I=1,8)
          READ(5,101) (RMASS(I),I=9,NDOF)
C
C         INPUT THE P-DELTA RELATIONSHIP FOR THE HYSTERESIS LOOP
```

```
C          S
C          BY READING IN RLOAD(1....6) AND DELTA(1....6).
C
           DO 200 I=1,6
           READ(5,201) RLOAD(I),DELTA(I)
       201 FORMAT(2F10.0)
       200 CONTINUE
C
C          NOW THAT THE P-DELTA RELATIONSHIP HAS BEEN READ IN
C          THE SLOPE OF EACH STRAIGHT LINE SEGMENT WHICH MAKES UP
C             THE
C          HYSTERESIS LOOP IS COMPUTED.THEN THE VECTOR OF SHEAR S
C             TIFFNESSES
C          FOR THE BEAM SEGMENTS (TK) IS COMPUTED.
C
           RK(1)=18.3
           RK(2)=(RLOAD(2)-RLOAD(1))/(DELTA(2)-DELTA(1))
           RK(3)=(RLOAD(3)-RLOAD(2))/(DELTA(3)-DELTA(2))
           RK(4)=(RLOAD(4)-RLOAD(3))/(DELTA(4)-DELTA(3))
           RK(5)=18.3
           RK(6)=RK(2)
           RK(7)=RK(3)
           RK(8)=RK(4)
           DO 700 I=1,8
           WRITE(6,701) RK(I)
       701 FORMAT(10X,E14.7)
       700 CONTINUE
C
C          THE MATRICES DELTAN AND RLOADN STORE THE SLIP AND SHEA
C             R STRESS
C          WHICH DEFINE THE HYSTERESIS LOOPS FOR EACH BEAM SEGMEN
C             T.
C          INITIALLY THE HYSTERESIS LOOPS CORRESPONDING TO THE SE
C             COND CYCLE
C          ARE INPUT FOR ALL BEAM SEGMENTS.
C
           DO 703 I=1,NSEG
           DELTAN(I,1)=DELTA(1)
           DELTAN(I,2)=DELTA(2)
           DELTAN(I,3)=DELTA(3)
           DELTAN(I,4)=DELTA(4)
           DELTAN(I,5)=DELTA(5)
           DELTAN(I,6)=DELTA(6)
           RLOADN(I,1)=RLOAD(1)
           RLOADN(I,2)=RLOAD(2)
           RLOADN(I,3)=RLOAD(3)
           RLOADN(I,4)=RLOAD(4)
           RLOADN(I,5)=RLOAD(5)
           RLOADN(I,6)=RLOAD(6)
       703 CONTINUE
           DO 10 I=1,NSEG
           CK(I)=RK(1)
        10 CONTINUE
           UL=2.5
```

```
      CALL STIFF(N,NSEG,IROT,ROTK,TRANSK,KREF,ISTIFF,UL)
      CALL JACOBY(NDOF,K)
      CALL RATIO(N,BETA2,CTRANS,CROT,TRANSK,ROTK,UL)
      CALL INDAMP(NDOF)
      DO 102 I=1,NH
      NFLAG=0
      IF (I.EQ.1) GO TO 300
      IF (H.LT.0.) GO TO 999
      CALL STIFF(N,NSEG,IROT,ROTK,TRANSK,KREF,ISTIFF,UL)
      CALL INQUAK(T,NTP,NQUAKE,H,IFLAG)
      CALL NUMINT(H,T,BETA,NDOF,IROT,ENDTIM,R)
      IF (T.GT.ENDTIM) GO TO 105
  300 CALL INHYST(H,T,OH,NSEG,JFLAG,PRINT,KREF,NFLAG)
      IF (I.EQ.1) GO TO 102
      IF (NFLAG.EQ.1) GO TO 102
      CALL CYCLE(NSEG,LFLAG,DINC)
  102 CONTINUE
  100 FORMAT(2F10.0,5I5)
  101 FORMAT(8F10.0)
  106 FORMAT(I5,2F10.0)
  110 FORMAT(5I5)
  999 WRITE(6,998) T,H
  998 FORMAT(/10X,2E14.7)
  105 STOP
      END
      SUBROUTINE STIFF(N,NTR,IROT,ROTK,TRANSK,KREF,ISTIFF,UL
     C )
C     THIS SUBROUTINE COMPUTES THE GLOBAL STIFFNESS MATRIX W
C        HICH
C     IS STORED IN GLOK. THE VECTOR TK CONTAINS THE SHEAR
C     FLEXIBILITIES OF THE CONTAINMENT VESSEL. 1./SHEARK(I)
C        IS
C     THE ELASTIC FLEXIBILITY OF THE UNCRACKED CONCRETE. FOR
C        THE
C     ITH BEAM SEGMENT NCR(I)/(AS(I)*CK(I)) IS THE TOTAL SHE
C        AR
C     FLEXIBILITY OF ALL THE HORIZONTAL CRACKS IN THE BEAM S
C        EGMENT.
C
      COMMON /DYN/RMASS(12),DAMP(12,12),CK(6),CFORCE(12),EQF
     C OR(12),
     1RKFOR(12),OLDFOR(12),RINFOR(12),ACC(12),DISP(12),VEL(1
     C 2),
     2OLDVEL(12),OLDACC(12),SHEAR(12),OLDSHR(12),REL(12),OLD
     C AMP(12),
     3SHEARK(5),GLOK(12,12),NCR(5),OLDCK(6),NLDIPD(5),OLDREL
     C (12),RK(8)
     4,TK(6),OLDISP(12)
      COMMON /PROP/AS(5),RIZ(5),SL(5),E,G,SIZ(5)
      DIMENSION ELK(4,4),VK(5)
      DIMENSION A(5),B(5),C(5)
C
C     IF IROT=1 THEN SOIL STRUCTURE INTERACTION IS TO BE INC
C        LUDED.
```

```
C
      IF (KREF.EQ.0) GO TO 45
      NN=N
      DO 1 I=1,NTR
      TK(I)=(NCR(I)/(CK(I)*AS(I)))+(1./SHEARK(I))
    1 CONTINUE
   20 CONTINUE
C
C     SET UP THE GLOBAL STIFFNESS MATRIX ,GLOK(N,N).
C
      N1=N-1
      NN=N+2
      DO 13 I=1,NN
      DO 13 J=1,NN
      GLOK(I,J)=0.
   13 CONTINUE
      DO 10 I=1,N1,2
      IF (ISTIFF.GT.3) GO TO 222
C
C     SET UP THE BEAM ELEMENT STIFFNESS MATRIX ELK(4,4) FOR
C        THE LTH
C     BEAM SEGMENT.
C
      L=(I+1)/2
      EI=E*RIZ(L)
      SUM=0.
      SUM2=0.
      NC=NCR(L)
      RNC=NCR(L)
      DO 22 K=1,NC
      AK=K
      RX=(2.*AK-1.)/(2.*RNC)
      SUM=SUM+RX
      SUM2=SUM2+RX**2
   22 CONTINUE
      A(L)=((1./SIZ(L))-(1./RIZ(L)))*SL(L)**2*UL*SUM2/E
      B(L)=((1./SIZ(L))-(1./RIZ(L)))*SL(L)*UL*SUM/E
      C(L)=((1./SIZ(L))-(1./RIZ(L)))*UL*NCR(L)/E
  222 CONTINUE
      L=(I+1)/2
      EI=E*RIZ(L)
      DET=SL(L)**4/(12.*EI**2)+TK(L)*SL(L)/EI+A(L)*SL(L)/EI+
     C  C(L)*
     1(SL(L)**3/(3.*EI)+TK(L)+A(L))-B(L)*SL(L)**2/EI-B(L)**2
      X=1./DET
      ELK(1,1)=X*((SL(L)/EI)+C(L))
      ELK(1,2)=-X*((SL(L)**2/(2.*EI))+B(L))
      ELK(1,3)=-ELK(1,1)
      ELK(1,4)=X*(B(L)-(SL(L)**2/(2.*EI))-C(L)*SL(L))
      ELK(2,2)=X*((SL(L)**3/(3.*EI))+TK(L)+A(L))
      ELK(2,3)=-ELK(1,2)
      ELK(2,4)=X*(SL(L)**3/(6.*EI)+B(L)*SL(L)-TK(L)-A(L))
      ELK(3,3)=ELK(1,1)
      ELK(3,4)=-ELK(1,2)
```

```
      ELK(4,4)=ELK(2,2)
      DO 3 K=1,4
      DO 3 J=1,K
    3 ELK(K,J)=ELK(J,K)
      GLOK(I,I)=ELK(1,1)+GLOK(I,I)
      GLOK(I+1,I+1)=ELK(2,2)+GLOK(I+1,I+1)
      GLOK(I+1,I)=ELK(2,1)+GLOK(I+1,I)
      GLOK(I+2,I)=ELK(3,1)
      GLOK(I+3,I)=ELK(4,1)
      GLOK(I+2,I+1)=ELK(3,2)
      GLOK(I+3,I+1)=ELK(4,2)
      GLOK(I+2,I+2)=ELK(3,3)
      GLOK(I+3,I+2)=ELK(4,3)
      GLOK(I+3,I+3)=ELK(4,4)
   10 CONTINUE
      DO 11 I=1,NN
      DO 11 J=1,NN
   11 GLOK(I,J)=GLOK(J,I)
      IF (IROT.EQ.0) GO TO 44
C
C
C     ADD TO THE GLOBAL STIFFNESS MATRIX THE TRANSLATIONAL
C     TRANSK) AND ROTATIONAL (ROTK) SOIL SPRINGS WHICH MODEL
C     THE STIFFNESS OF THE UNDERLYING SOIL.
C
      GLOK(NN-1,NN-1)=GLOK(NN-1,NN-1)+TRANSK
      GLOK(NN,NN)=GLOK(NN,NN)+ROTK
   44 ISTIFF=ISTIFF+1
   45 CONTINUE
      RETURN
      END
      SUBROUTINE NUMINT(H,T,BETA,N,IROT,ENDTIM,R)
C
C     THIS SUBROUTINE CALCULATES THE CHANGES IN DISPLACEMENT
C         ,
C     VELOCITY AND ACCELERATION FOR EACH TIME STEP IN THE SE
C         ISMIC
C     ANALYSIS. DDF(I) AND DSF(I) ARE THE CHANGES FOR EACH T
C         IME
C     STEP IN DAMPING AND SRING FORCE FOR THE ITH DEGREE OF
C         FREEDOM.
C     CFORCE(I),RKFOR(I) AND RINFOR(I) CONTAIN THE TOTAL DAM
C         PING
C     FORCES,SPRING FORCES AND INERTIAL FORCES AT TIME T. DI
C         SP(I)
C     ,VEL(I) AND ACC(I) ARE THE DISPLACEMENT,VELOCITY AND
C     ACCELERATION FOR THE ITH DEGREE OF FREEDOM AT TIME T.
C         SHEAR(I)
C     CONTAINS THE SHEAR FORCE IN THE ITH BEAM SEGMENT. REL(
C         I) IS
C     THE CRACK SLIP FOR THE CRACKS IN THE ITH BEAM SEGMENT.
C     OLDSHR(I),OLDAMP(I),OLDFOR(I),OLDACC(I),OLDVEL(I) AND
C     OLDISP(I) CONTAIN THE SHEAR, DAMPING FORCE,SPRING FORC
C         E,ACC-
C     ELERATION,VELOCITY AND DISPLACEMENT FOR THE ITH DEGREE
```

```
C          OF
C       FREEDOM AT THE PREVIOUS TIME POINT.
C
        DIMENSION ZMOM(5),ZMAX(5)
        DIMENSION DELACC(12),DELDSP(12),DELVEL(12)
        COMMON /PROP/AS(5),RIZ(5),SL(5),E,G,SIZ(5)
        DIMENSION X(12)
        COMMON /DYN/RMASS(12),DAMP(12,12),CK(6),CFORCE(12),EQF
     C   OR(12),
     1RKFOR(12),OLDFOR(12),RINFOR(12),ACC(12),DISP(12),VEL(1
     C   2),
     2OLDVEL(12),OLDACC(12),SHEAR(12),OLDSHR(12),REL(12),OLD
     C   AMP(12),
     3SHEARK(5),GLOK(12,12),NCR(5),OLDCK(6),NLDIPD(5),OLDREL
     C   (12),RK(8)
     4,TK(6),OLDISP(12)
        DIMENSION DDF(12),DSF(12),EQEFR(12)
        DIMENSION SHRMAX(12),DISMAX(12),RELMAX(12)
C
C       THE VELOCITIES AND DISPLACEMENTS OF THE LUMPED MASSES
C       ARE SET EQUAL TO THEIR INITIAL VALUE.
C
        IF (T.GT.0.) GO TO 302
        NP=N
        N1=NP-1
        NP2=N/2
        IF (IROT.EQ.0) GO TO 447
        NP=N-2
        N1=NP-1
        NP2=NP/2
  447   CONTINUE
        DO 32 I=1,N
        DDF(I)=0.
        DSF(I)=0.
        CFORCE(I)=0.
        RKFOR(I)=0.
        DISP(I)=0.
        VEL(I)=0.
        ACC(I)=EQFOR(I)/RMASS(I)
        RINFOR(I)=RMASS(I)*ACC(I)
        DELDSP(I)=0.
        DELVEL(I)=0.
        DELACC(I)=0.
        SHEAR(I)=0.
        REL(I)=0.
        OLDSHR(I)=0.
        OLDAMP(I)=0.
        OLDISP(I)=0.
        OLDREL(I)=0.
        OLDFOR(I)=0.
        OLDACC(I)=0.
        OLDVEL(I)=0.
        SHRMAX(I)=SHEAR(I)
        DISMAX(I)=DISP(I)
```

```
      RELMAX(I)=REL(I)
   32 CONTINUE
      DO 23 I=1,NP2
      ZMAX(I)=0.
   23 CONTINUE
      GO TO 84
C
C     THE CHANGES IN DISPLACEMENT AND VELOCITY FOR THIS TIME
C        STEP ARE
C     CALCULATED ACCORDING TO THE NEWMARK BETA METHOD. FIRST
C        THE VALUE
C     FOR THE CHANGE IN ACCELERATION (DELACC) FOR THE PREVIO
C        US TIME
C     STEP IS ASSUMED FOR THE PRESENT TIME STEP. THE CHANGE
C        IN THE
C     VELOCITY (DELVEL) AND DISPLACEMENT (DELDSP) CAN THEN B
C        E SOLVED
C     FOR.
C
  302 ITER=0
  300 ITER=ITER+1
      DO 49 L=1,N
      X(L)=DELDSP(L)
      DELVEL(L)=(2.*ACC(L)+DELACC(L))*H/2.
      DELDSP(L)=(VEL(L)*H)+(.5-BETA)*ACC(L)*H**2 + BETA*(ACC
   C  (L)
     1+DELACC(L))*H**2
   49 CONTINUE
      IF (ITER.LT.4) GO TO 48
      JOUT=0
      DO 45 I=1,N
      IF (DELDSP(I).EQ.0.) GO TO 45
      IF (ABS((DELDSP(I)-X(I))/DELDSP(I)).LE..001) GO TO 45
      JOUT=1
   45 CONTINUE
      IF (JOUT.EQ.0) GO TO 350
   48 DO 44 I=1,N
      DO 99 K=1,N
      DDF(I)=DAMP(I,K)*DELVEL(K)+DDF(I)
      DSF(I)=GLOK(I,K)*DELDSP(K)+DSF(I)
   99 CONTINUE
C
C     EQERR IS THE ERROR IN EQUILIBRIUM DUE TO THE ASSUMPTIO
C        N OF
C     VALUES FOR DELACC.
C
      EQERR(I)=(RINFOR(I)+RMASS(I)*DELACC(I))+(CFORCE(I)+DDF
   C  (I))
     1+(RKFOR(I)+DSF(I))-EQFOR(I)
      DSF(I)=0.
      DDF(I)=0.
   44 CONTINUE
      DO 47 I=1,N
      DELACC(I)=(RMASS(I)*DELACC(I)-EQERR(I))/(RMASS(I))
```

```
   47 CONTINUE
      GO TO 300
  350 CONTINUE
      DO 98 I=1,N
      DO 97 K=1,N
      DSF(I)=GLOK(I,K)*DELDSP(K)+DSF(I)
      DDF(I)=DAMP(I,K)*DELVEL(K)+DDF(I)
   97 CONTINUE
      OLDFOR(I)=RKFOR(I)
      OLDISP(I)=DISP(I)
      OLDVEL(I)=VEL(I)
      OLDACC(I)=ACC(I)
      OLDSHR(I)=SHEAR(I)
      OLDAMP(I)=CFORCE(I)
      OLDREL(I)=REL(I)
C
C
C     THE VALUES OF DISPLACEMENT,VELOCITTY AND ACCELERATION
C        FOT TIME
C     T ARE CALCULATED.
C
      DISP(I)=DISP(I)+DELDSP(I)
      VEL(I)=VEL(I)+DELVEL(I)
      ACC(I)=ACC(I)+DELACC(I)
      RKFOR(I)=RKFOR(I)+DSF(I)
      RINFOR(I)=RMASS(I)*ACC(I)
      CFORCE(I)=CFORCE(I)+DDF(I)
      SHEAR(I)=0.
      DDF(I)=0.
      DSF(I)=0.
   98 CONTINUE
      DO 401 I=1,NP2
      IS=2*I-1
      DO 72 K=1,IS,2
      SHEAR(I)=RKFOR(K)+SHEAR(I)
      IF (I.GT.1) GO TO 28
      ZMOM(1)=RKFOR(1)*SL(1)
      GO TO 72
   28 ZMOM(I)=ZMOM(I-1)+SHEAR(I)*SL(I)
   72 CONTINUE
  401 CONTINUE
      DO 201 I=1,NP2
      SHEAR(I)=SHEAR(I)/AS(I)
      ZMOM(I)=ZMOM(I)*R/RIZ(I)
  201 CONTINUE
      DO 540 I=1,NP2
      REL(I)=OLDREL(I)+(SHEAR(I)-OLDSHR(I))/CK(I)
  540 CONTINUE
      DO 501 I=1,N
      IF (ABS(DISMAX(I)).GE.ABS(DISP(I))) GO TO 501
      DISMAX(I)=DISP(I)
  501 CONTINUE
      DO 701 I=1,NP2
      IF (ABS(SHRMAX(I)).GE.ABS(SHEAR(I))) GO TO 601
      SHRMAX(I)=SHEAR(I)
```

```
  601 IF (ABS(ZMAX(I)).GE.ABS(ZMOM(I))) GO TO 801
      ZMAX(I)=ZMOM(I)
  801 IF (ABS(RELMAX(I)).GE.ABS(REL(I))) GO TO 701
      RELMAX(I)=REL(I)
  701 CONTINUE
      IF (T.LT.ENDTIM) GO TO 84
      WRITE(6,1)
    1 FORMAT(/11X,'MAXIMUM SHEAR',3X,'MAXIMUM DISPLACEMENT',
   C  3X,
     1'MAX CRACK DISPLACEMENT',3X,'MAX BENDING STRESS')
      DO 411 I=1,NP2
  411 WRITE(6,2) SHRMAX(I),DISMAX(I),RELMAX(I),ZMAX(I)
    2 FORMAT(10X,E14.7,6X,E14.7,10X,E14.7,9X,E14.7)
      DO 412 I=6,N
  412 WRITE(6,3) DISMAX(I)
    3 FORMAT(30X,E14.7)
      WRITE(6,333) (CK(I),I=1,5)
  333 FORMAT(/10X,5E14.7)
      CALL PRINT5(GLOK,12)
   84 RETURN
      END
      SUBROUTINE RATIO(N,BETA2,CTRANS,CROT,TRANSK,ROTK,UL)
      COMMON /DYN/RMASS(12),DAMP(12,12),CK(6),CFORCE(12),EQF
   C  OR(12),
     1RKFOR(12),OLDFOR(12),RINFOR(12),ACC(12),DISP(12),VEL(1
   C  2),
     2OLDVEL(12),OLDACC(12),SHEAR(12),OLDSHR(12),REL(12),OLD
   C  AMP(12),
     3SHEARK(5),GLOK(12,12),NCR(5),OLDCK(6),NLDIPD(5),OLDREL
   C  (12),RK(8)
     4,TK(6),OLDISP(12)
      COMMON /EIG/OMEGA(12),A(12,12),ATR(12,12),D(12)
      COMMON /PROP/AS(5),RIZ(5),SL(5),E,G,SIZ(5)
      DIMENSION V(5),RMOM(5)
      DIMENSION EN(12,12),ET(12),B(12)
C
C
C     THIS SUBROUTINE IS CALLED ONLY IF SOIL STRUCTURE INTER
C        ACTION
C     IS TO BE INCLUDED IN THE ANALYSIS. SINCE THE CRITICAL
C        DAMPING
C     RATIOS IN THE STRUCTURAL AND SOIL DEGREES OF FREEDOM U
C        SUALLY
C     DIFFER BY A LARGE AMOUNT SOME COMMON MODAL DAMPING VAL
C        UES
C     ARE REQUIRED. THE SUBREGIONED ENERGY PROPORTION METHOD
C     IS USED TO DO THIS. THE STEPS INVOLVED IN THE METHOD A
C        RE
C     EXPLAINED BELOW.
C
C     FIRST SET UP THE VECTOR B WHICH CONTAINS THE CRITICAL
C        DAMPING
C     RATIO FOR EACH MASS. THE DAMPING RATIO FOR ALL THE STR
C        UCTURAL
C     MASSES IS BETA2. THE TRANSLATIONAL SOIL DAMPING RATIO
```

```
C           IS CTRANS
C         AND THE ROTATIONAL SOIL DAMPING RATIO IS CROT.
C
          NM=12
          N2=N/2
          DO 100 I=1,N
          B(I)=BETA2
  100 CONTINUE
          B(N+1)=CTRANS
          B(N+2)=CROT
C
C         NOW COMPUTE THE STRAIN ENERGY IN THE ITH MASS. THE STR
C           AIN
C         ENERGY FOR EACH LUMPED MASS FOR EACH MODE IS STORED IN
C         THE MATRIX EN.THE INTERNAL MODAL STRAIN ENERGY IS ONE
C         HALF THE PRODUCT OF THE AVERAGE INTERNAL FORCES AT THE
C         LUMPED MASS AND THE MODAL DISPLACEMENT.
C
          DO 1 J=1,NM
          DO 2 I=1,N2
          SK=NCR(I)/(CK(I)*AS(I))+(1./SHEARK(I))
          EI=E*RIZ(I)
          SUM=0.
          SUM2=0.
          NC=NCR(I)
          RNC=NCR(I)
          DO 22 K=1,NC
          AK=K
          RX=(2.*AK-1.)/(2.*RNC)
          SUM=SUM+RX
          SUM2=SUM2+RX**2
   22 CONTINUE
          XF=(1./SIZ(I)-1./RIZ(I))/E
          S=XF*UL*SL(I)**2*SUM2
          T=XF*UL*SL(I)*SUM
          C=XF*UL*NCR(I)
          AA=XF*UL**3*SUM2/6.
          BB=XF*UL**2*SUM/2.
          DET=SL(I)**4/(12.*EI**2)+SL(I)*SK/EI+S*SL(I)/EI+C*
        1(SL(I)**3/EI+SK+S)-T*SL(I)**2/EI-T**2
          RMOM(I)=((A(2*I+1,J)-A(2*I-1,J))*(SL(I)**2/EI+T)+A(2*I
        C   ,J)*
        1(SL(I)**3/EI+SK+S)+A(2*I+2,J)*(SL(I)**3/EI+T*SL(I)
        2-SK-S))/DET
          V(I)=((A(2*I-1,J)-A(2*I+1,J))*(SL(I)/EI+C)-A(2*I,J)*(S
        C   L(I)**2
        1/(2.*EI)+T)+A(2*I+2,J)*(T-SL(I)**2/(2.*EI)-SL(I)*C))/D
        C   ET
          EN(2*I-1,J)=V(I)**2*SK/2.
          EN(2*I,J)=(1./(2.*E*RIZ(I)))*(RMOM(I)**2*SL(I)+RMOM(I)
        C   *V(I)
        1*SL(I)**2+V(I)**2*SL(I)**3/3.)
          EN(2*I,J)=EN(2*I,J)+RMOM(I)**2*UL*XF/2.+RMOM(I)*V(I)*B
        C   B+
```

```
      1V(I)**2*AA
    2 CONTINUE
      EN(N+1,J)=TRANSK*A(N+1,J)**2*.5
      EN(N+2,J)=ROTK*A(N+2,J)**2*.5
    1 CONTINUE
C
C
C     COMPUTE THE TOTAL ENERGY IN EACH MODE AND STORE IN VEC
C        TOR
C     ET.
C
      DO 7 I=1,NM
      ET(I)=0.
      DO 7 J=1,NM
      ET(I)=EN(J,I)+ET(I)
    7 CONTINUE
C
C
C     NOW COMPUTE THE MODAL DAMPING RATIOS (STORED IN VECTOR
C        D).
C
      DO  8 I=1,NM
      D(I)=0.
      DO 8 J=1,NM
      D(I)=EN(J,I)*B(J)+D(I)
    8 CONTINUE
      DO 13 I=1,NM
      D(I)=D(I)/ET(I)
   13 CONTINUE
      DO 9 I=1,NM
      WRITE(6,12) I,D(I)
    9 CONTINUE
   12 FORMAT(/10X,'MODAL DAMPING FOR MODE',I1,'=',E10.3)
      RETURN
      END
      SUBROUTINE INDAMP(N)
      COMMON /DYN/RMASS(12),DAMP(12,12),CK(6),CFORCE(12),EQF
     C  OR(12),
     1RKFOR(12),OLDFOR(12),RINFOR(12),ACC(12),DISP(12),VEL(1
     C  2),
     2OLDVEL(12),OLDACC(12),SHEAR(12),OLDSHR(12),REL(12),OLD
     C  AMP(12),
     3SHEARK(5),GLOK(12,12),NCR(5),OLDCK(6),NLDIPD(5),OLDREL
     C  (12),RK(8)
     4,TK(6),OLDISP(12)
      COMMON /EIG/OMEGA(12),A(12,12),ATR(12,12),D(12)
      DIMENSION C(12,12)
C
C
C     FROM MODAL ANALYSIS,DAMP(N,N)=INV(ATR(N,N))*CBAR(N,N)*
C        INV(A(N,N))
C     WHERE CBAR(N,N) IS A DIAGONAL MATRIX WITH THE TERMS C(
C        I,I)2.*D(I)
C     *OMEGA(I).THE FOLLOWING STATEMENTS COMPUTE DAMP(N,N) U
C        SING THE
C     FACT THAT INV(A(N,N))=ATR(N,N)*RMASS(N,N).
C
```

```
      DO 1 I=1,N
      DO 1 J=1,N
      C(I,J)=2.*D(J)*OMEGA(J)*A(I,J)*RMASS(I)
    1 CONTINUE
      CALL MULT(C,ATR,DAMP,N)
      DO 2 I=1,N
      DO 2 J=1,N
      DAMP(I,J)=DAMP(I,J)*RMASS(J)
    2 CONTINUE
      DO 3 I=1,N
    3 WRITE(6,4) (DAMP(I,J),J=1,N)
    4 FORMAT(/10X,7E14.7)
      RETURN
      END
      SUBROUTINE INQUAK(T,NTP,N,H,IFLAG)
      COMMON /DYN/RMASS(12),DAMP(12,12),CK(6),CFORCE(12),EQF
     C  OR(12),
     1RKFOR(12),OLDFOR(12),RINFOR(12),ACC(12),DISP(12),VEL(1
     C  2),
     2OLDVEL(12),OLDACC(12),SHEAR(12),OLDSHR(12),REL(12),OLD
     C  AMP(12),
     3SHEARK(5),GLOK(12,12),NCR(5),OLDCK(6),NLDIPD(5),OLDREL
     C  (12),RK(8)
     4,TK(6),OLDISP(12)
C
C
C     THIS SUBROUTINE READS IN THE GROUND ACCELERATION HISTO
C        RY AND
C     KEEPS TRACK OF THE CURRENT VALUE OF THE GROUND ACCELER
C        ATION.
C
      DIMENSION GRACC(10),TIME(10)
      IF (IFLAG.EQ.1) GO TO 44
      IFLAG=1
      DO 100 I=1,NTP
      READ(5,101) TIME(I),GRACC(I)
  101 FORMAT(2F10.0)
  100 CONTINUE
      DO 55 I=1,N,2
      EQFOR(I)=-RMASS(I)*GRACC(1)*38.64
      EQFOR(I+1)=0.
   55 CONTINUE
      GO TO 200
C
C     NOW FIND THE CURRENT VALUE OF THE GROUND ACCELERATION
C        X.
C
   44 CONTINUE
      IF (T.GT.TIME(NTP)) GO TO 200
      I=1
  102 I=I+1
      IF (I.GT.NTP) GO TO 150
      IF (T.GT.TIME(I)) GO TO 102
      IF (T.LT.TIME(I-1)) GO TO 102
      J=I-1
```

```
C
C       J IDENTIFIES WHICH OF THE STRAIGHT LINE SEGMENTS CONTA
C         INS THE
C       CURRENT GROUND ACCELERATION.
C
        SLOPE=(GRACC(J+1)-GRACC(J))/(TIME(J+1)-TIME(J))
        X=GRACC(J)+(T-TIME(J))*SLOPE
        DO 98 I=1,N,2
        EQFOR(I)=-RMASS(I)*X*386.4
        EQFOR(I+1)=0.
   98 CONTINUE
        GO TO 200
  150 WRITE(6,151)
  151 FORMAT(20X,'THE GROUND ACCELERATION CORRESPONDING TO T
    C  IME T HAS
    1NOT BEEN FOUND'/)
  200 CONTINUE
        RETURN
        END
        SUBROUTINE JACOBY(N,K)
        COMMON /DYN/RMASS(12),DAMP(12,12),CK(6),CFORCE(12),EQF
    C  OR(12),
    1RKFOR(12),OLDFOR(12),RINFOR(12),ACC(12),DISP(12),VEL(1
    C  2),
    2OLDVEL(12),OLDACC(12),SHEAR(12),OLDSHR(12),REL(12),OLD
    C  AMP(12),
    3SHEARK(5),GLOK(12,12),NCR(5),OLDCK(6),NLDIPD(5),OLDREL
    C  (12),RK(8)
    4,TK(6),OLDISP(12)
        COMMON /EIG/OMEGA(12),A(12,12),ATR(12,12),D(12)
        DIMENSION EM(12),STB(12,12),T(12,12),TT(12,12),B(12,12
    C  ),
    1ST(12,12),A1(12,12)
        DIMENSION C(12,12)
C
C       THIS SUBROUTINE CALCULATES EIGENVECTORS AND EIGENVALUE
C         S
C       FROM A GIVEN STIFFNESS MATRIX AND MASS VECTOR. N IS TH
C         E
C       NUMBER OF STRUCTURAL DEGREES OF FREEDOM IN THE SYSTEM,
C       EM IS THE MASS VECTOR AND ST IS THE STRUCTURAL STIFFNE
C         SS MATRIX.
C       ONLY THE STRUCTURAL PORTION OF THE GLOBAL STIFFNESS MA
C         TRIX
C       IS DIAGONALIZED SO THE FREQUENCIES AND MODE SHAPES ARE
C         FOR
C       A FIXED BASE STRUCTURE.
C
        DO 75 I=1,N
        DO 75 J=1,N
        ST(I,J)=GLOK(I,J)
   75 CONTINUE
        DO 76 I=1,N
        EM(I)=RMASS(I)
```

```
   76 CONTINUE
      CALL PRINT5(ST,N)
      CALL UNIT(A1,N)
C
C     STB=(1/SQRT(EM))*(ST)*(1/SQRT(EM)). THE STIFFNESS MATR
C       IX
C     ST IS TRANSFORMED INTO A FORM IN WHICH THE JACOBI METH
C       OD
C     CAN BE APPLIED.
C
      DO 10 I=1,N
   10 EM(I)=SQRT(EM(I))
      DO 12 I=1,N
      DO 12 J=1,N
   12 STB(I,J)=ST(I,J)/(EM(J)*EM(I))
      DO 20 KK=1,K
      DO 15 I=1,N
      DO 15 J=I,N
      IF (I-J) 14,15,14
C
C     T IS A UNIT MATRIX EXCEPT FOR T(I,I),T(J,J),T(I,J),
C     AND T(J,I). BY PRE AND POST MULTIPLYING STB BY T THE
C     ELEMENT STB(I,J) IS SET=0. THIS ACTUALLY A SERIES OF
C     ORTHOGONAL TRANSFORMATIONS TO DIAGONALIZE STB.AFTER ST
C       B
C     IS DIAGONALIZED IT WILL CONTAIN THE EIGENVALUES ON ITS
C     MAIN DIAGONAL.
C
   14 IF (ABS(STB(I,J)).LT.1.0E-10) GO TO 15
      CALL UNIT(T,N)
      DIFF=STB(I,I)-STB(J,J)
      IF (ABS(DIFF)-.00005D0) 30,30,32
   30 TH=.785398E0
      GO TO 33
   32 THC=2.0E0*STB(I,J)/DIFF
      TH=.5E0*ATAN(THC)
   33 T(I,I)=COS(TH)
      T(J,J)=T(I,I)
      T(I,J)=-SIN(TH)
      T(J,I)=-T(I,J)
C
C     CALCULATE THE TRANSPOSE OF T (TT).
C
      CALL TRA(T,TT,N)
C
C     TT*STB*T=STB
C
      CALL PRMULT(STB,TH,I,J,N)
      CALL POMULT(STB,TH,I,J,N)
C
C     A1*T=A1. A1 STORES THE RESULTS OF
C     T1*T2*T3....TK.(THERE ARE K ITERATIONS).A1=SQRT(EM)*A
C     WHERE A IS THE MODAL MATRIX.T1 IS T FOR THE FIRST ITERA
C       TION
```

```
C      T2 IS T FOR THE SECOND ITERATION UP TO TK FOR THE KTH
C      ITERATION.
C
       CALL POMULT(A1,TH,I,J,N)
   15 CONTINUE
C
C      THE MODAL MATRIX A=(1/SQRT(EM))*A1.THE FIRST ROW OF A
C      IS NORMALIZED TO 1
C
       DO 18 J=1,N
       DO 18 I=1,N
   18 A(I,J)=A1(I,J)/EM(I)
   20 CONTINUE
       DO 50 I=1,N
       OMEGA(I)=SQRT(STB(I,I))
   50 CONTINUE
C
C      SORT FREQUENCIES AND EIGENVECTORS STARTING FROM MODE 1
C          (LOWEST)
C      AND GOING UP TO MODE N.
C
       NN=N-1
       DO 80 I=1,NN
       L=I+1
       DO 9 K=L,N
       IF (OMEGA(K).GT.OMEGA(I)) GO TO 9
       WX=OMEGA(I)
       OMEGA(I)=OMEGA(K)
       OMEGA(K)=WX
       DO 300 II=1,N
       AX=A(II,I)
       A(II,I)=A(II,K)
       A(II,K)=AX
  300 CONTINUE
    9 CONTINUE
   80 CONTINUE
C
C      PRINT OUT THE NATURAL FREQUENCIES AND EIGENVECTORS.
C
       DO 11 I=1,N
   11 WRITE(6,122) I,OMEGA(I)
  122 FORMAT(/10X,'FREQUENCY',I5,'=',F10.2)
       CALL PRINT5(A,N)
       CALL TRA(A,ATR,N)
       RETURN
       END
       SUBROUTINE MULT(A,B,C,N)
       DIMENSION A(12,12),B(12,12),C(12,12)
       DO 10 I=1,N
       DO 10 J=1,N
       C(I,J)=0.0E0
       DO 10 L=1,N
   10 C(I,J)=C(I,J)+A(I,L)*B(L,J)
       RETURN
```

```fortran
      END
      SUBROUTINE UNIT(A,N)
      DIMENSION A(12,12)
      DO 10 I=1,N
      DO 8 J=1,N
    8 A(I,J)=0.0E0
   10 A(I,I)=1.0E0
      RETURN
      END
      SUBROUTINE TRA(A,B,N)
      DIMENSION A(12,12),B(12,12)
      DO 10 I=1,N
      DO 10 J=1,N
   10 B(I,J)=A(J,I)
      RETURN
      END
      SUBROUTINE POMULT(STB,TH,I,J,N)
      DIMENSION STB(12,12),C(12,2)
      DO 1 II=1,N
      C(II,1)=STB(II,I)*COS(TH)+STB(II,J)*SIN(TH)
      C(II,2)=STB(II,J)*COS(TH)-STB(II,I)*SIN(TH)
    1 CONTINUE
      DO 2 II=1,N
      STB(II,I)=C(II,1)
      STB(II,J)=C(II,2)
    2 CONTINUE
      RETURN
      END
      SUBROUTINE PRMULT(STB,TH,I,J,N)
      DIMENSION STB(12,12),C(2,12)
      DO 1 JJ=1,N
      C(1,JJ)=STB(I,JJ)*COS(TH)+STB(J,JJ)*SIN(TH)
      C(2,JJ)=STB(J,JJ)*COS(TH)-STB(I,JJ)*SIN(TH)
    1 CONTINUE
      DO 2 JJ=1,N
      STB(I,JJ)=C(1,JJ)
      STB(J,JJ)=C(2,JJ)
    2 CONTINUE
      RETURN
      END
      SUBROUTINE PRINT5(A,N)
      DIMENSION A(12,12)
      WRITE(6,20)
      DO 10 I=1,N
   10 WRITE(6,12) (A(I,J),J=1,N)
   12 FORMAT(10X,10E10.3)
   20 FORMAT(//)
      RETURN
      END
      SUBROUTINE CYCLE(N,LFLAG,DINC)
C
C     THIS SUBROUTINE KEEPS TRACK OF WHICH CYCLE OF LOADING
C     EACH CRACK IN THE VESSEL IS ON. THE LOAD CYCLE NUMBER
C       FOR ALL
```

```
C     THE CRACKS IN THE ITH BEAM SEGMENT IS STORED IN NCYCLE
C         (I).
C     AT T=0, NCYCLE(I)=1. THE FIRST CYCLE CRACK STIFFNESS I
C         S
C     LINEAR WITH NO HYSTERESIS LOOP.
C
      COMMON /DYN/RMASS(12),DAMP(12,12),CK(6),CFORCE(12),EQF
C     OR(12),
     1RKFOR(12),OLDFOR(12),RINFOR(12),ACC(12),DISP(12),VEL(1
C     2),
     2OLDVEL(12),OLDACC(12),SHEAR(12),OLDSHR(12),REL(12),OLD
C     AMP(12),
     3SHEARK(5),GLOK(12,12),NCR(5),OLDCK(6),NLDIPD(5),OLDREL
C     (12),RK(8)
     4,TK(6),OLDISP(12)
      COMMON /B/RLOAD(6),DELTA(6),IPD(5),NCYCLE(5),RLOADN(5,
C     6),
     1DELTAN(5,6)
      DIMENSION PEAK(5)
      IF (LFLAG.GT.0) GO TO 2
      LFLAG=1
      DO 1 I=1,N
      PEAK(I)=0.
    1 NCYCLE(I)=1
      GO TO 45
C
C     THE PEAK SHEAR STRESS FOR THE CURRENT LOAD CYCLE IS ST
C         ORED
C     IN PEAK(I) FOR THE ITH BEAM SEGMENT.
C
    2 DO 10 I=1,N
      IF (ABS(SHEAR(I)).LE.ABS(PEAK(I))) GO TO 10
      PEAK(I)=SHEAR(I)
   10 CONTINUE
C
C     FOR THE FIRST CYCLE, IF ABS(PEAK(I)) IS GT RLOAD(1) AN
C         D
C     UNLOADING IS OCCURING THEN THE SECOND CYCLE HYSTERESIS
C     LOOP IS SWITCHED TO.
C
      DO 3 I=1,N
      IF (ABS(SHEAR(I)).GE.ABS(OLDSHR(I))) GO TO 3
      IF (NCYCLE(I).GT.1) GO TO 4
      IF (ABS(PEAK(I)).LT.RLOAD(1)) GO TO 3
      IF (PEAK(I).LT.0.) GO TO 8
      IPD(I)=3
      CK(I)=RK(3)
      PEAK(I)=0.
      NCYCLE(I)=NCYCLE(I)+1
      GO TO 3
C
C     AFTER THE FIRST CYCLE THE DEFINITION OF AN ADDITIONAL
C     LOAD CYCLE CHANGES. IF ABS(PEAK(I)) GT .1KSI AND ABS(
C     SHEAR(I)) LT .05 KSI THEN NCYCLE(I) IS INCREASED BY 1.
```

```
C      THE HYSTERESIS LOOP FOR THE ITH BEAM SEGMENT, AS DEFIN
C         ED BY
C      DELTAN(I,1.....6) AND RLOADN(I,1....6) ARE CHANGED
C      ACCORDINGLY.
C

    8 IPD(I)=7
      CK(I)=RK(7)
      PEAK(I)=0.
      NCYCLE(I)=NCYCLE(I)+1
      GO TO 3
    4 IF (IPD(I).EQ.3) GO TO 5
      IF (IPD(I).EQ.7) GO TO 6
      GO TO 3
    5 IF (ABS(PEAK(I)).LT..1) GO TO 3
      IF (SHEAR(I).GT..05) GO TO 3
      GO TO 7
    6 IF (ABS(PEAK(I)).LT..1) GO TO 3
      IF (SHEAR(I).LT.(-.05)) GO TO 3
    7 NCYCLE(I)=NCYCLE(I)+1
      PEAK(I)=0.
      DELTAN(I,1)=DELTAN(I,1)+DINC
      DELTAN(I,2)=DELTAN(I,2)+DINC
      DELTAN(I,4)=-DELTAN(I,1)
      DELTAN(I,5)=-DELTAN(I,2)
      DELTAN(I,3)=(RLOAD(2)-RLOAD(4)+RK(4)*DELTAN(I,4)-RK(3)
    C  *DELTAN(
     1I,2))/(RK(4)-RK(3))
      RLOADN(I,3)=RK(4)*(DELTAN(I,3)-DELTAN(I,4))+RLOAD(4)
      DELTAN(I,6)=-DELTAN(I,3)
      RLOADN(I,6)=-RLOADN(I,3)
    3 CONTINUE
   45 RETURN
      END
      SUBROUTINE INHYST(H,T,OH,N,JFLAG,PRINT,KREF,NFLAG)
C
C      INHYST KEEPS TRACK OF WHERE THE SHEAR STRESS IN EACH B
C         EAM
C      SEGMENT IS IN THE CYCLE DEPENDENT HYSTERESIS LOOPS.
C      THE CRACK STIFFNESS FOR THE ITH BEAM SEGMENT IS CK(I).
C
      DIMENSION TI(10),VPRINT(10)
      COMMON /DYN/RMASS(12),DAMP(12,12),CK(6),CFORCE(12),EQF
    C  OR(12),
     1RKFOR(12),OLDFOR(12),RINFOR(12),ACC(12),DISP(12),VEL(1
    C  2),
     2OLDVEL(12),OLDACC(12),SHEAR(12),OLDSHR(12),REL(12),OLD
    C  AMP(12),
     3SHEARK(5),GLOK(12,12),NCR(5),OLDCK(6),NLDIPD(5),OLDREL
    C  (12),RK(8)
     4,TK(6),OLDISP(12)
      COMMON /B/RLOAD(6),DELTA(6),IPD(5),NCYCLE(5),RLOADN(5,
    C  6),
     1DELTAN(5,6)
      IF (JFLAG.GT.0) GO TO 202
```

```
      JFLAG=1
      PRTIM=0.
      OLDTIM=0.
      READ(5,13) NTI
   13 FORMAT(I5)
      PRTOL=H/10.
      READ(5,101) (TI(I),I=1,NTI)
      READ(5,101) (VPRINT(I),I=1,NTI)
      PRINT=VPRINT(1)
      JJ=1
  101 FORMAT(10F8.0)
C
C     THE INITIAL STIFFNESS IS ASSUMED TO BE RK(1)
C
      DO 46 I=1,N
      CK(I)=RK(1)
      IPD(I)=1
      NCYCLE(I)=1
   46 CONTINUE
      GO TO 500
C
C     IPD IDENTIFIES WHICH LINEAR SEGMENT OF THE HYSTERESIS
C        LOOP YOU
C     ARE ON.
C
  202 CONTINUE
      DO 131 L=1,N
      OLDCK(L)=CK(L)
      NLDIPD(L)=IPD(L)
  131 CONTINUE
      DO 299 I=1,N
      IF (IPD(I).EQ.8) GO TO 212
      IF (IPD(I).GE.3) GO TO 205
      IF (IPD(I).GT.1) GO TO 204
C
C     IPD HAS BEEN TESTED TO SEE IF IT IS EQUAL TO 1.THE
C     SHEAR STRESS IS THEN CHECKED TO SEE IF IT IS NEGATIVE.
C        IF SO,
C     THE STIFFNESS CK IS SET EQUAL TO RK(5),THE INITIAL
C     NEGATIVE STIFFNESS.
C
      IF (SHEAR(I).GE.0.) GO TO 299
      IPD(I)=5
      CK(I)=RK(5)
      GO TO 299
C
C     CHECK TO SEE IF A CHANGE OF STIFFNESS HAS OCCURED DURI
C        NG THE
C     LAST TIME STEP.IN THIS CASE THE STIFFNESS CK HAS CHANG
C        ED
C     FROM RK(1) TO RK(2).
C
C
C     THE STATEMENTS BELOW PERTAIN TO CRACKS ON THE RK(2) SE
```

```
C          CTION OF
C       THE LOOP. A CHECK IS MADE TO SEE WHETHER UNLOADING HAS
C          STARTED
C       DURING THE LAST TIME STEP. IF SO, THE STIFFNESS BECOME
C        S RK(3).
C
  204 IF (SHEAR(I).GE.OLDSHR(I)) GO TO 299
      IPD(I)=3
      CK(I)=RK(3)
      GO TO 299
  205 IF (IPD(I).GT.3) GO TO 207
C
C       THE FOLLOWING STATEMENTS DEAL WITH CRACKS ON THE RK=RK
C        (3)
C       SECTION OF THE HYSTERESIS LOOP. A CHECK IS MADE TO SEE
C          IF THE
C       RK(4) BRANCH HAS BEEN REACHED.
C
      IF (SHEAR(I).LT.OLDSHR(I)) GO TO 29
      IF (SHEAR(I).LT.RLOAD(1)) GO TO 68
      IPD(I)=2
      CK(I)=RK(2)
      GO TO 299
   68 IPD(I)=4
      CK(I)=RK(4)
      GO TO 299
   29 FLAG3=RLOADN(I,3)+(REL(I)-DELTAN(I,3))*RK(4)
      IF (SHEAR(I).GT.(FLAG3+.05*RLOAD(1))) GO TO 299
C
C       NOW CHECK TO SEE HOW MUCH FLAG3 HAS BEEN EXCEEDED BY.
C          THE
C       ACCEPTABLE ERROR IS 5 PER CENT. IF THE ERROR IS GREATE
C        R THAN
C       THIS GO BACK TO THE LAST TIME STEP AND USE A SMALLER H
C         .
C
      ERROR=SHEAR(I)-FLAG3
      IF (ABS(ERROR).LE.ABS(.05*RLOAD(1))) GO TO 300
      IF (OLDSHR(I).GT.FLAG3) GO TO 90
      OLDCK(I)=RK(4)
      NLDIPD(I)=4
      KREF=1
      GO TO 60
   90 H=((FLAG3-OLDSHR(I))/(SHEAR(I)-OLDSHR(I)))*H
      GO TO 59
  300 CONTINUE
  301 IPD(I)=4
      CK(I)=RK(4)
      GO TO 299
C
C       THE FOLLOWING STATEMENTS CHECK TO SEE IF THE CRACK STI
C          FFNESS
C       EQUALS RK(4). IF SO ,A CHECK IS MADE TO SEE IF RELOADI
C          NG IS
```

```
C       OCCURING. IF IT IS AND SHEAR(I) IS GREATER THAN RLOAD(
C          1) THEN THE
C       STIFFNESS IS CHANGED TO RK(2). IF NO RELOADING HAS OCC
C          URED
C       A CHECK IS MADE TO SEE IF A CHANGE TO RK(6) SHOULD BE
C          MADE.
C
  207 IF (IPD(I).GT.4) GO TO 209
      IF (SHEAR(I).LE.OLDSHR(I)) GO TO 208
      IF (SHEAR(I).LT.RLOAD(1)) GO TO 299
      IPD(I)=2
      CK(I)=RK(2)
      GO TO 299
  208 IF (RLOAD(4).LT.SHEAR(I)) GO TO 299
      IPD(I)=6
      CK(I)=RK(6)
      GO TO 299
C
C       THE FOLLOWING STATEMENTS APPLY TO CK=RK(5). A CHANGE O
C          F
C       STIFFNESS IS CHECKED FOR.
C
  209 IF (IPD(I).GT.5) GO TO 210
      IF (SHEAR(I).LT.0.) GO TO 299
      IPD(I)=1
      CK(I)=RK(1)
      GO TO 299
C
C       THE FOLLOWING STATEMENTS APPLY TO CK=RK(6). RELOADING
C          IS CHECKED
C       FOR.
C
  210 IF (IPD(I).GT.6) GO TO 211
      IF (SHEAR(I).LE.OLDSHR(I)) GO TO 299
      IPD(I)=7
      CK(I)=RK(7)
      GO TO 299
C
C       THE FOLLOWING STATEMENTS APPLY TO CK=RK(7). A CHANGE O
C          F STIFFNESS
C       IS CHECKED FOR.
C
  211 IF (SHEAR(I).GT.OLDSHR(I)) GO TO 39
      IF (SHEAR(I).GT.RLOAD(4)) GO TO 78
      IPD(I)=6
      CK(I)=RK(6)
      GO TO 299
   78 IPD(I)=8
      CK(I)=RK(8)
      GO TO 299
   39 FLAG6=RLOADN(I,6)+(REL(I)-DELTAN(I,6))*RK(8)
      IF (SHEAR(I).LT.(FLAG6-.05*RLOAD(1))) GO TO 299
C
C       CHECK TO SEE HOW MUCH FLAG6 HAS BEEN EXCEEDED BY. THE
```

```
C        ACCEPTABLE ERROR IS 5 PER CENT. IF THIS IS EXCEEDED TH
C          EN GO BACK T
C        LAST TIME STEP AND USE A SMALLER H.
C
         ERROR=SHEAR(I)-FLAG6
         IF (ABS(ERROR).LE.ABS(.05*RLOAD(1))) GO TO 400
         IF (OLDSHR(I).LT.FLAG6) GO TO 91
         OLDCK(I)=RK(8)
         NLDIPD(I)=8
         KREF=1
         GO TO 60
   91 H=((FLAG6-OLDSHR(I))/(SHEAR(I)-OLDSHR(I)))*H
         GO TO 59
  400 CONTINUE
  401 IPD(I)=8
         CK(I)=RK(8)
         GO TO 299
C
C        THE FOLLOWING STATEMENTS APPLY TO IPD=1,CK=RK(8).CHANG
C          E OF
C        STIFFNESS AND UNLOADING ARE CHECKED FOR.
C
  212 IF (SHEAR(I).GE.OLDSHR(I)) GO TO 213
         IF (SHEAR(I).GT.RLOAD(4)) GO TO 299
         IPD(I)=6
         CK(I)=RK(6)
         GO TO 299
  213 IF (SHEAR(I).LT.RLOAD(1)) GO TO 299
         IPD(I)=2
         CK(I)=RK(2)
  299 CONTINUE
         H=OH
         KREF=0
         DO 99 I=1,N
         IF (NLDIPD(I).EQ.IPD(I)) GO TO 99
         KREF=1
   99 CONTINUE
         IF (T.LT.10.) GO TO 94
         IF (T.GT.10.8) GO TO 94
         WRITE(6,93) T,SHEAR(5),REL(5),NLDIPD(5)
   93 FORMAT(/10X,3E14.7,I5)
   94 CONTINUE
         IF ((T+PRTOL-PRTIM).LT.0.) GO TO 450
         IF (ABS(T-PRTIM).LE.PRTOL) GO TO 17
         H=PRTIM-OLDTIM
   59 CONTINUE
         KREF=0
   60 NFLAG=1
         T=OLDTIM
         DO 89 K=1,N
         IPD(K)=NLDIPD(K)
         SHEAR(K)=OLDSHR(K)
         REL(K)=OLDREL(K)
         CK(K)=OLDCK(K)
```

```
   89 CONTINUE
      DO 189 K=1,12
      DISP(K)=OLDISP(K)
      VEL(K)=OLDVEL(K)
      ACC(K)=OLDACC(K)
      RKFOR(K)=OLDFOR(K)
      RINFOR(K)=RMASS(K)*ACC(K)
      CFORCE(K)=OLDAMP(K)
  189 CONTINUE
      GO TO 461
C
C     PRINT OUT DYNAMIC RESULTS AT TIME=T.
C
   17 CONTINUE
      WRITE(6,12) (NCYCLE(I),I=1,N)
   12 FORMAT(/10X,5I5)
      WRITE(6,22) T
   22 FORMAT(/10X,'FOR TIME = ',F8.2,8X,'DISPLACEMENT',8X,
     1'SHEAR STRESS',9X,'CRACK DISP',10X,'STIFFNESS'/)
      DO 73  I=1,N
      WRITE(6,76) DISP(2*I-1),SHEAR(I),REL(I),OLDCK(I)
   76 FORMAT(36X,E14.7,6X,E14.7,6X,E14.7,6X,E14.7)
   73 CONTINUE
      IF (T.LT.TI(JJ)) GO TO 5
      JJ=JJ+1
      PRINT=VPRINT(JJ)
    5 PRTIM=PRTIM+PRINT
  450 OLDTIM=T
  461 T=T+H
  500 RETURN
      END
```

TABLE 2.1

INCREMENTAL LOADS FOR THE SAP IV MODEL

Step	Load*	Bars with E_2 Modulus
1	20 $\cos\phi$	None
2	1 $\cos\phi$	1, 10, 19
3	2 $\cos\phi$	1, 2, 10, 11, 19, 20
4	4 $\cos\phi$	1-3, 10-12, 19-21
5	6 $\cos\phi$	1-4, 10-13, 19-22
6	9 $\cos\phi$	1-5, 10-14, 19-23
7	23 $\cos\phi$	1-6, 10-15, 19-24
8	77 $\cos\phi$	1-7, 10-16, 19-25
9	138 $\cos\phi$	1-8, 10-17, 19-26
Total	280 $\cos\phi$	

* These loads are shear stress distributions which are converted to equivalent nodal loads using equations (2.4).

TABLE 3.1

BEAM ELEMENT STIFFNESS MATRIX

$$[K_E] = \frac{EI}{1 + 4\lambda} \begin{bmatrix} \frac{12}{L^3} & -\frac{6}{L^2} & -\frac{12}{L^3} & -\frac{6}{L^2} \\ -\frac{6}{L^2} & \frac{4}{L}(1 + \lambda) & \frac{6}{L^2} & \frac{2}{L}(1 - 2\lambda) \\ -\frac{12}{L^3} & \frac{6}{L^2} & \frac{12}{L^3} & \frac{6}{L^2} \\ -\frac{6}{L^2} & \frac{2}{L}(1 - 2\lambda) & \frac{6}{L^2} & \frac{4}{L}(1 + \lambda) \end{bmatrix}$$

$$\lambda = \frac{3EI}{L^3} \frac{L}{A_s G}$$

TABLE 3.2

GLOBAL STIFFNESS MATRIX

$$
\begin{array}{ccccc}
u_1\theta_1 & u_2\theta_2 & u_3\theta_3 & u_4\theta_4 & u_5\theta_5 \\
\end{array}
$$

$$
\begin{bmatrix}
K_{11} & -K_{12} & 0 & 0 & 0 \\
-K_{21} & K_{11}' + K_{22} & K_{23} & 0 & 0 \\
0 & -K_{32} & K_{22}' + K_{33} & -K_{34} & 0 \\
0 & 0 & -K_{43} & K_{33}' + K_{44} & -K_{45} \\
0 & 0 & 0 & -K_{54} & K_{44}' + K_{55}
\end{bmatrix}
$$

$$
K_{ii} = \frac{EI_i}{1+4\lambda_i}
\begin{bmatrix}
\dfrac{12}{L_i^{\,3}} & -\dfrac{6}{L_i^{\,2}} \\[2ex]
-\dfrac{6}{L_i^{\,2}} & \dfrac{4}{L_i}(1+\lambda_i)
\end{bmatrix}
\qquad
K_{ii}' = \frac{EI_i}{1+4\lambda_i}
\begin{bmatrix}
\dfrac{12}{L_i^{\,3}} & \dfrac{6}{L_i^{\,2}} \\[2ex]
\dfrac{6}{L_i^{\,2}} & \dfrac{4}{L_i}(1+\lambda_i)
\end{bmatrix}
$$

$$
K_{ij} = \frac{EI_i}{1+4\lambda_i}
\begin{bmatrix}
-\dfrac{12}{L_i^{\,3}} & -\dfrac{6}{L_i^{\,2}} \\[2ex]
\dfrac{6}{L_i^{\,2}} & \dfrac{2}{L_i}(1-2\lambda_i)
\end{bmatrix}
\qquad
M_{ij} = K_{ij}^{\,T}
$$

TABLE 3.3

NATURAL FREQUENCIES (CYCLES/SEC)

Mode	10 DOF	5 DOF
1	6.0	7.5
2	15.3	18.4
3	24.0	31.2
4	30.2	43.9
5	43.2	51.0
6	43.5	----
7	50.6	----
8	68.2	----
9	94.5	----
10	109.2	----

TABLE 4.1

Soil Type	C_2(fps)	K_u(k/in)	K_ϕ(k-in/rad)
Soft Soil	500	30,647	2.184×10^{10}
Medium Soil	1,200	176,528	1.258×10^{11}
Hard Soil	2,000	490,356	3.494×10^{11}

TABLE 4.2

$$
\begin{array}{cccccc}
u_1\theta_1 & u_2\theta_2 & u_3\theta_3 & u_4\theta_4 & u_5\theta_5 & u_f\phi_f
\end{array}
$$

$$
\begin{bmatrix}
K_{11} & K_{12} & 0 & 0 & 0 & 0 \\
K_{21} & K_{11}' + K_{22} & K_{23} & 0 & 0 & 0 \\
0 & K_{32} & K_{22}' + K_{33} & K_{34} & 0 & 0 \\
0 & 0 & K_{43} & K_{33}' + K_{44} & K_{45} & 0 \\
0 & 0 & 0 & K_{54} & K_{44}' + K_{55} & K_{5f} \\
0 & 0 & 0 & 0 & K_{f5} & K_{55}' + K_{ff}
\end{bmatrix}
$$

$$
K_{ff} = \begin{bmatrix} K_u & 0 \\ 0 & K_\phi \end{bmatrix}
\qquad
K_{5f} = \frac{EI_5}{1 + 4\lambda_5} \begin{bmatrix} -\dfrac{12}{h_5^2} & -\dfrac{6}{h_5^2} \\[2ex] \dfrac{6}{h_5^2} & \dfrac{2}{h_5}(1 - 2\lambda_5) \end{bmatrix}
$$

$$
K_{f5} = K_{5f}^{T}
$$

TABLE 5.1

$$|K|_{Element} = \frac{1}{det} \begin{bmatrix} \left(\dfrac{L}{EI} + C\right) & -\left(\dfrac{L^2}{2EI} + B\right) & -\left(\dfrac{L}{EI} + C\right) & \left(B - \dfrac{L^2}{2EI} - CL\right) \\[3mm] -\left(\dfrac{L^2}{2EI} + B\right) & \left(\dfrac{L^3}{3EI} + \dfrac{L}{GA_s} + \dfrac{N}{K_c} + A\right) & \left(\dfrac{L^2}{2EI} + B\right) & \left(\dfrac{L^3}{6EI} + BL - \dfrac{L}{GA_s} - \dfrac{N}{K_c} - A\right) \\[3mm] -\left(\dfrac{L}{LI} + C\right) & \left(\dfrac{L^2}{2EI} + B\right) & \left(\dfrac{L}{EI} + C\right) & \left(\dfrac{L^2}{2EI} + B\right) \\[3mm] \left(B - \dfrac{L^2}{2EI} - CL\right) & \left(\dfrac{L^3}{6EI} + BL - \dfrac{L}{GA_s} - \dfrac{N}{K_c} - A\right) & \left(\dfrac{L^2}{2EI} + B\right) & \left(\dfrac{L^3}{3EI} + \dfrac{L}{GA_s} + \dfrac{N}{K_c} + A\right) \end{bmatrix}$$

$$A = \left(\frac{1}{I_c} - \frac{1}{I}\right) \frac{L^2 L_u}{E} \sum_{i=1}^{N} \left(\frac{2i-1}{2N}\right)^2 \qquad B = \left(\frac{1}{I_c} - \frac{1}{I}\right) \frac{LL_u}{E} \sum_{i=1}^{N} \left(\frac{2i-1}{2N}\right) \qquad C = \left(\frac{1}{I_c} - \frac{1}{I}\right) \frac{NL_u}{E}$$

$$det = \frac{L^4}{12E^2 I^2} + \frac{L}{EI}\left(\frac{L}{GA_s} + \frac{N}{K_c}\right) + \frac{AL}{EI} + C\left(\frac{L^3}{3EI} + \frac{L}{GA_s} + \frac{N}{K_c} + A\right) - \frac{BL^2}{EI} - B^2$$

TABLE 5.2

Run	Displacement (inches)	Shear Stress (psi)	Crack Slip (inches)	Cycles
1	1.330	288	-----	----
2	1.543	272	.0136	18
3	2.565	126	.0125	7
4	1.200	280	.0143	25

TABLE 5.3

Run	Concrete Stress (ksi)	Steel Stress (ksi)	Change in Crack Width (inches)
1	----	-----	-----
2	.599	25.10	.0022
3	.237	9.93	.0009
4	.696	29.17	.0025

TABLE 5.4

Beam	I (in^4)		I_c (in^4)		A_s (in^2)
1	4.483	10^{10}	1.074	10^{10}	97,270
2	6.202	10^{10}	1.179	10^{10}	142,000
3	6.202	10^{10}	1.179	10^{10}	142,000
4	6.202	10^{10}	1.179	10^{10}	142,000
5	6.202	10^{10}	1.179	10^{10}	142,000

TABLE 5.5

Run	Soil Type	Crack Spacing
1	Medium	-------
2	Medium	5' - 6"
3	Soft	5' - 6"
4	Hard	5' - 6"

TABLE 5.6

DOF	u_1, θ_1	u_2-u_5, θ_2-θ_5	u_f, ϕ_f
Mass $(k\text{-}sec^2/in)$	28.82	22.97	61.74
Mass Moment $(k\text{-}sec^2\text{-}in \times 10^6)$	8.17	8.29	12.74

DOF = Degree of Freedom

TABLE 5.7

Mode	1	2	3
a_1	240.38	1070.33	443.02
a_2	5.78	4.27	- 2.25
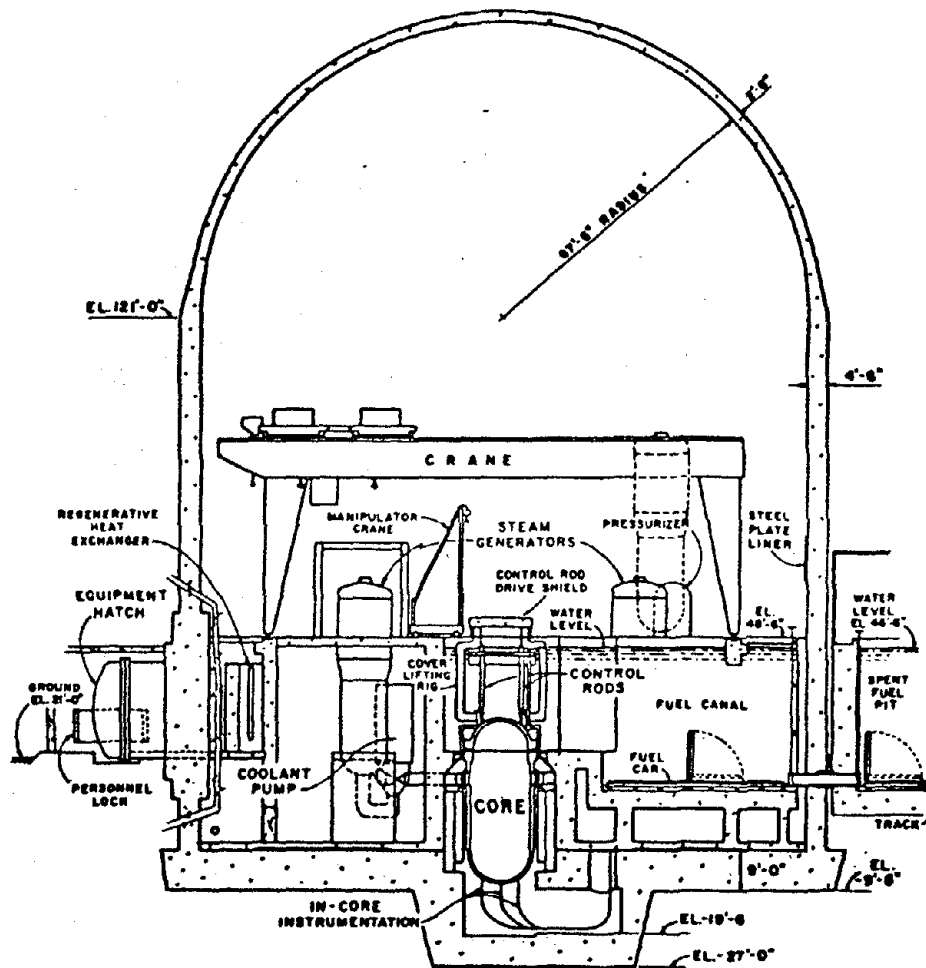
Figure 1.1 - Typical Nuclear Containment Vessel
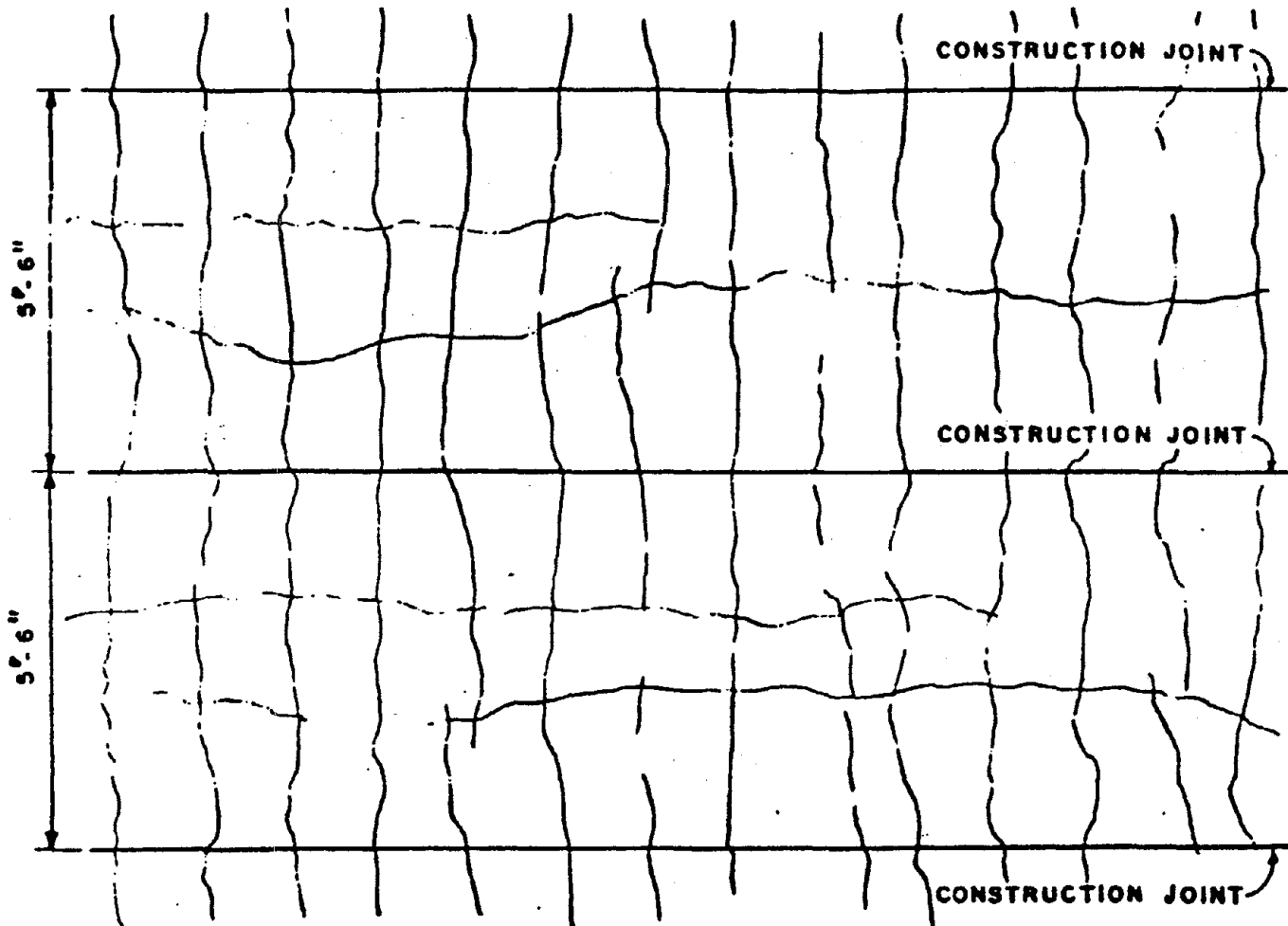
Vertical cracks at approximately 15" O.C. Maximum width .010"

Horizontal cracks at each construction joint plus one or two much

smaller cracks between joints.

No spalling of concrete.

Figure 1.2
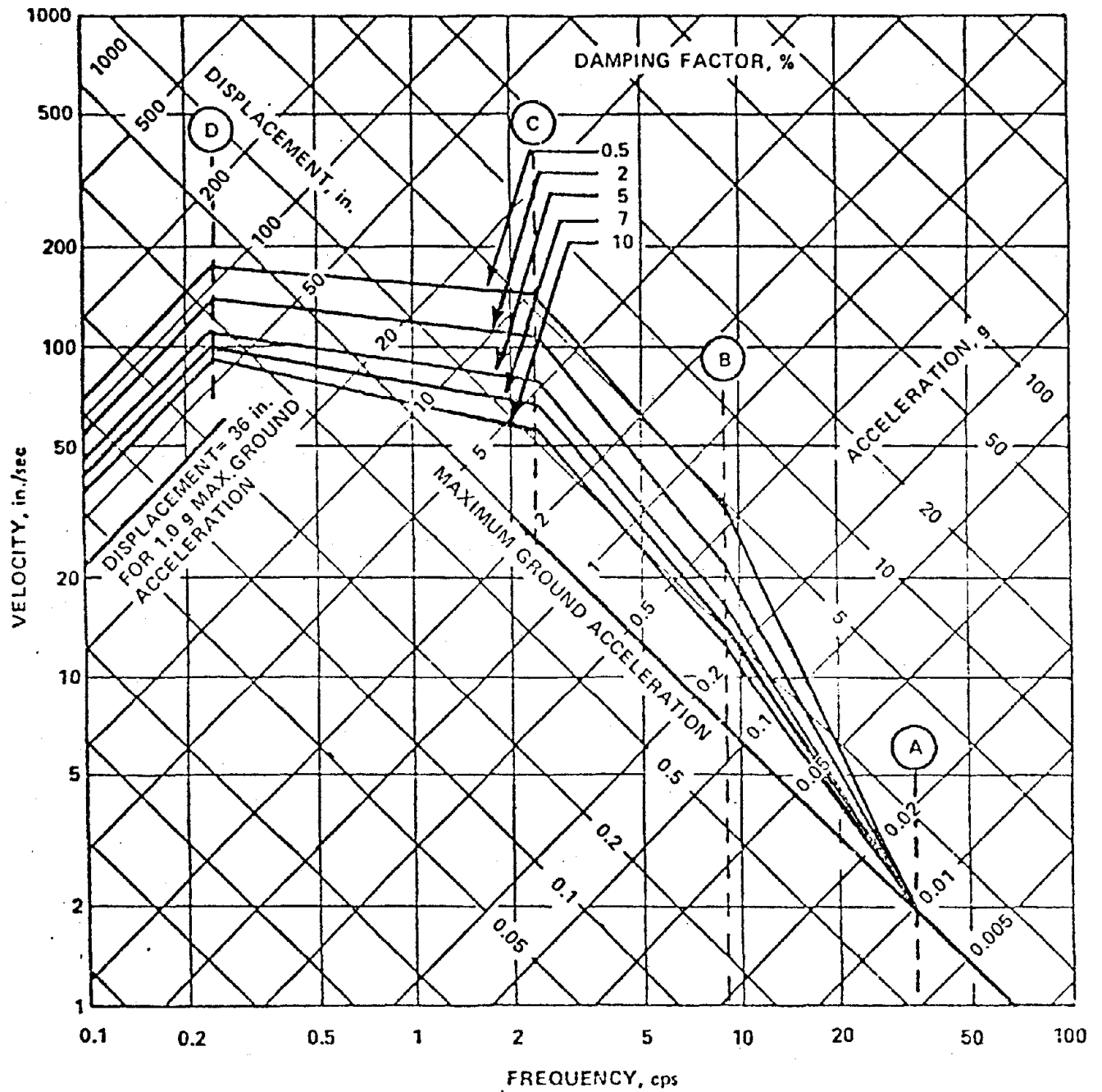
Horizontal design response soectra - scaled to 1g horizontal ground acceleration.

Figure 1.3
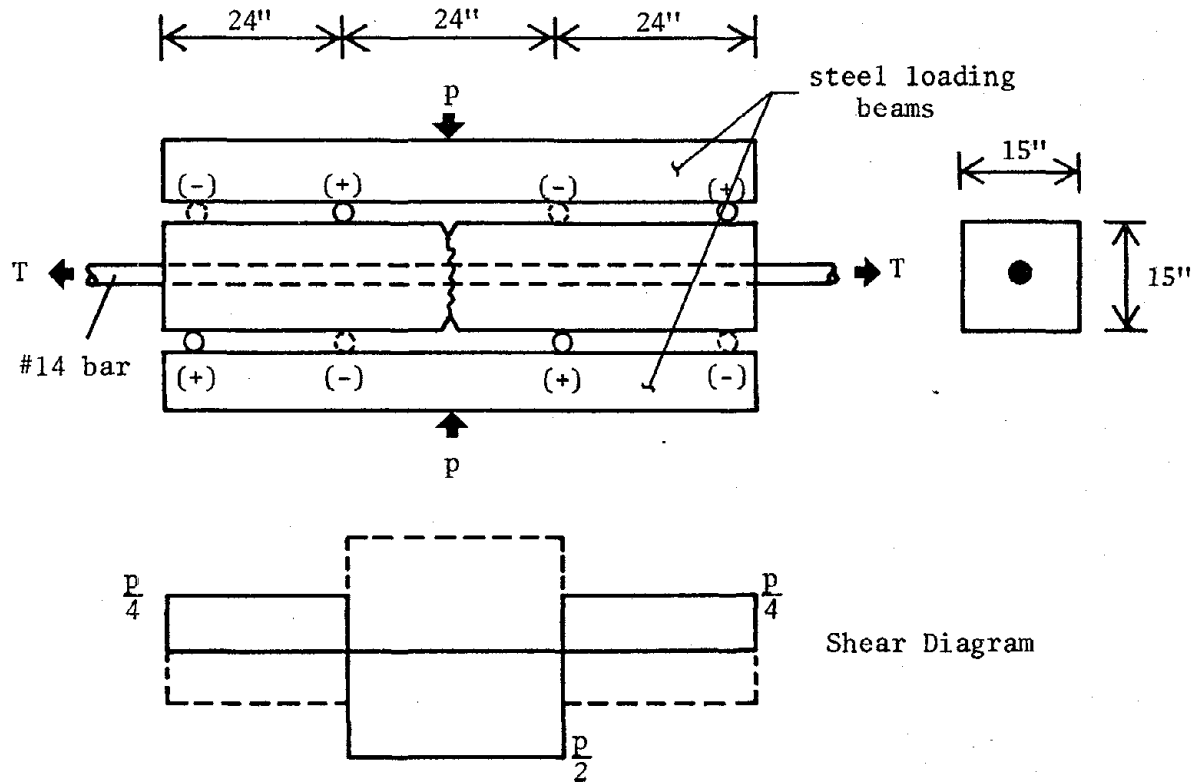
Figure 2.1 - Beam-type Specimen
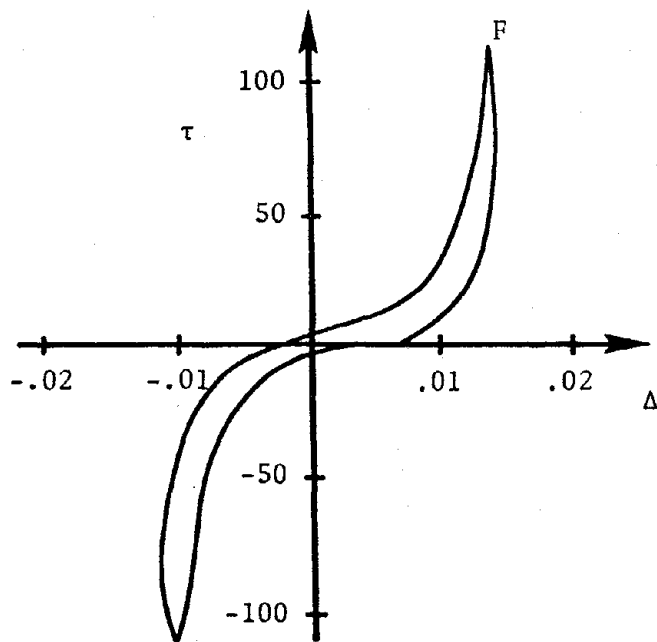
Figure 2.2
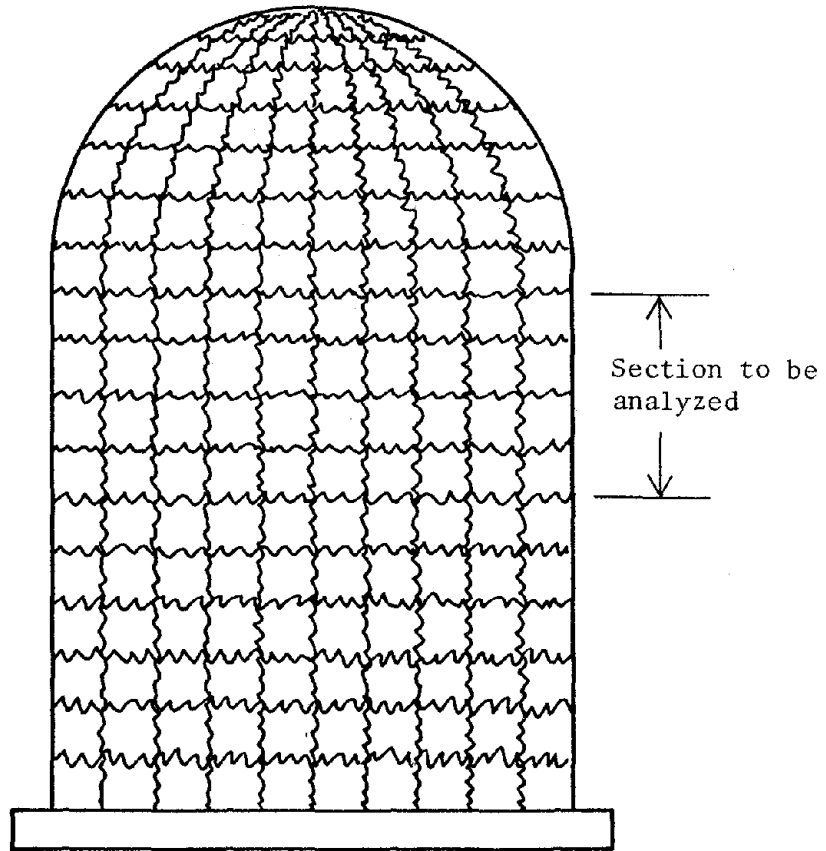
Figure 2.3 - Containment with Horizontal
and Vertical Cracking
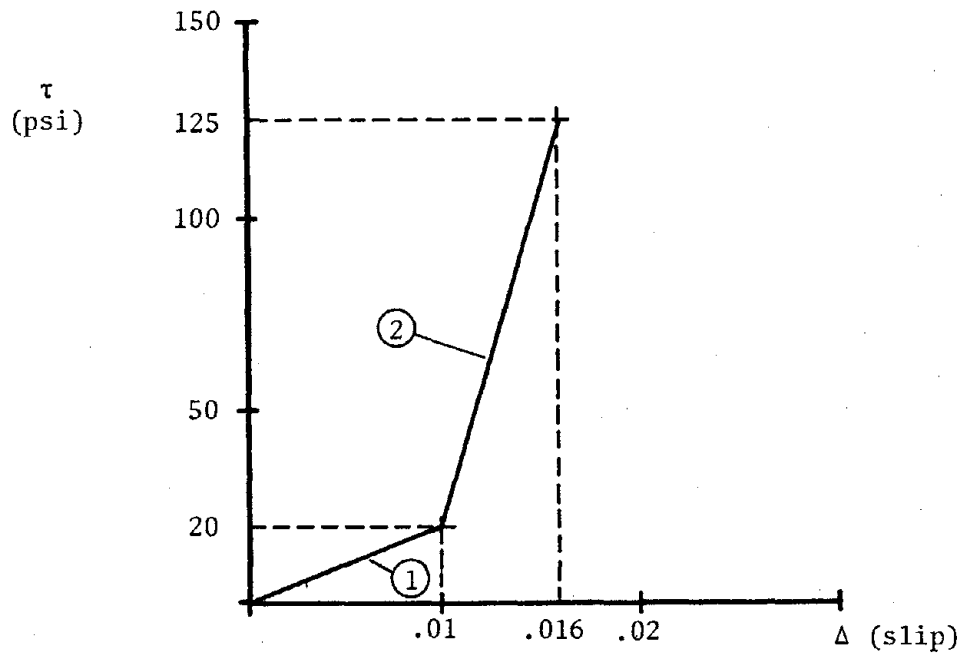
Figure 2.4 - Idealized Load-Slip Curve
(From Curve F of Figure 2.1)
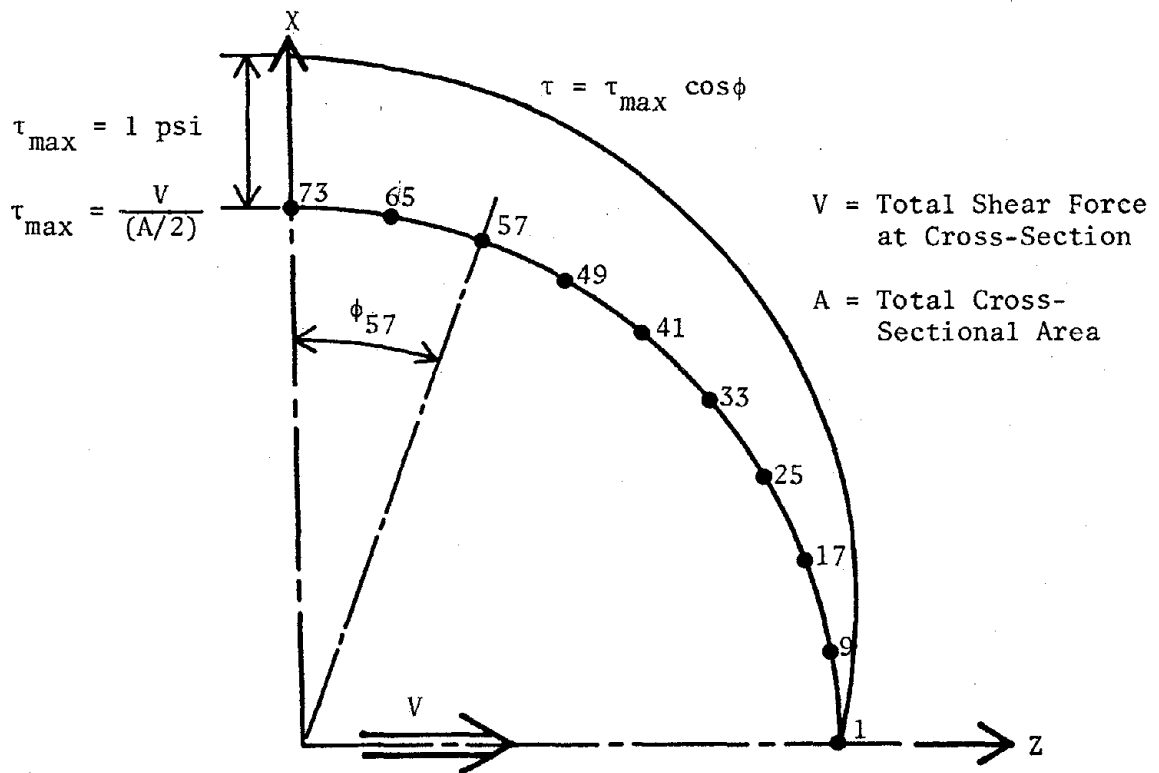
Figure 2.5 - Elastic Shear Stress Distribution

Figure 2.6

PLAN VIEW

ROLLOUT VIEW
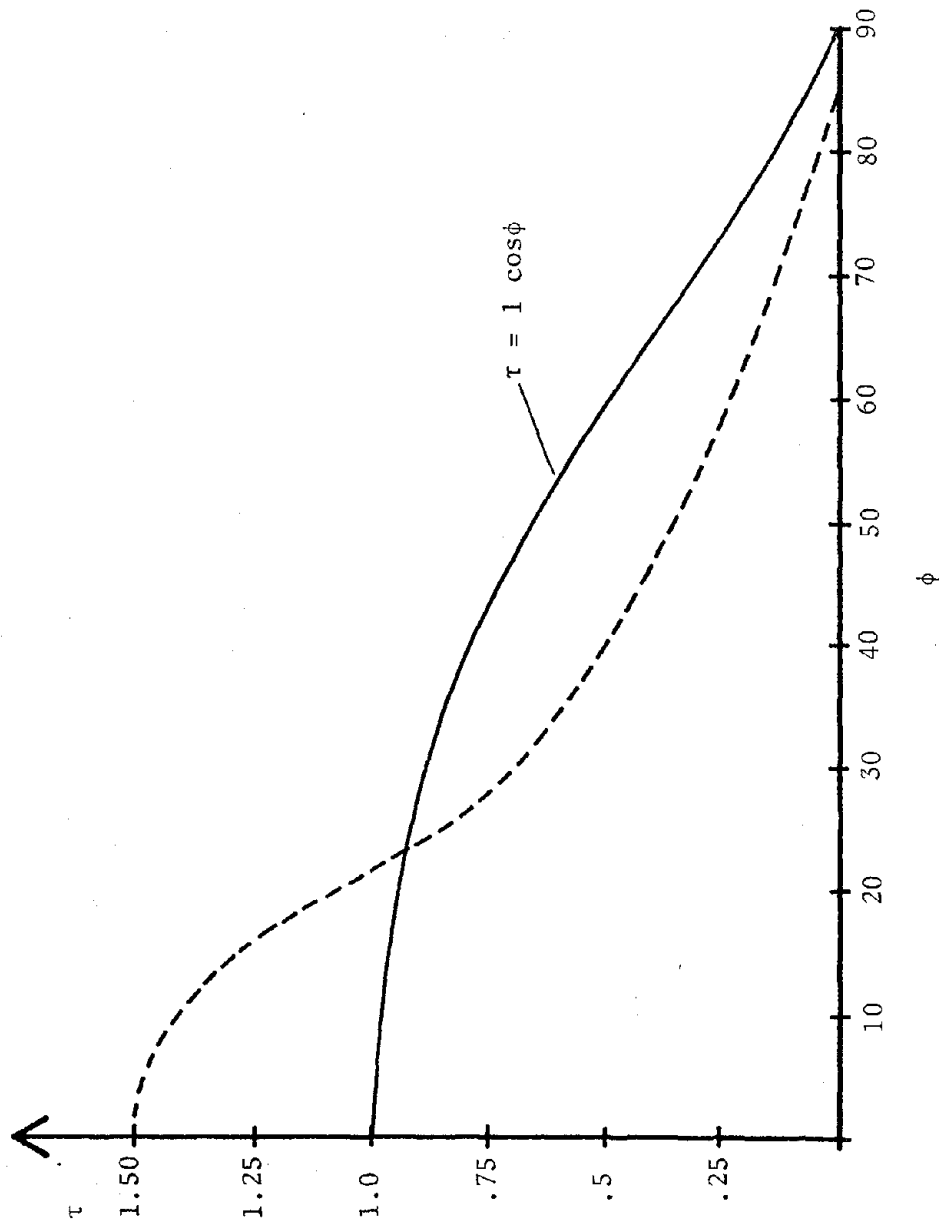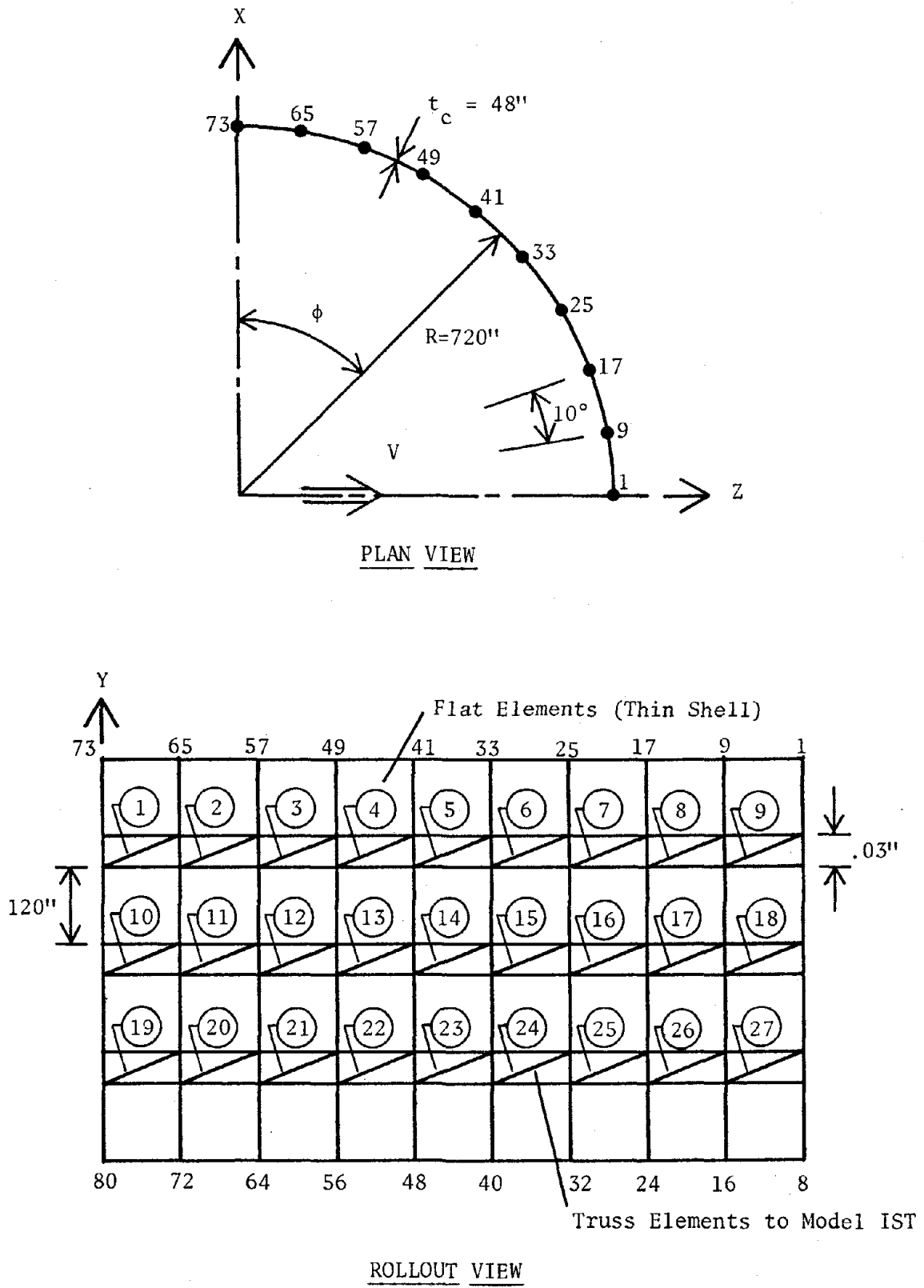
Figure 2.7 - SAP IV Model
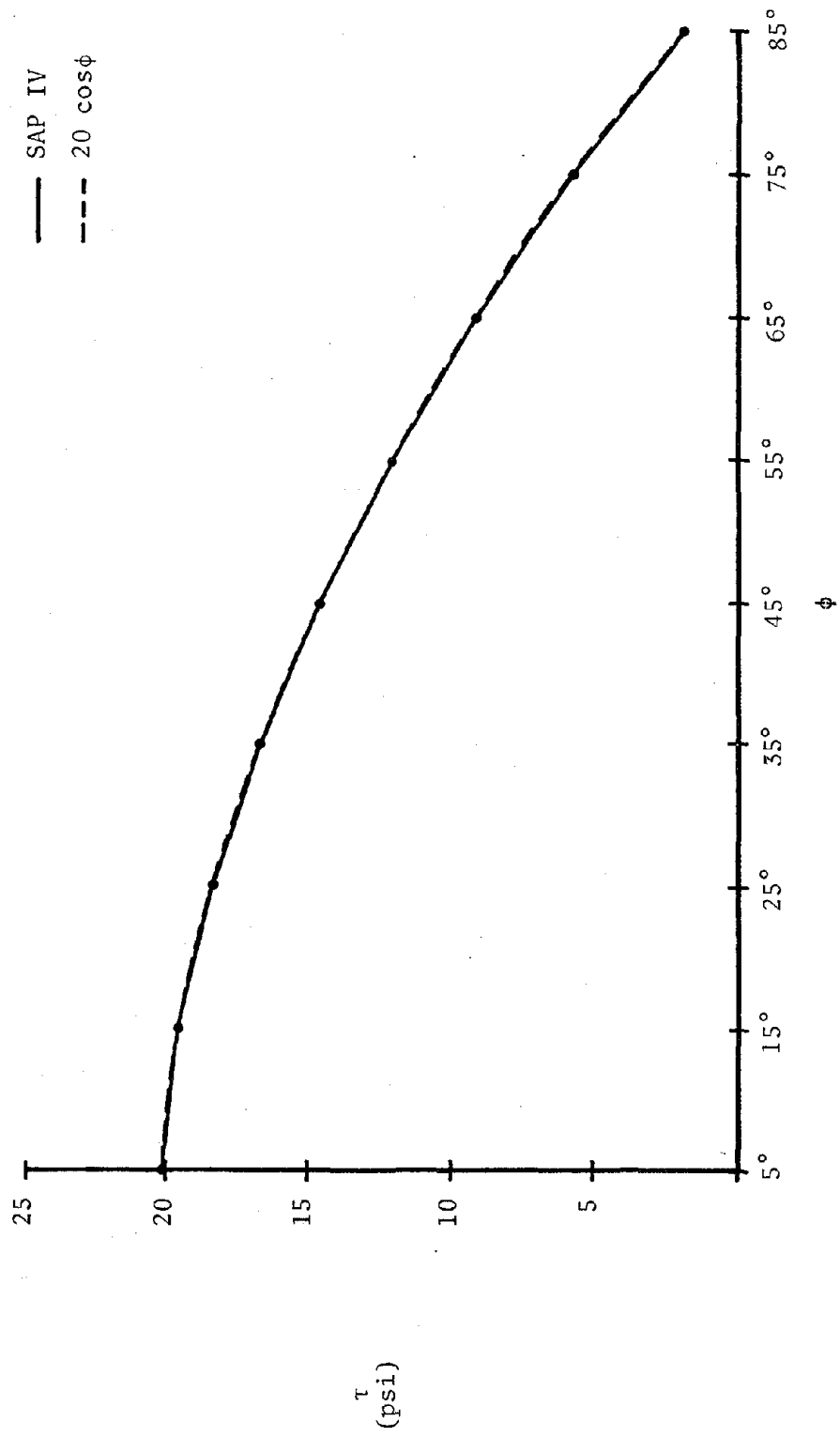
Figure 2.8
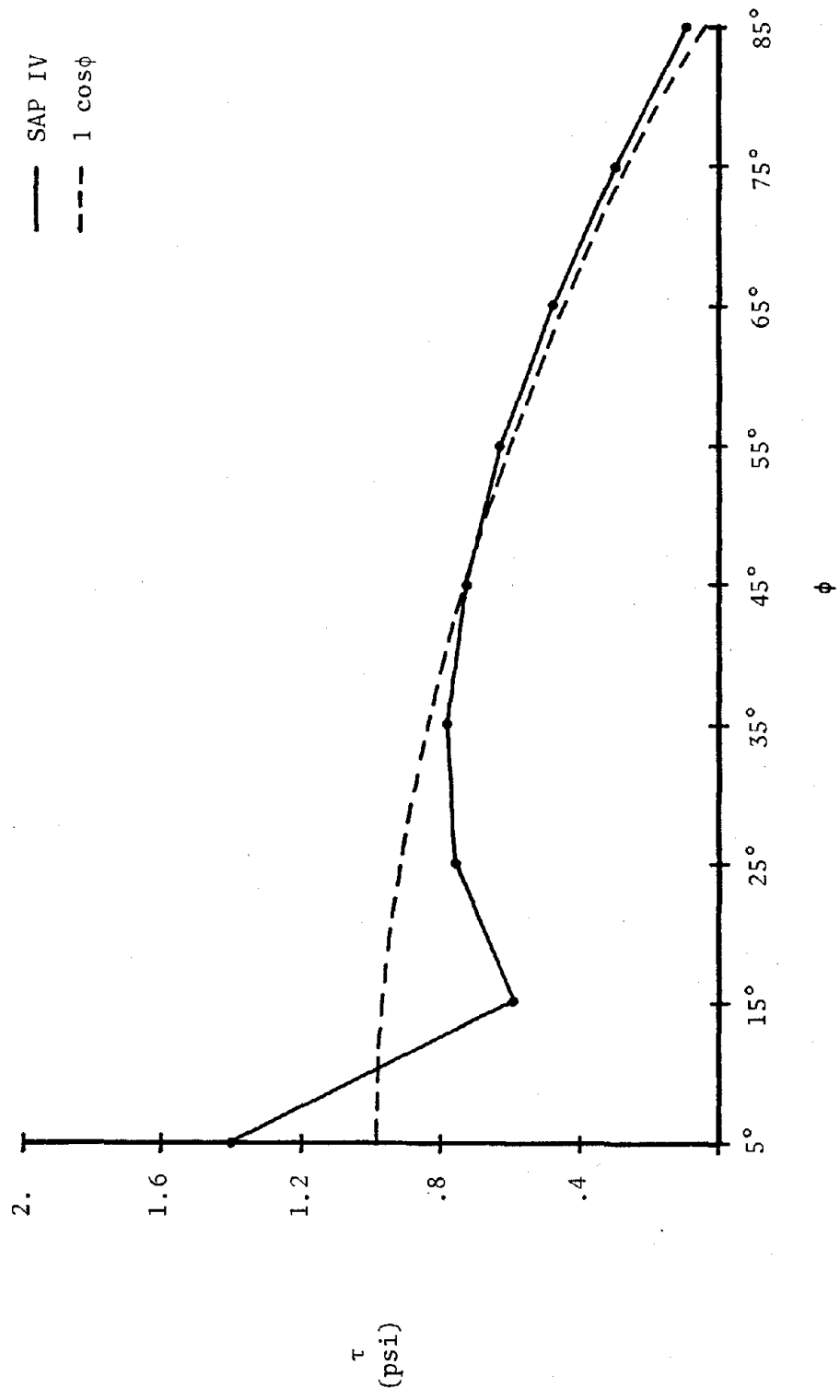
Figure 2.9 - $\phi = 0°$ to $10°$ Stiff (E_2)
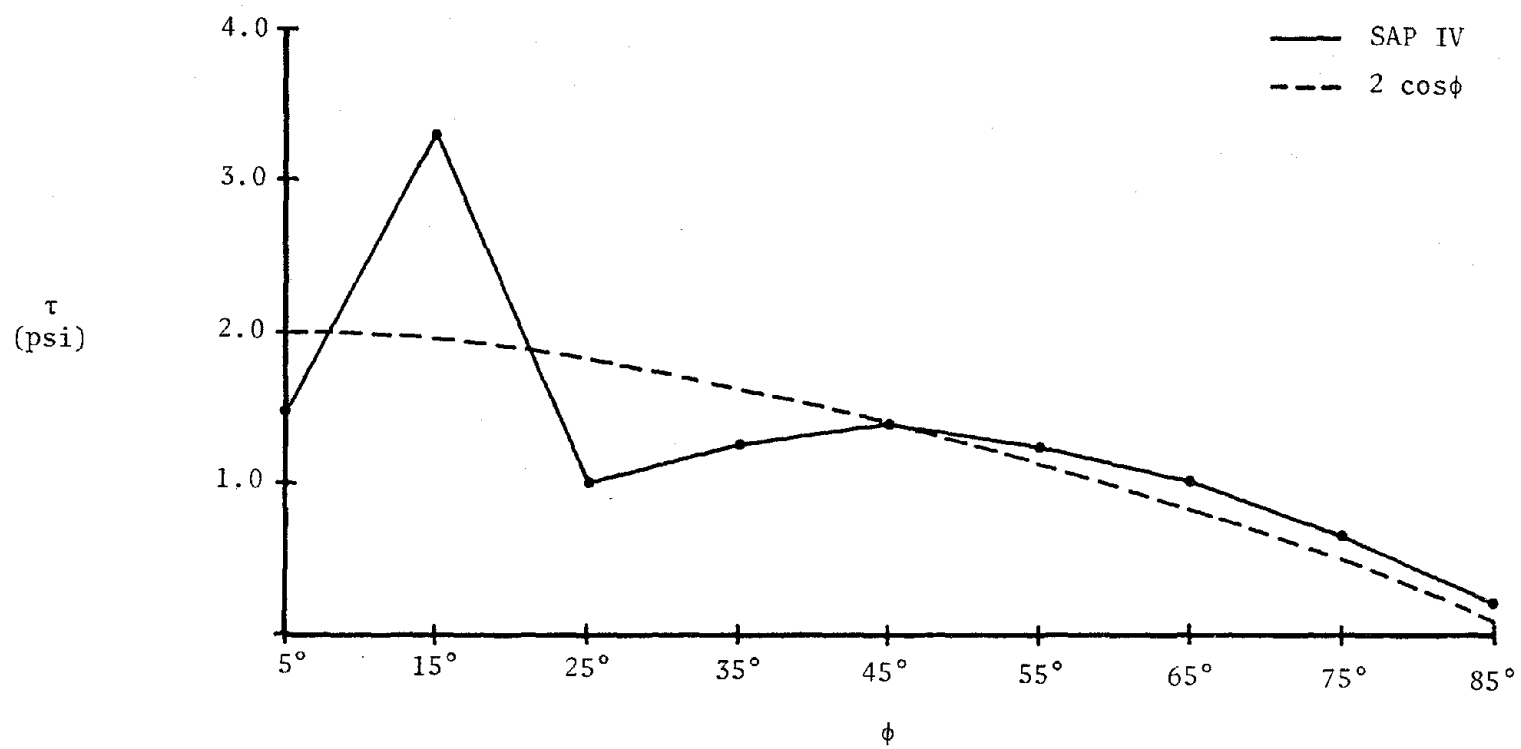
Figure 2.10 - $\phi = 0°$ to $20°$ Stiff
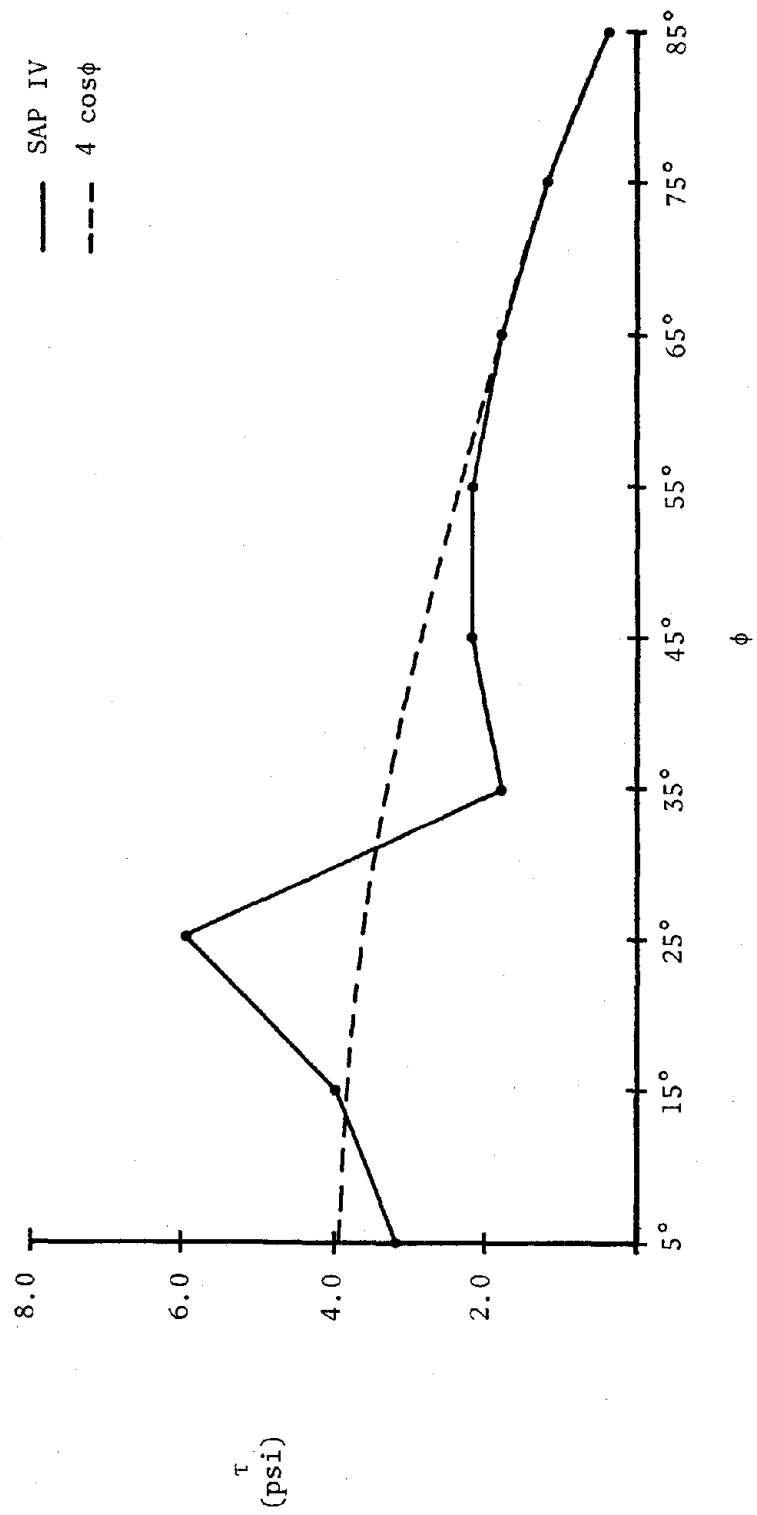
Figure 2.11 - $\phi = 0°$ to $30°$ Stiff
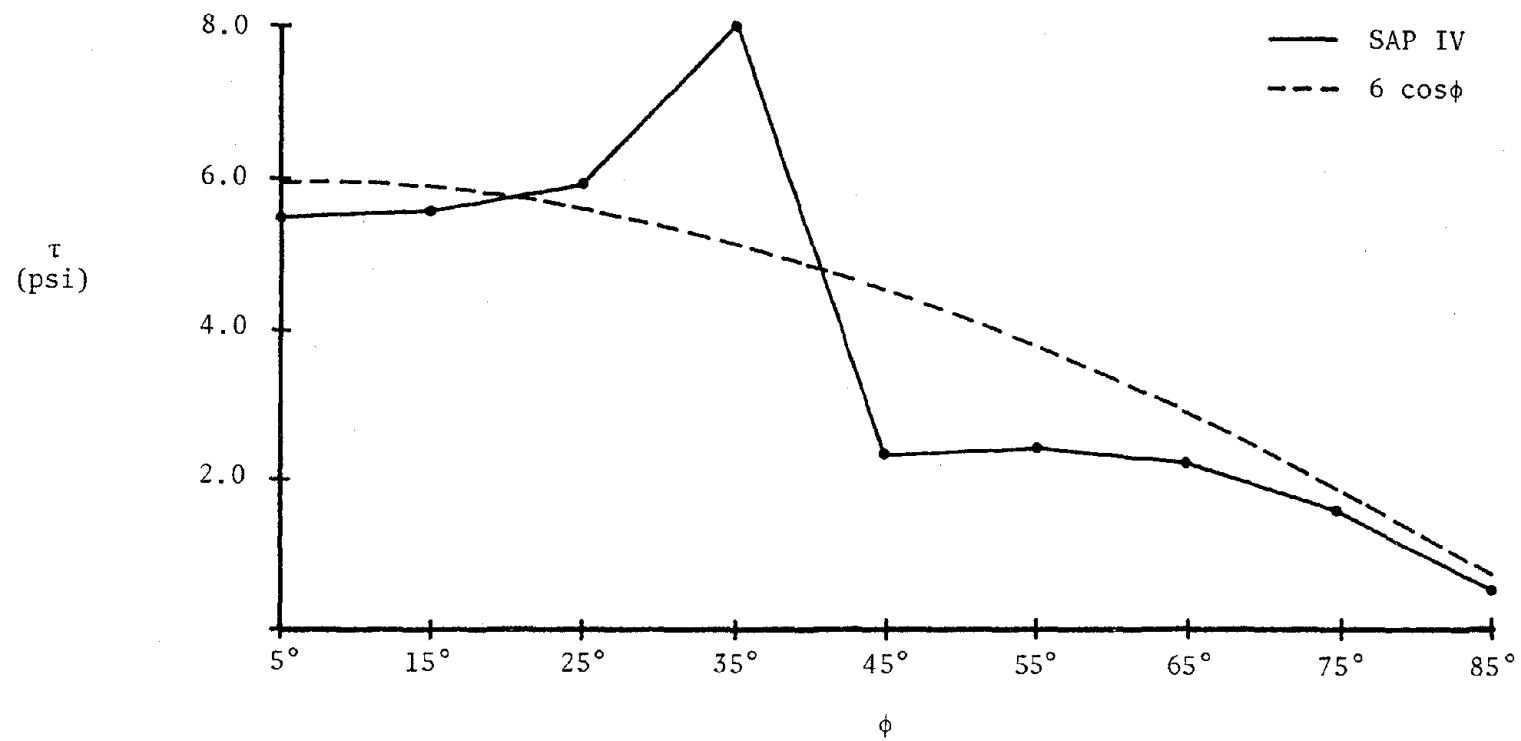
Figure 2.12 - ϕ = 0° to 40° Stiff
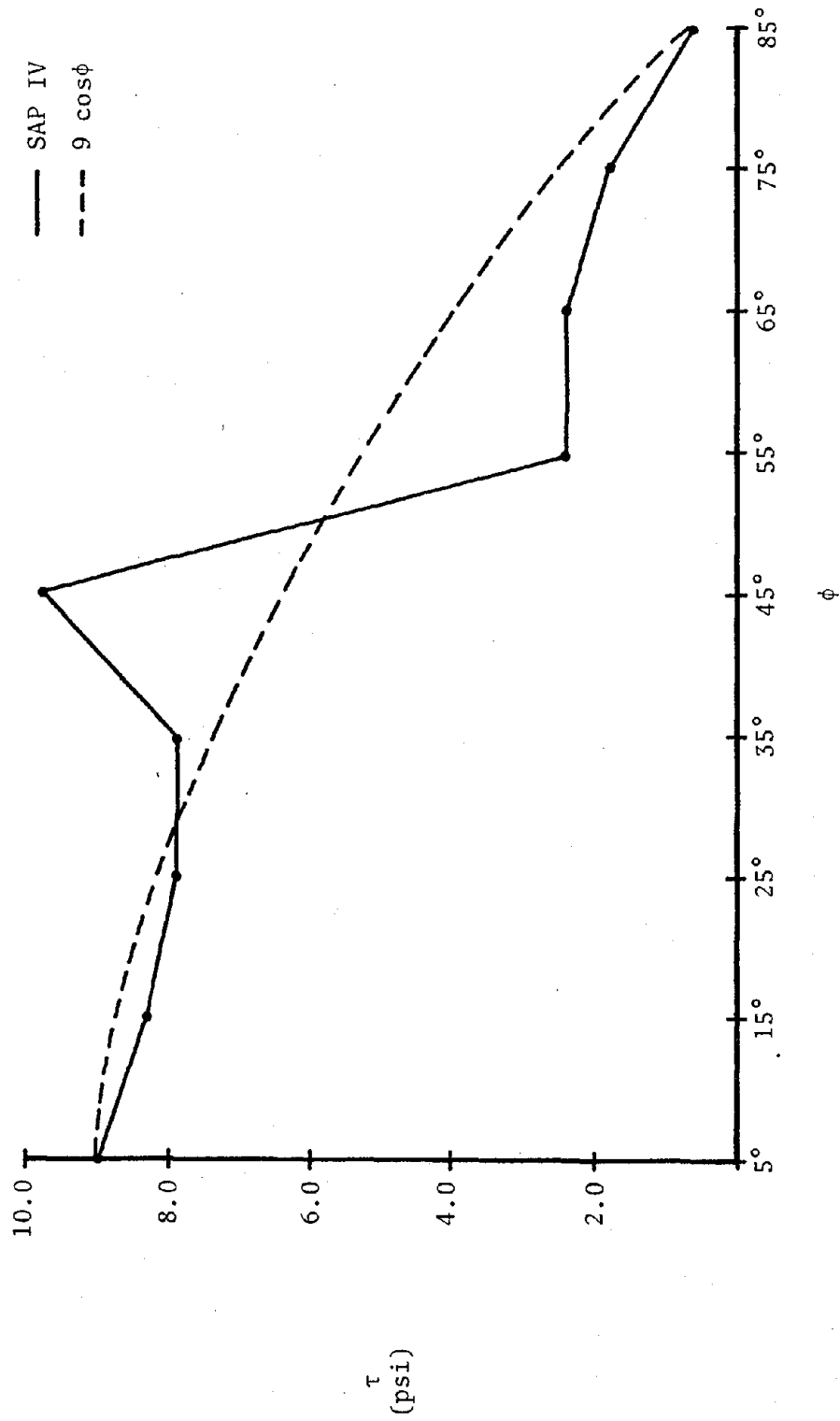
Figure 2.13 - $\phi = 0°$ to $50°$ Stiff
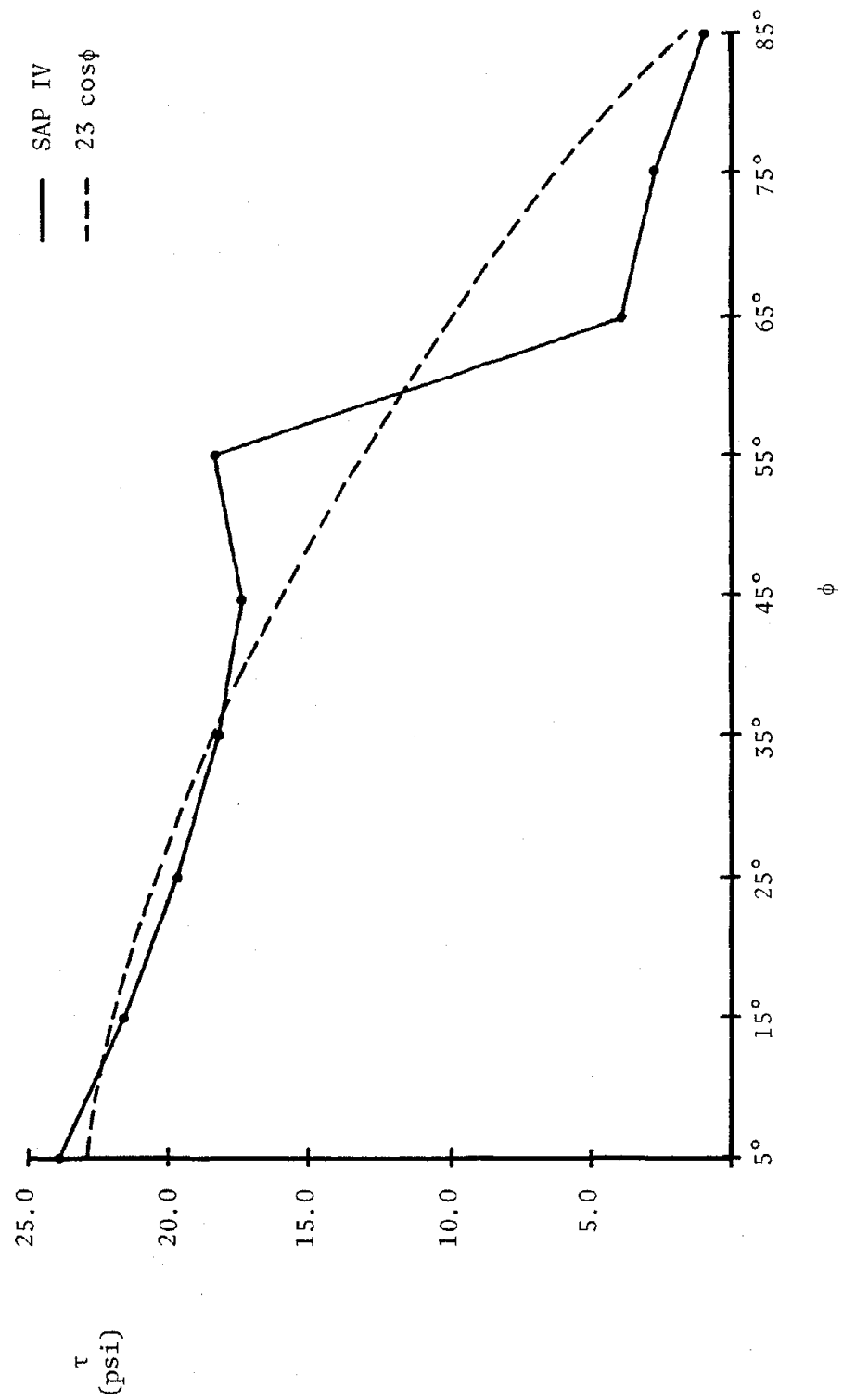
Figure 2.14 - $\phi = 0°$ to $60°$ Stiff
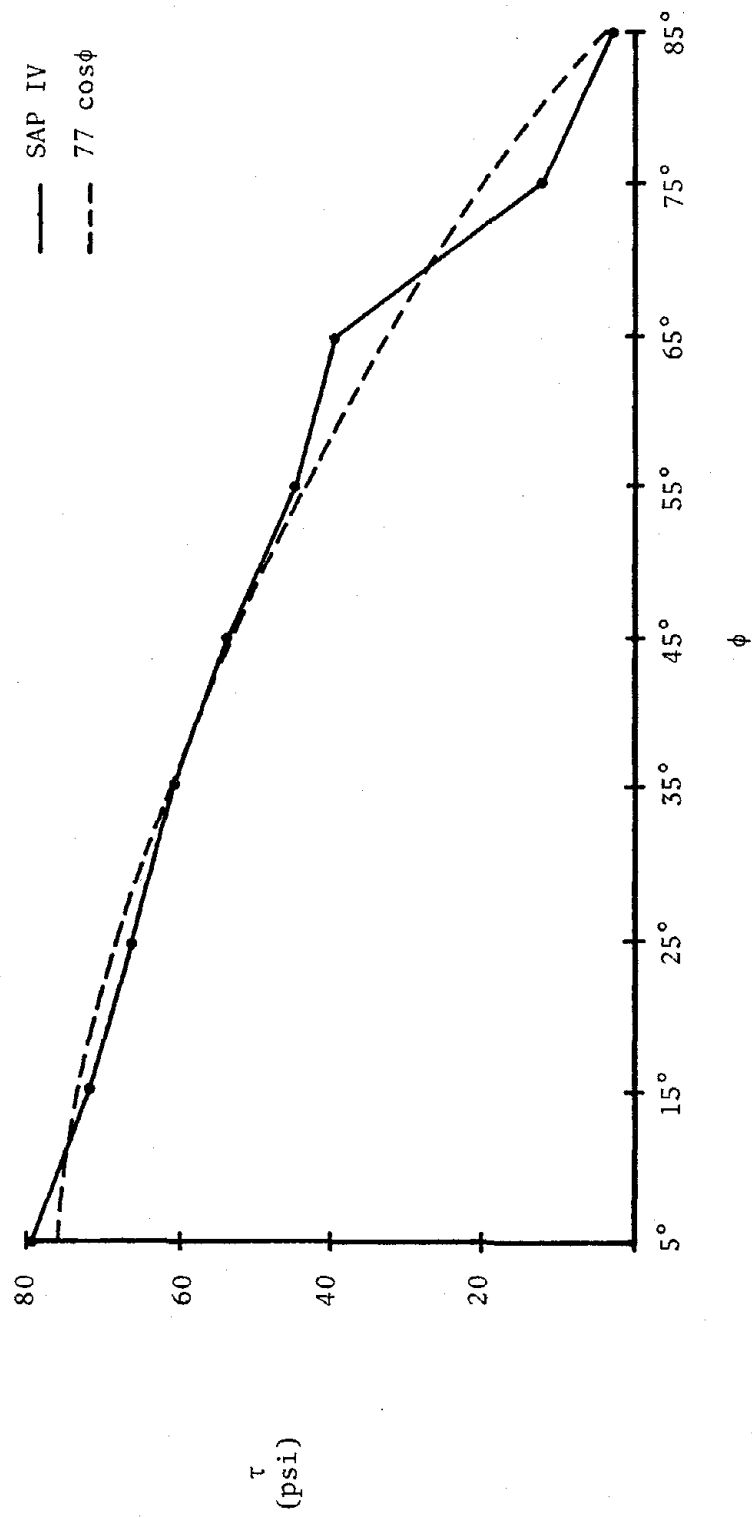
Figure 2.15 - $\phi = 0°$ to $70°$ Stiff
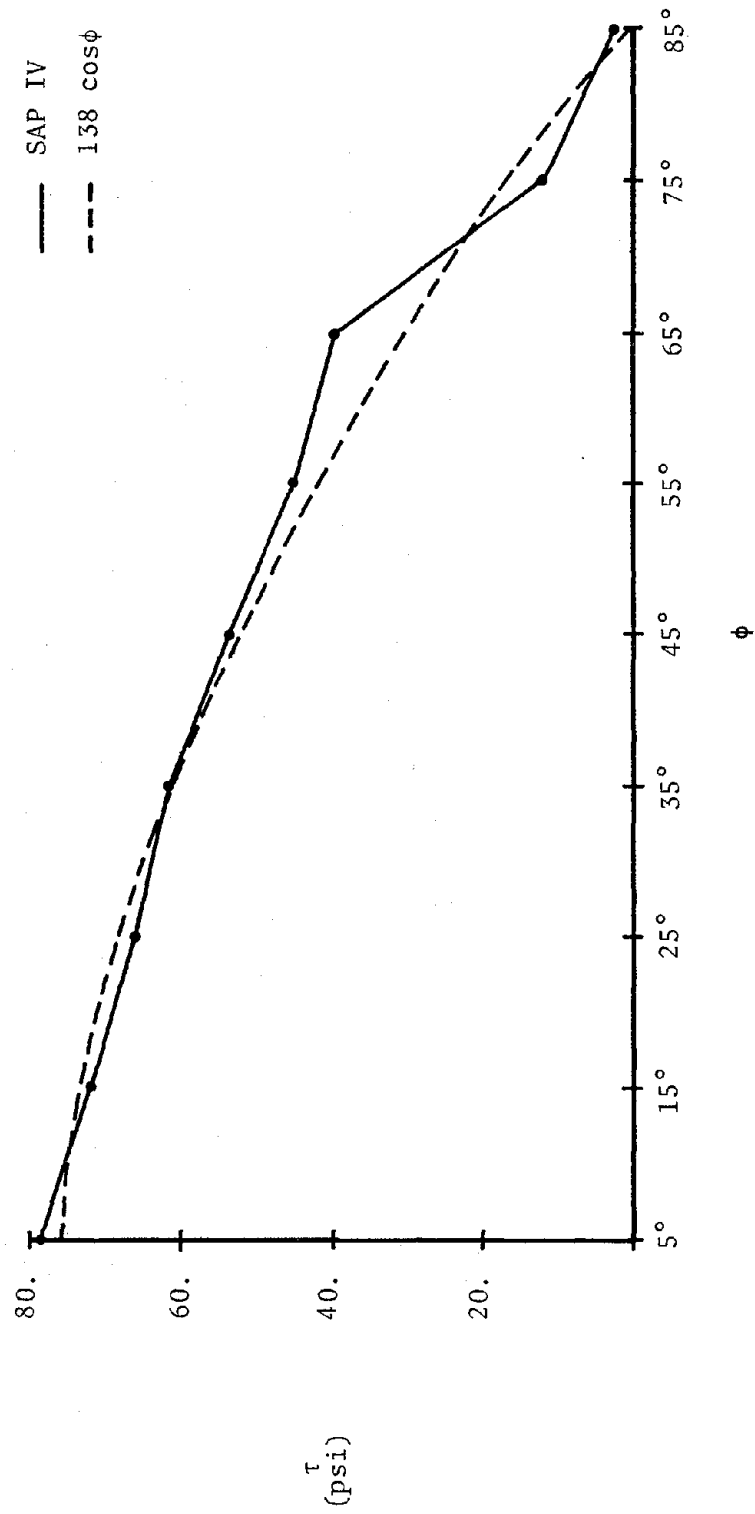
Figure 2.16 - $\phi = 0°$ to $80°$ Stiff
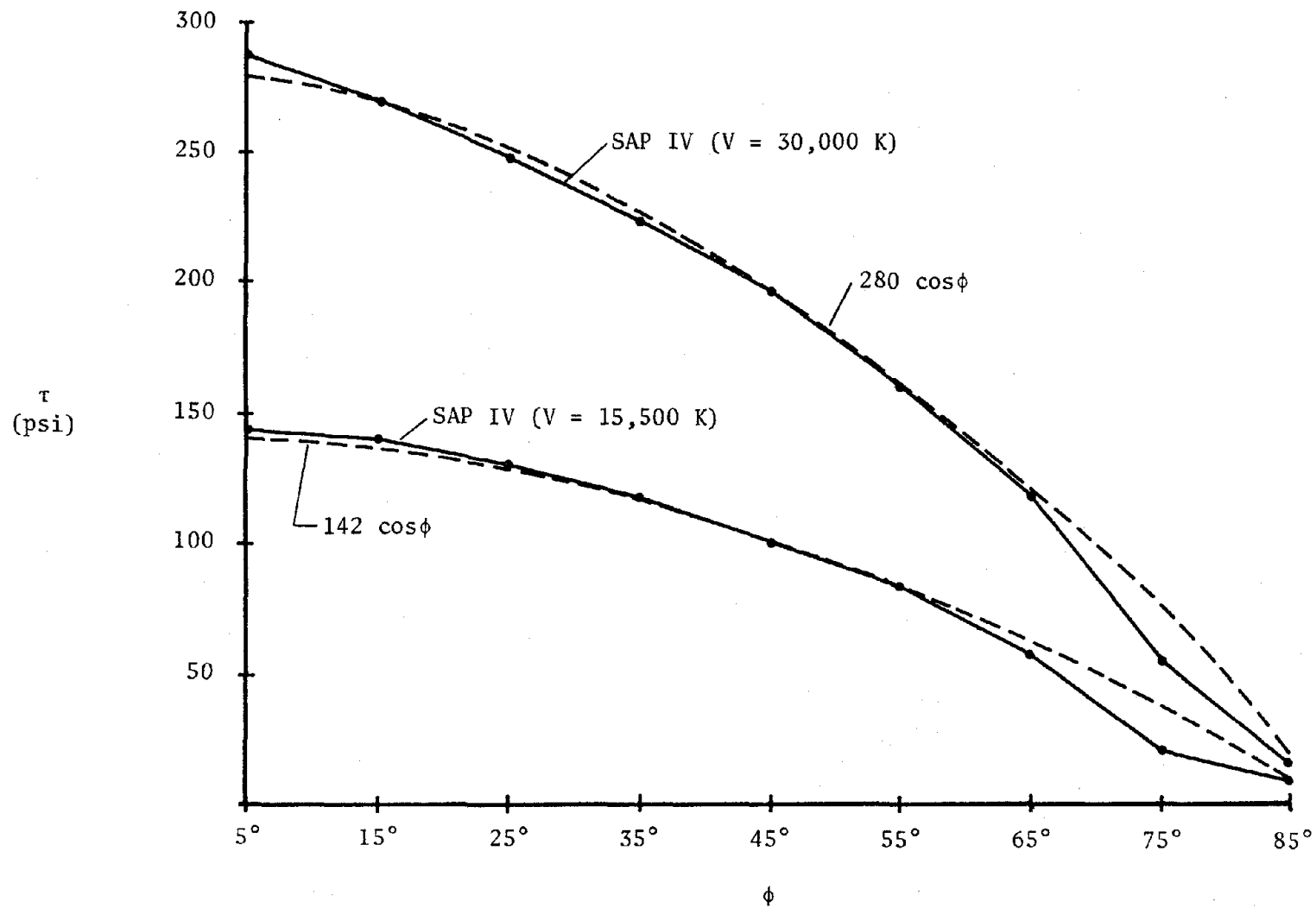
Figure 2.17 - Total Stresses fo V = 30,000 K and V = 15,5550 K
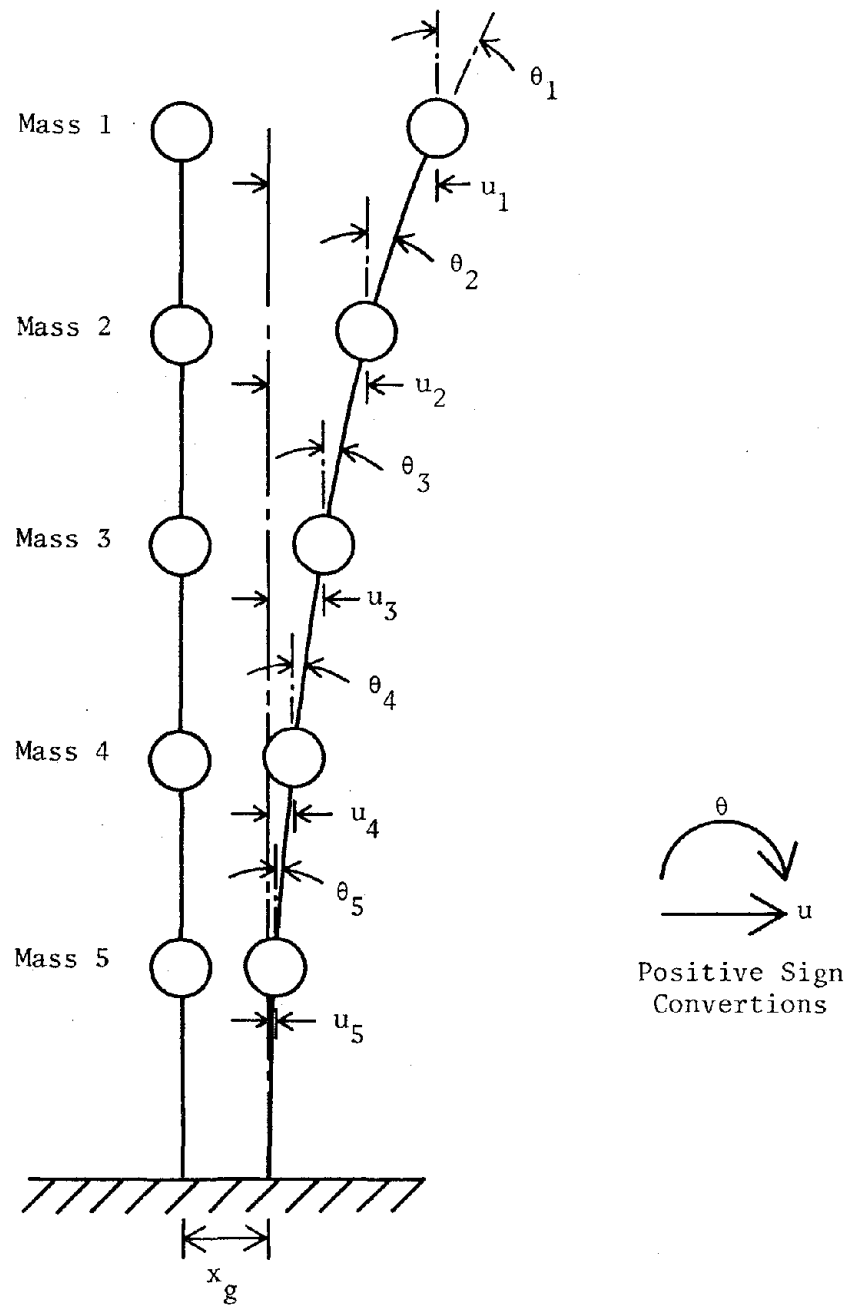
Figure 3.1 - The Structural Degrees of Freedom

a. Actual Containment Vessel   b. Lumped Mass
                                      Model
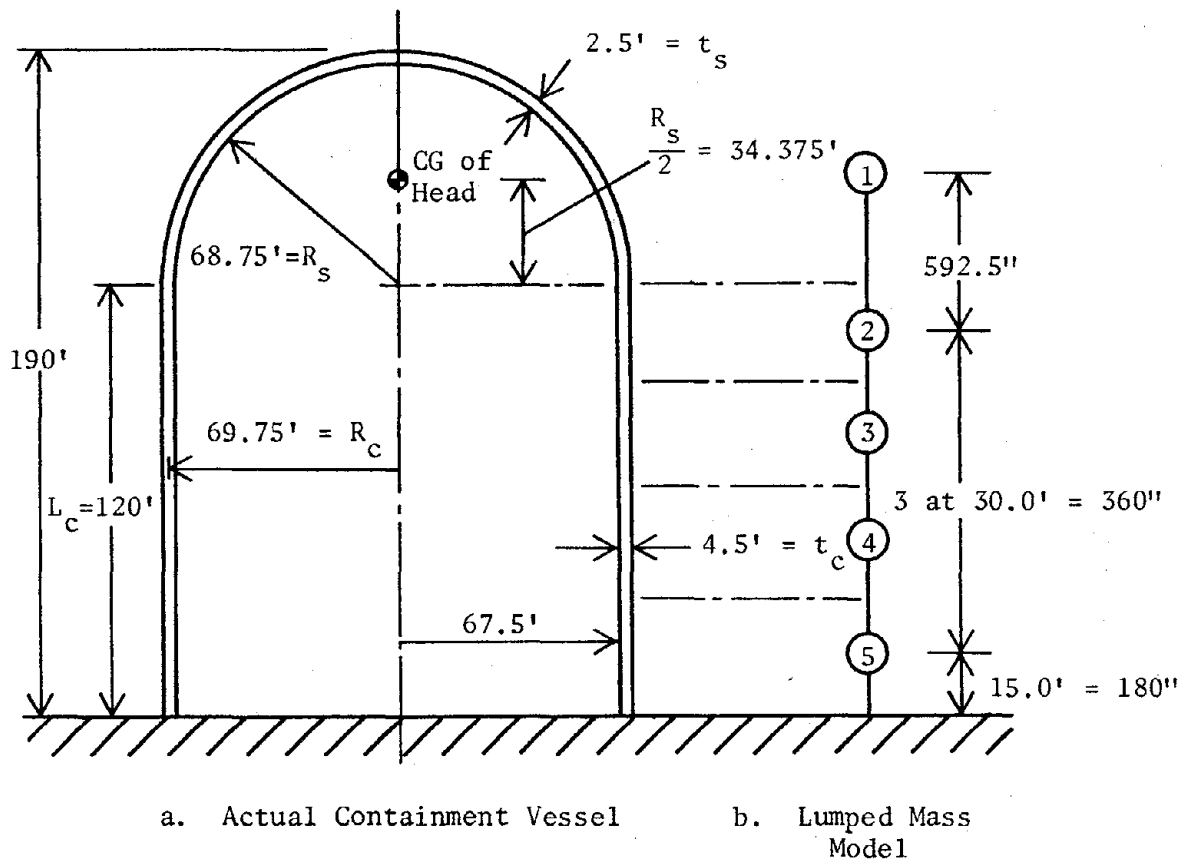
Node	Mass ($k-sec^2/in$)	Moment of Inertia (in^4)	Mass Moment ($k-sec^2-in$)	Shear Area (in^2)
1	28.822	6.7064×10^{10}	8.174×10^6	97,270
2	22.967	9.9476×10^{10}	8.293×10^6	142,000
3	22.967	9.9476×10^{10}	8.293×10^6	142,000
4	22.967	9.9476×10^{10}	8.293×10^6	142,000
5	22.967	9.9476×10^{10}	8.293×10^6	142,000

Figure 3.2
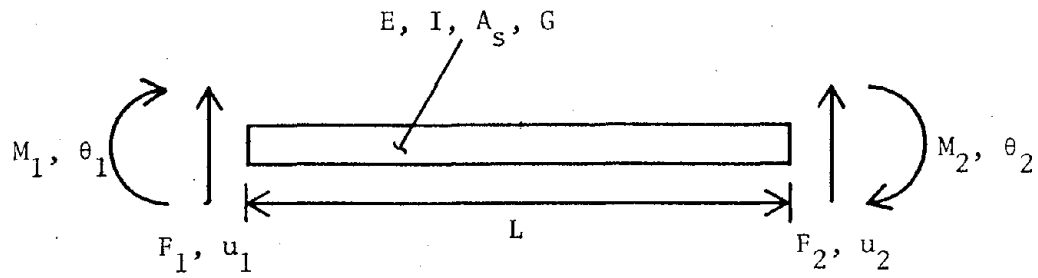
Figure 3.3 - Beam Element
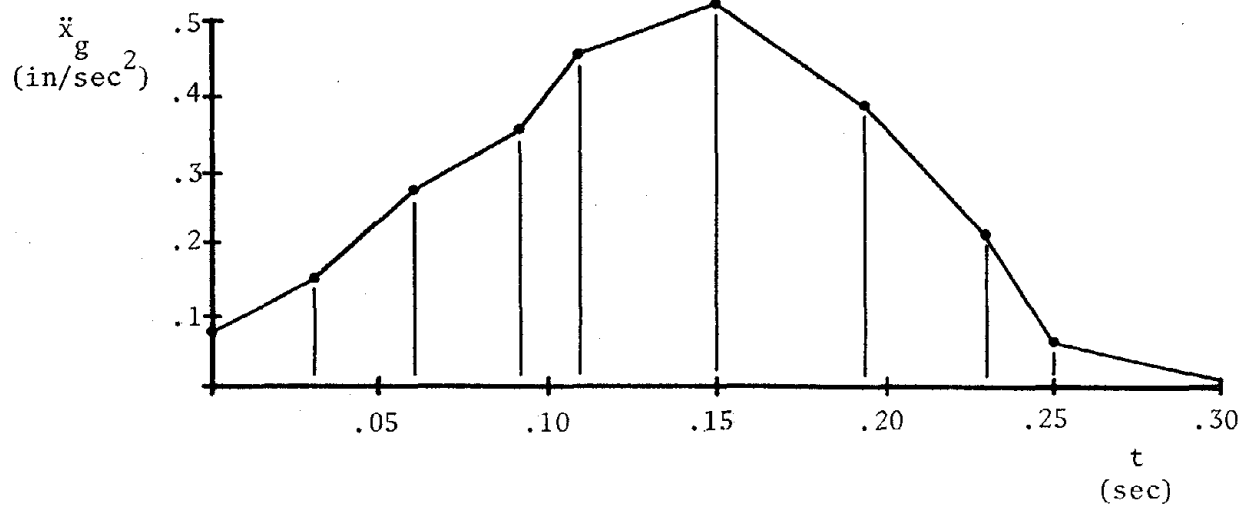
Figure 3.4 - Test Earthquake
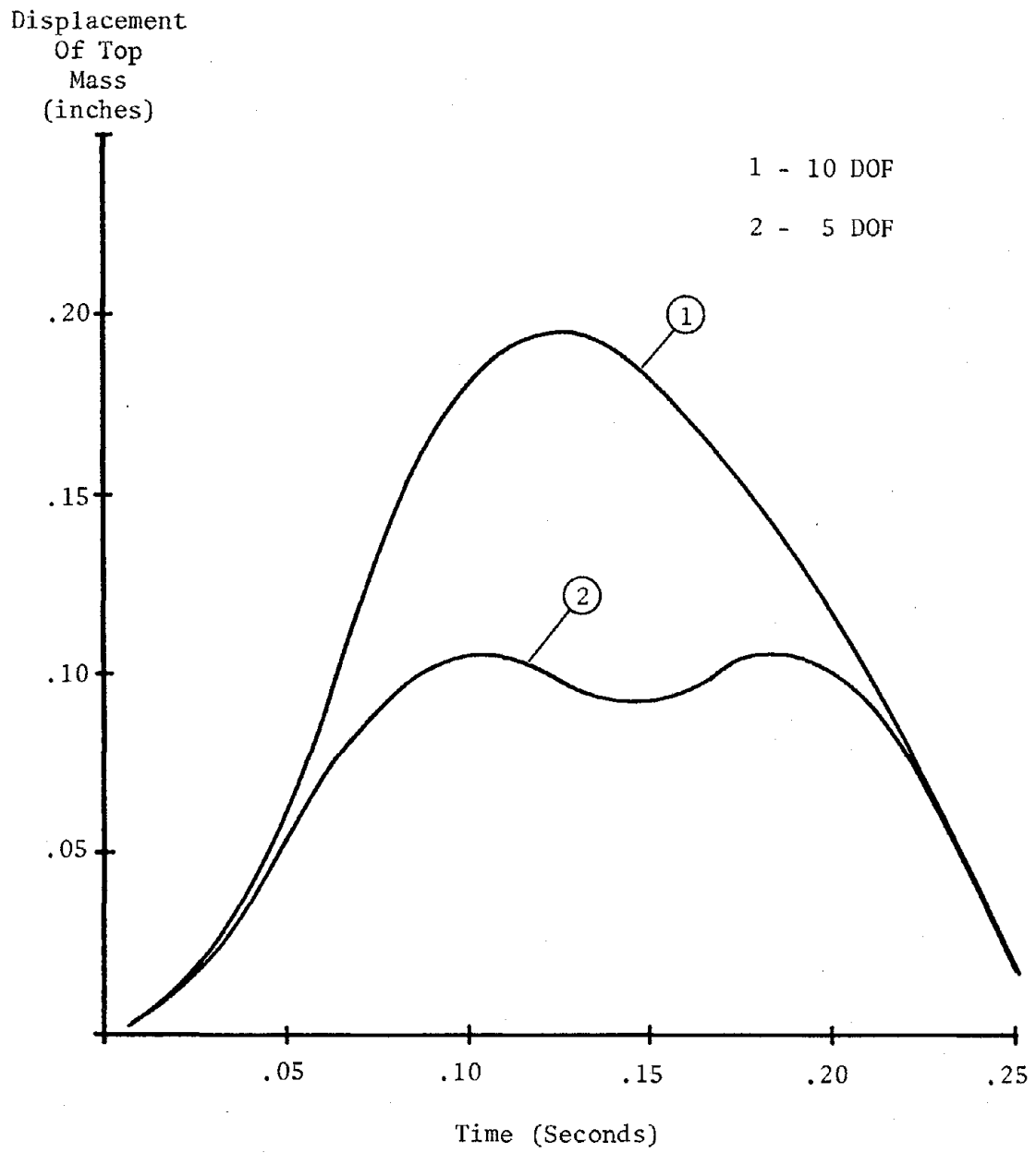
Figure 3.5
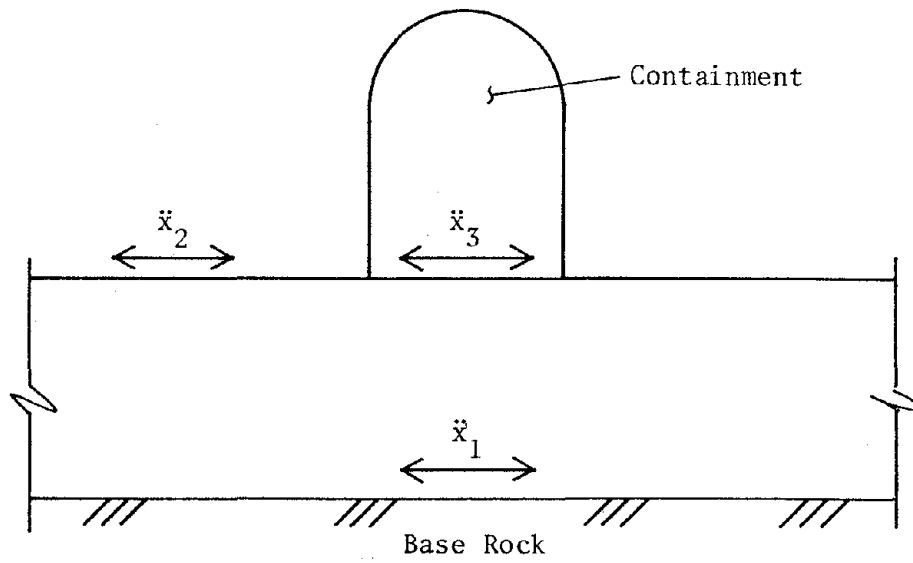
Figure 4.1
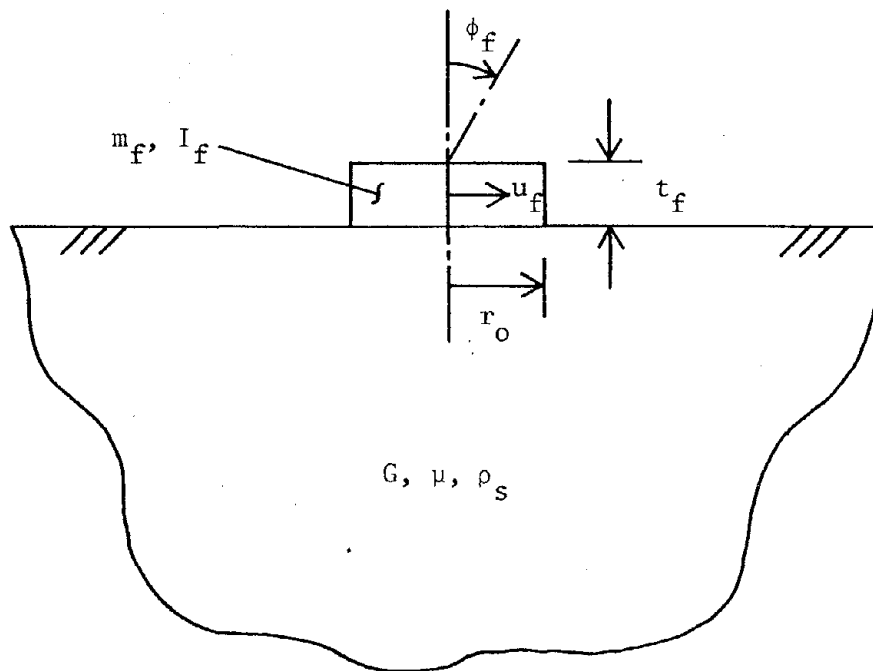
Figure 4.2
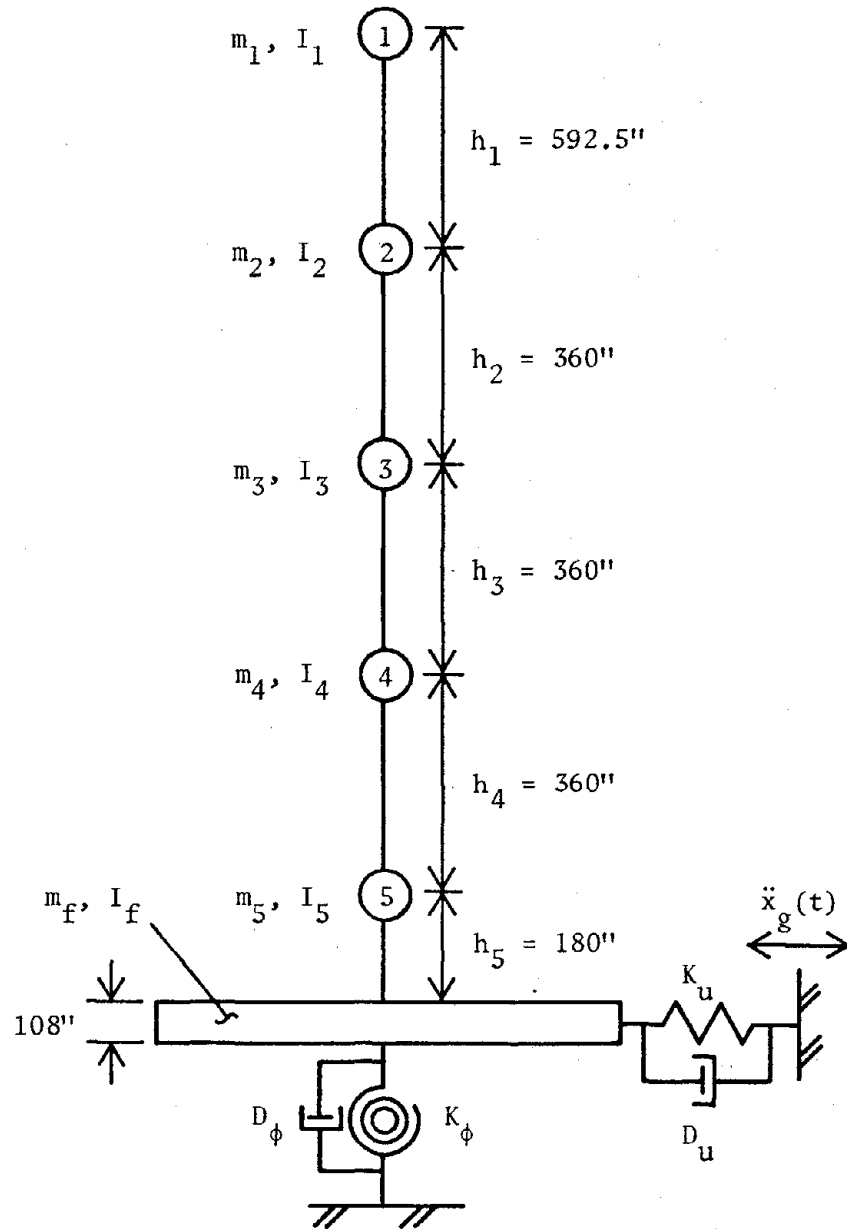
Figure 4.3 - Containment Model Including SSI
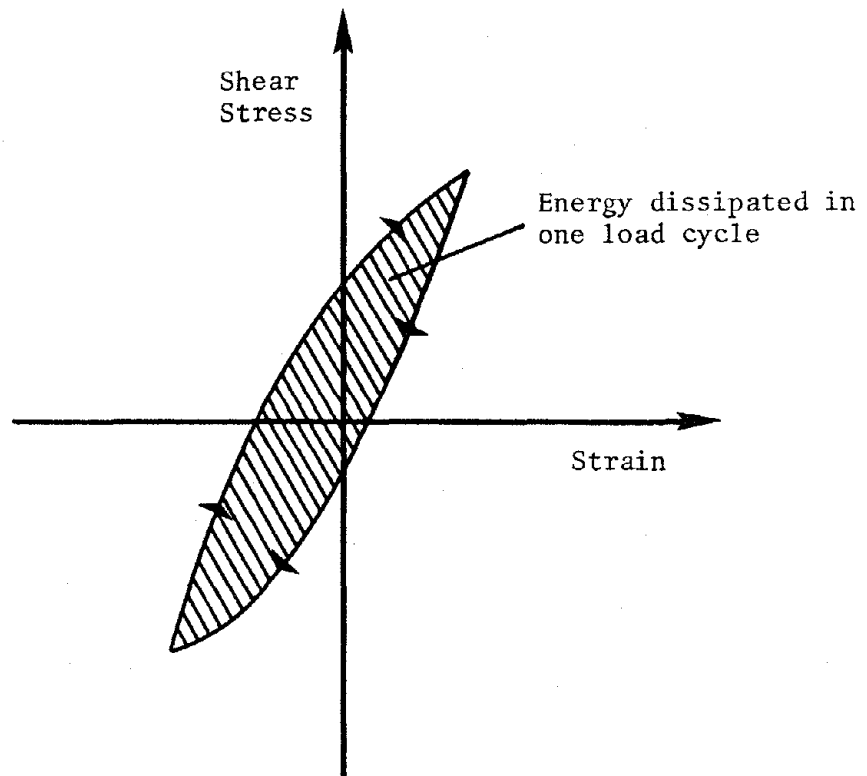
Figure 4.4 - Hysteresis In Soils

device for moving
vertical beams

hydraulic rams for
tensioning reinforcing bars

frame for tensioning
reinforcing bars

15" × 15" shear plane
of concrete specimen

shear
load rams

load
cell

vertical beam for
transmitting shear
load to specimen

rollers
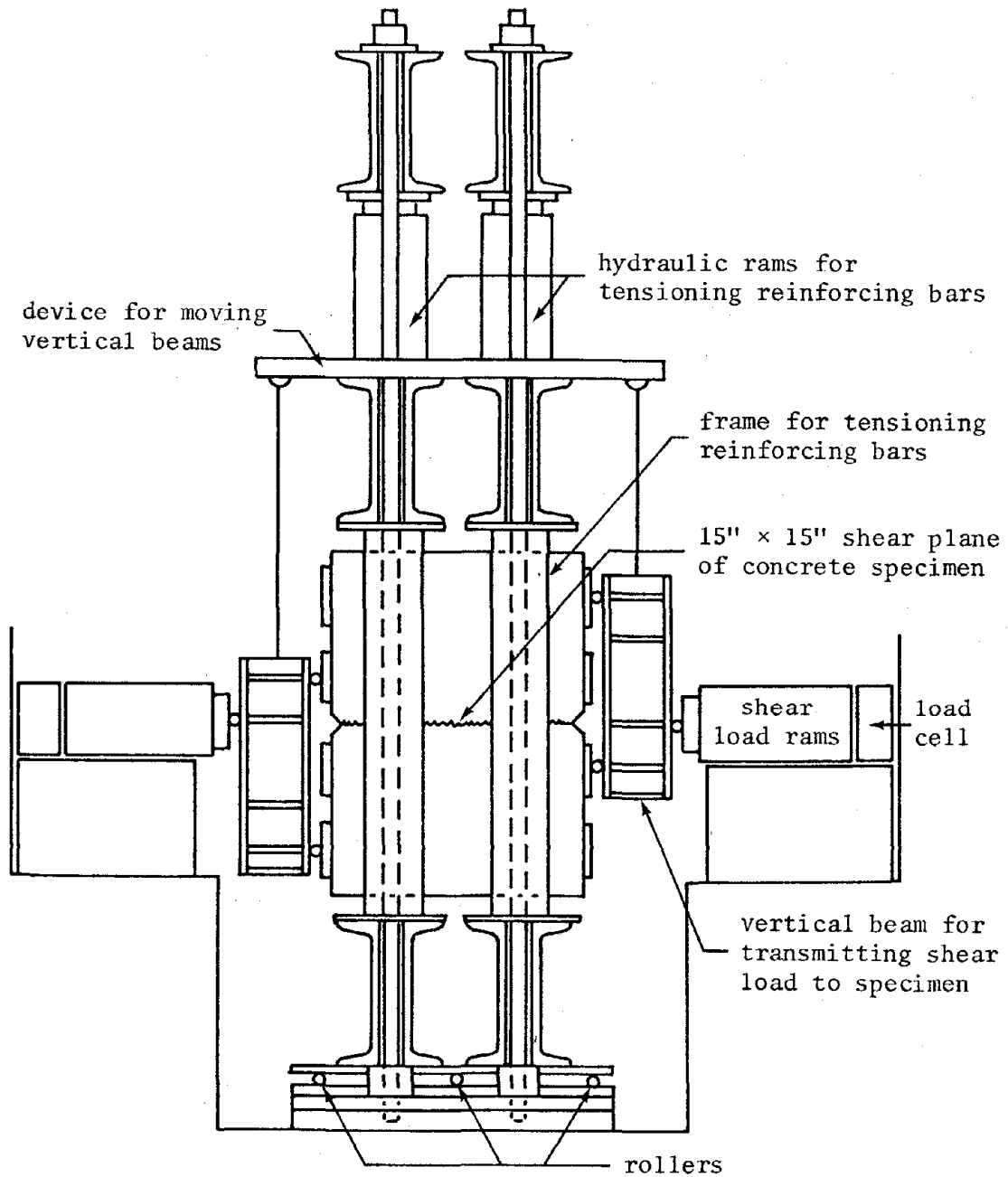
Figure 5.1 - Test Specimen (reinforced with 4 #9 bars)
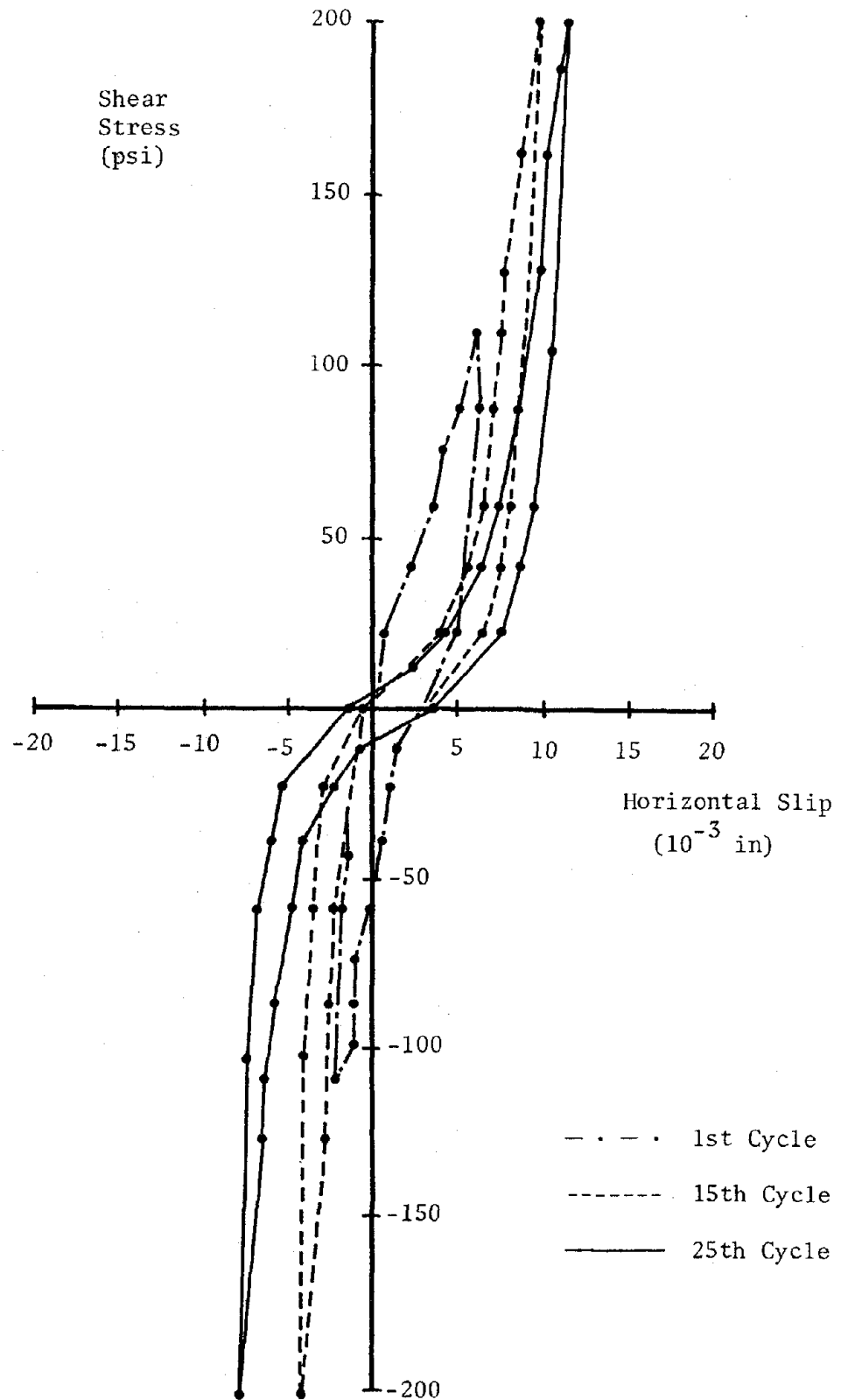
Figure 5.2 - Shear Stress VS. Horizontal Slip
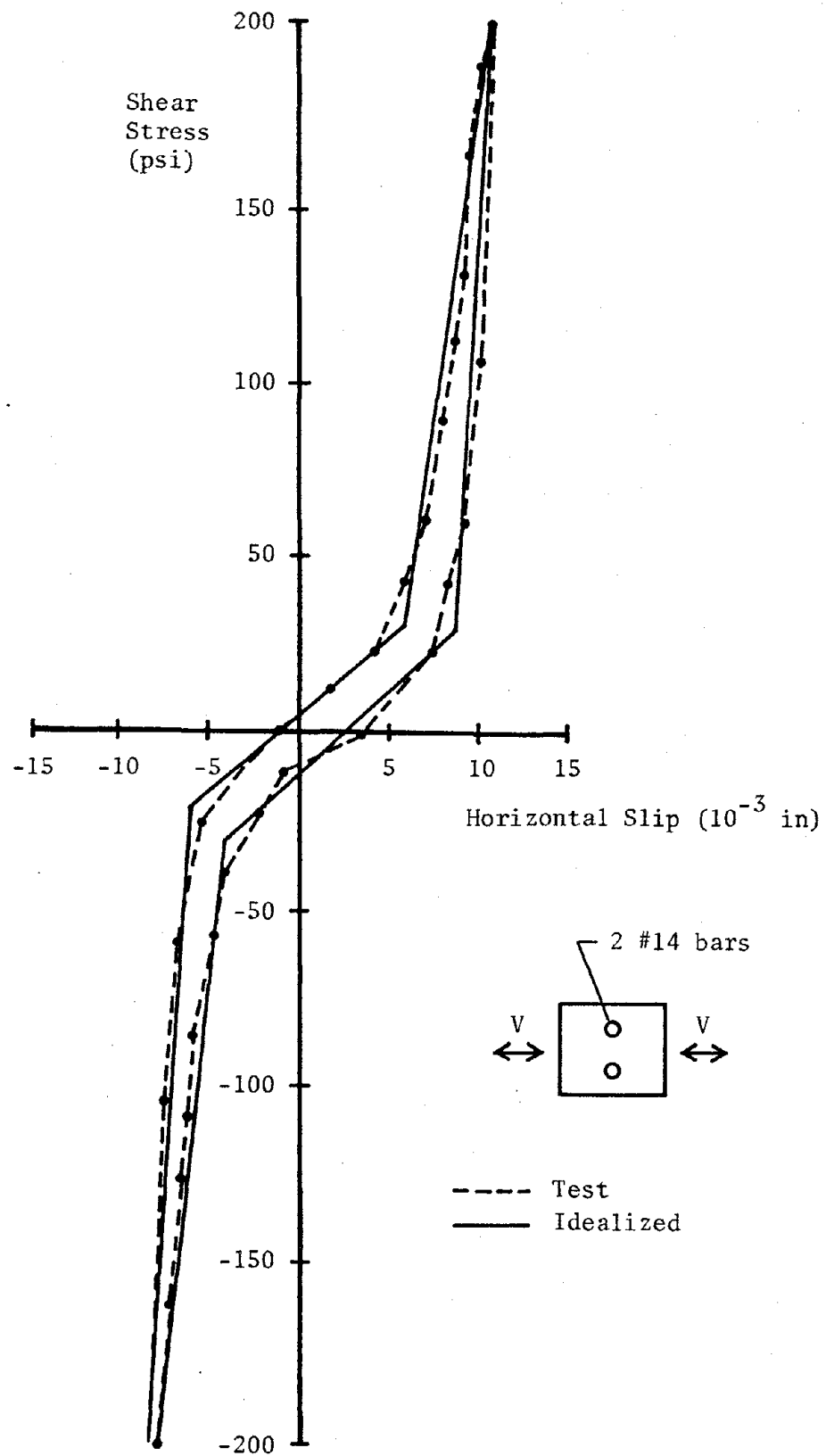
Figure 5.3 - Shear Stress Vs. Horizontal Slip - 25th Cycle
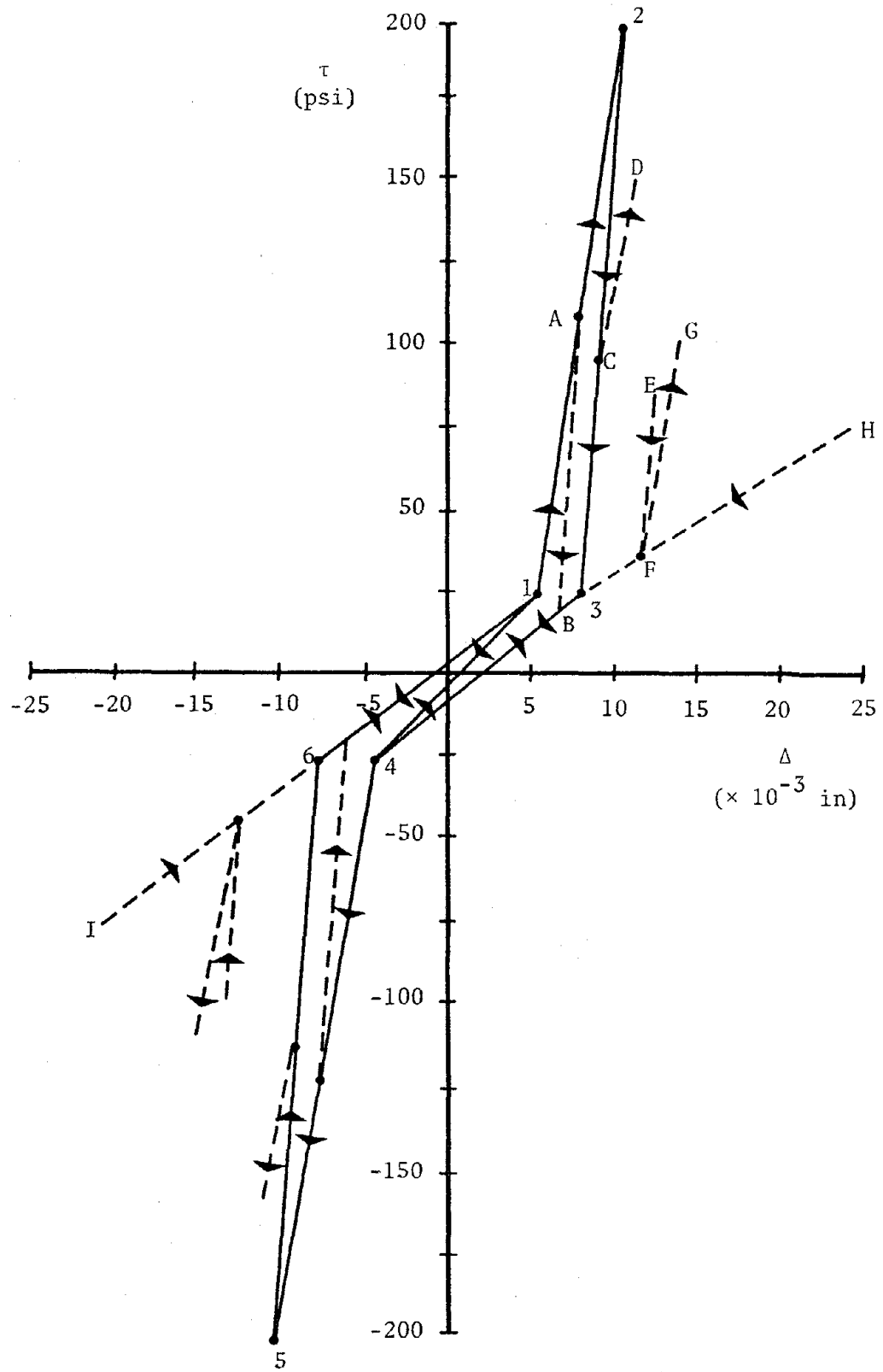
Figure 5.4 - Idealization of the 25th Cycle
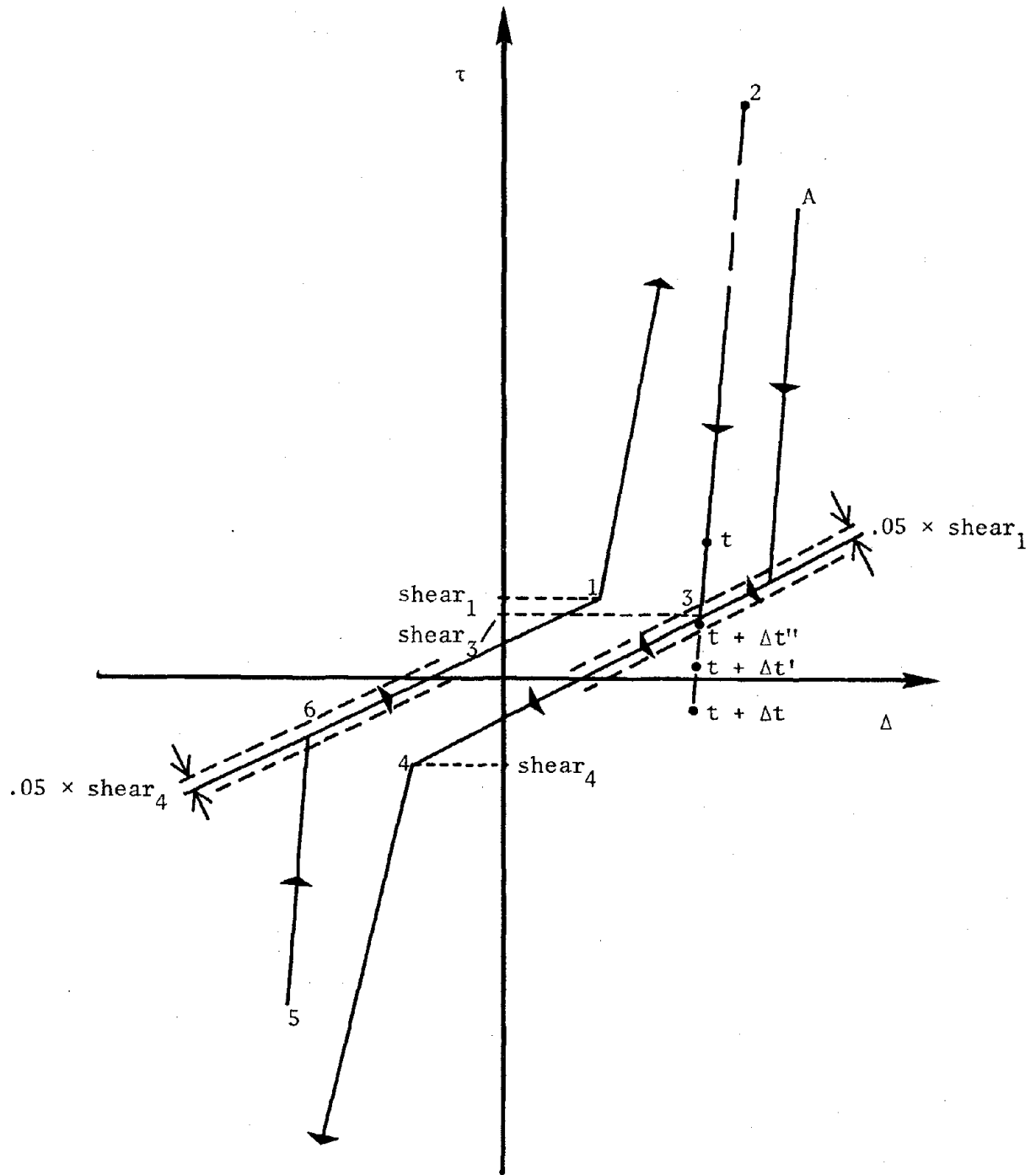
Figure 5.5
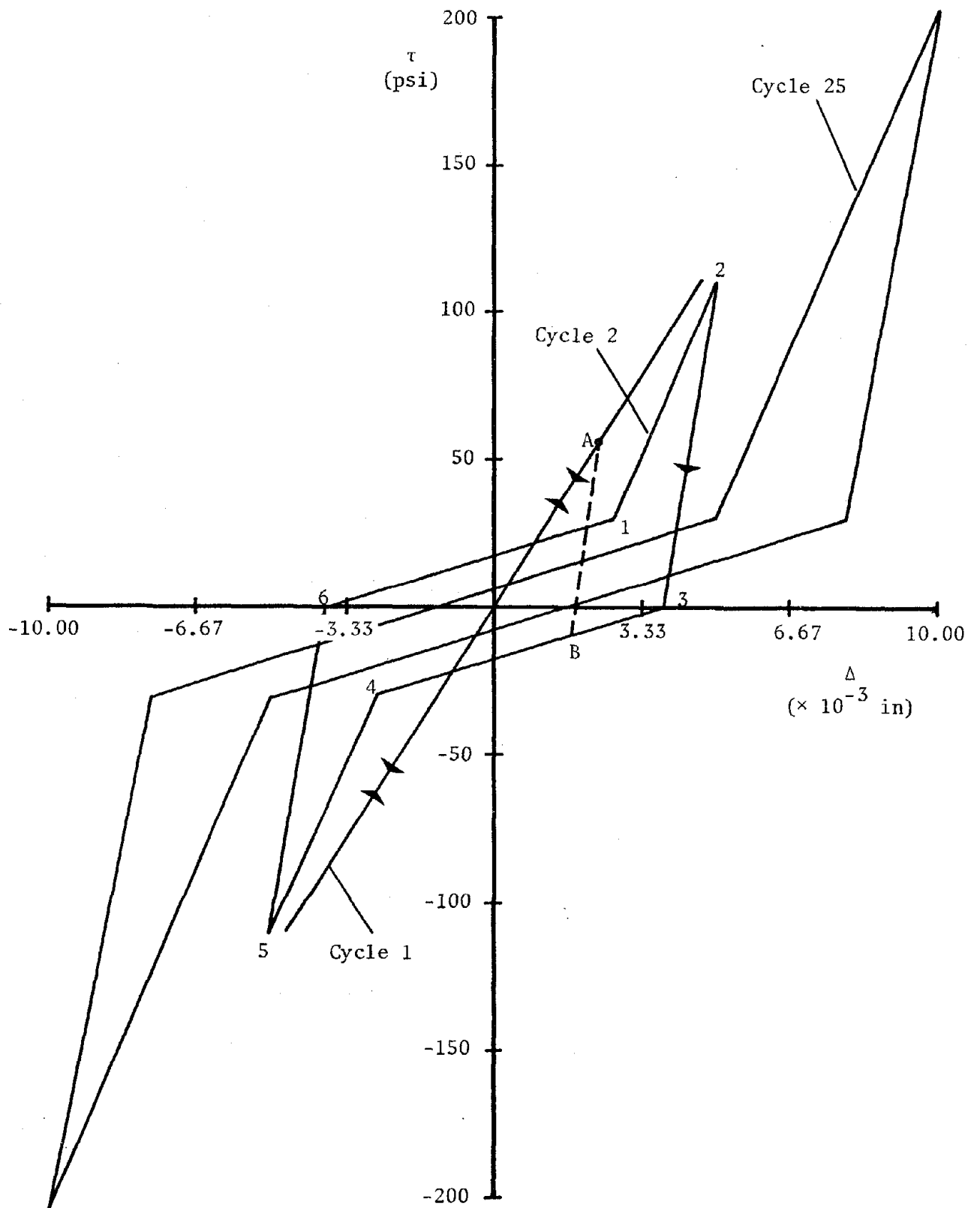
Figure 5.6
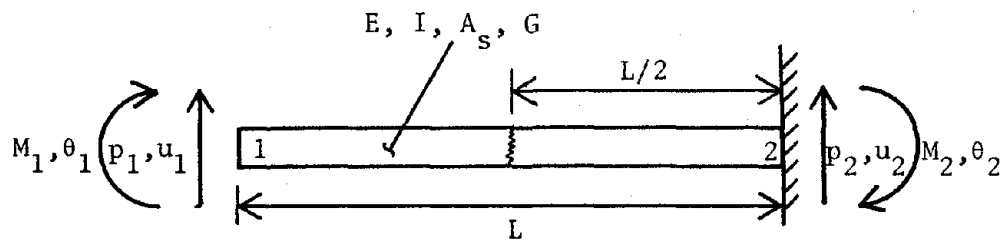
Figure 5.7 - Cracked Beam Element
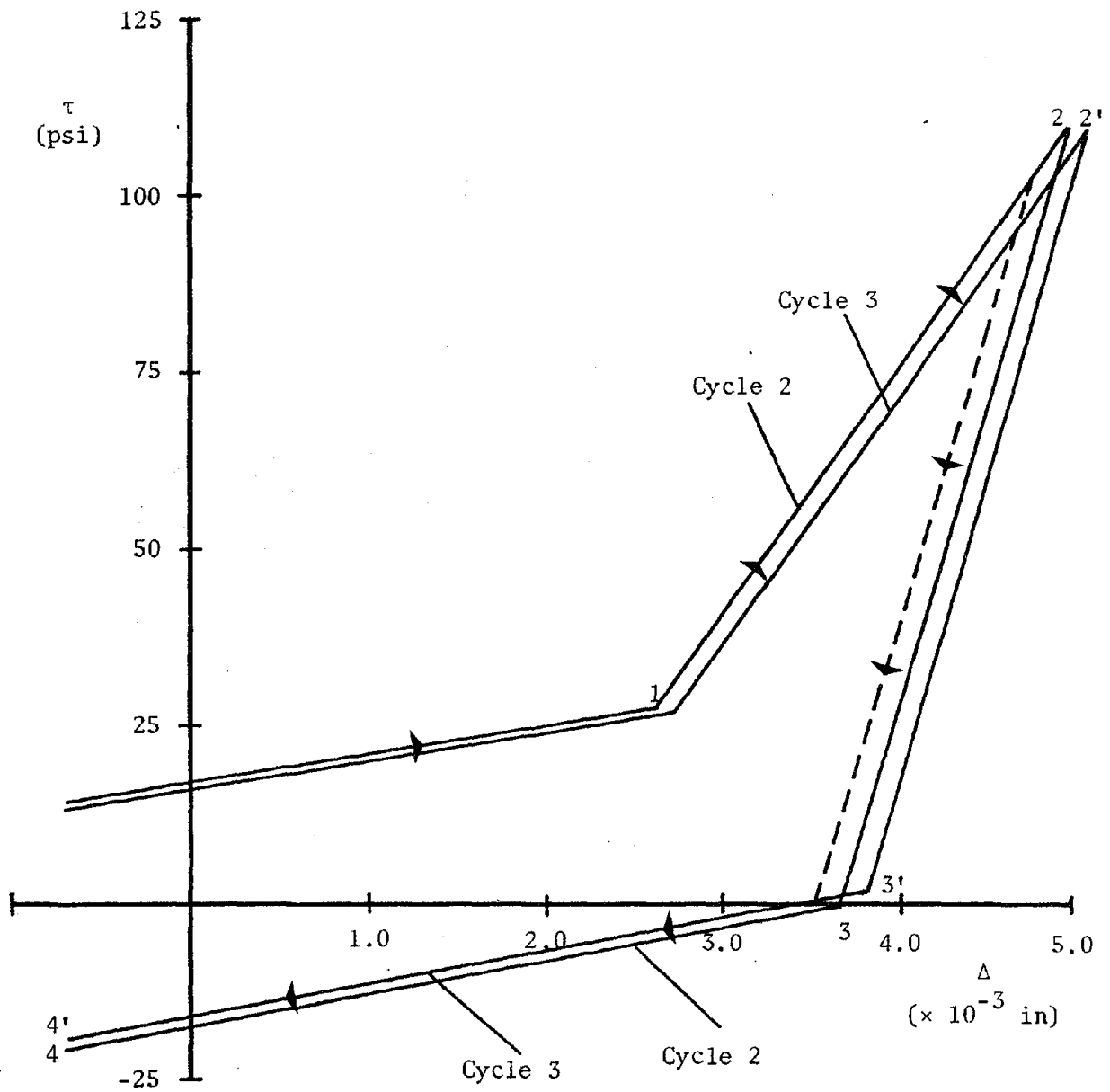
Figure 5.8
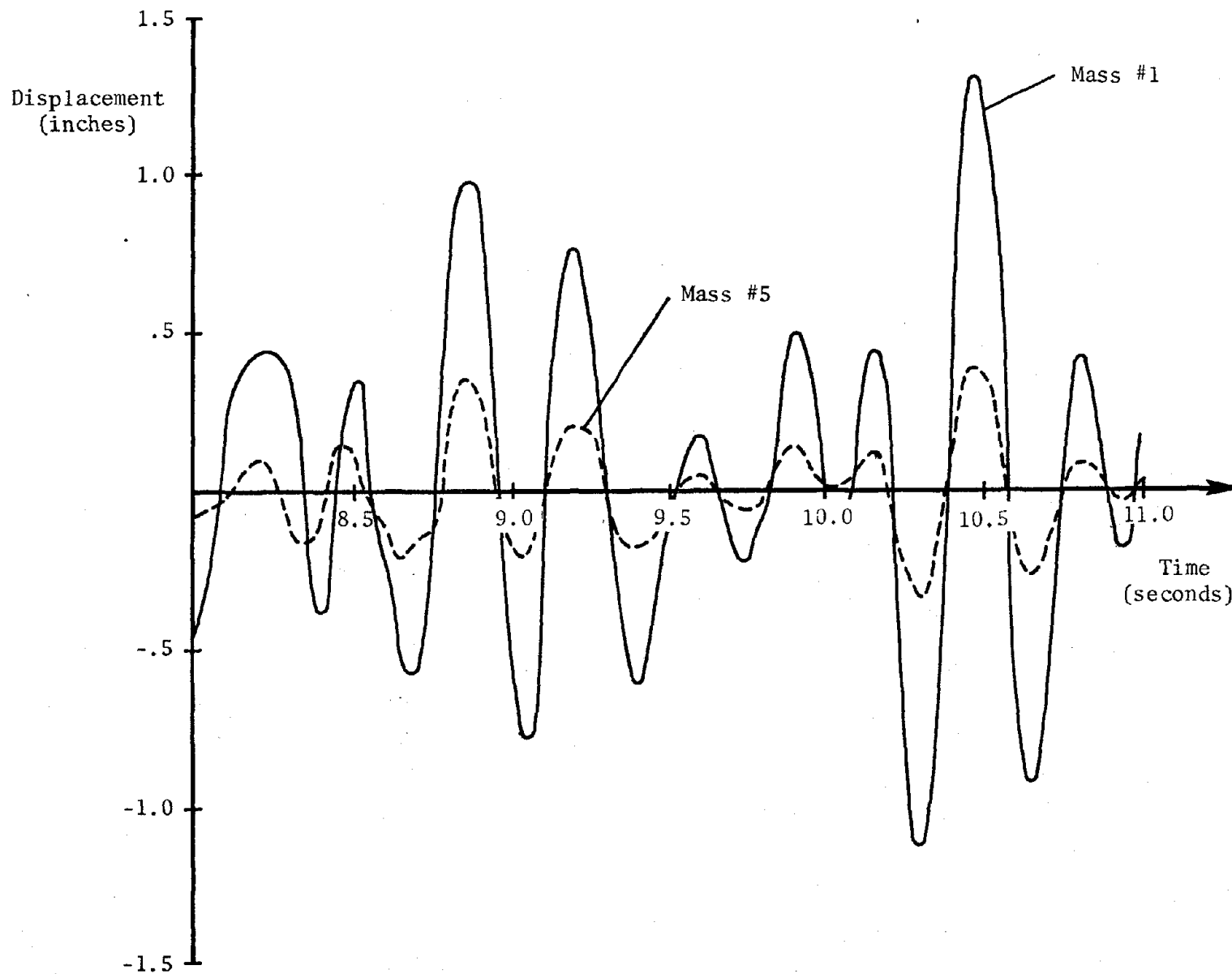
Figure 5.9- Displacement Vs. Time for Uncracked Containment
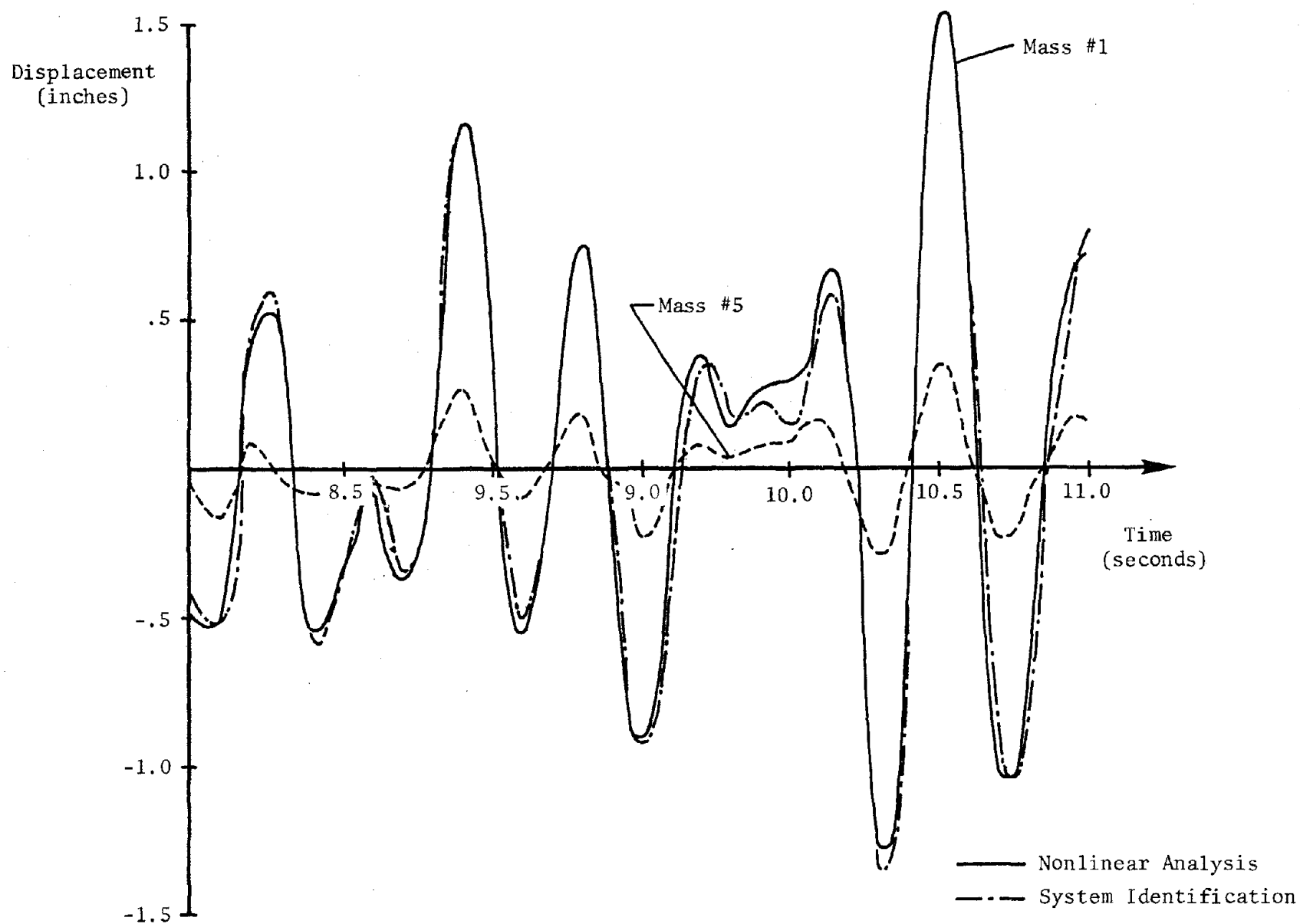
Figure 5.10 - Displacement Vs. Time for Medium Soil Stiffness
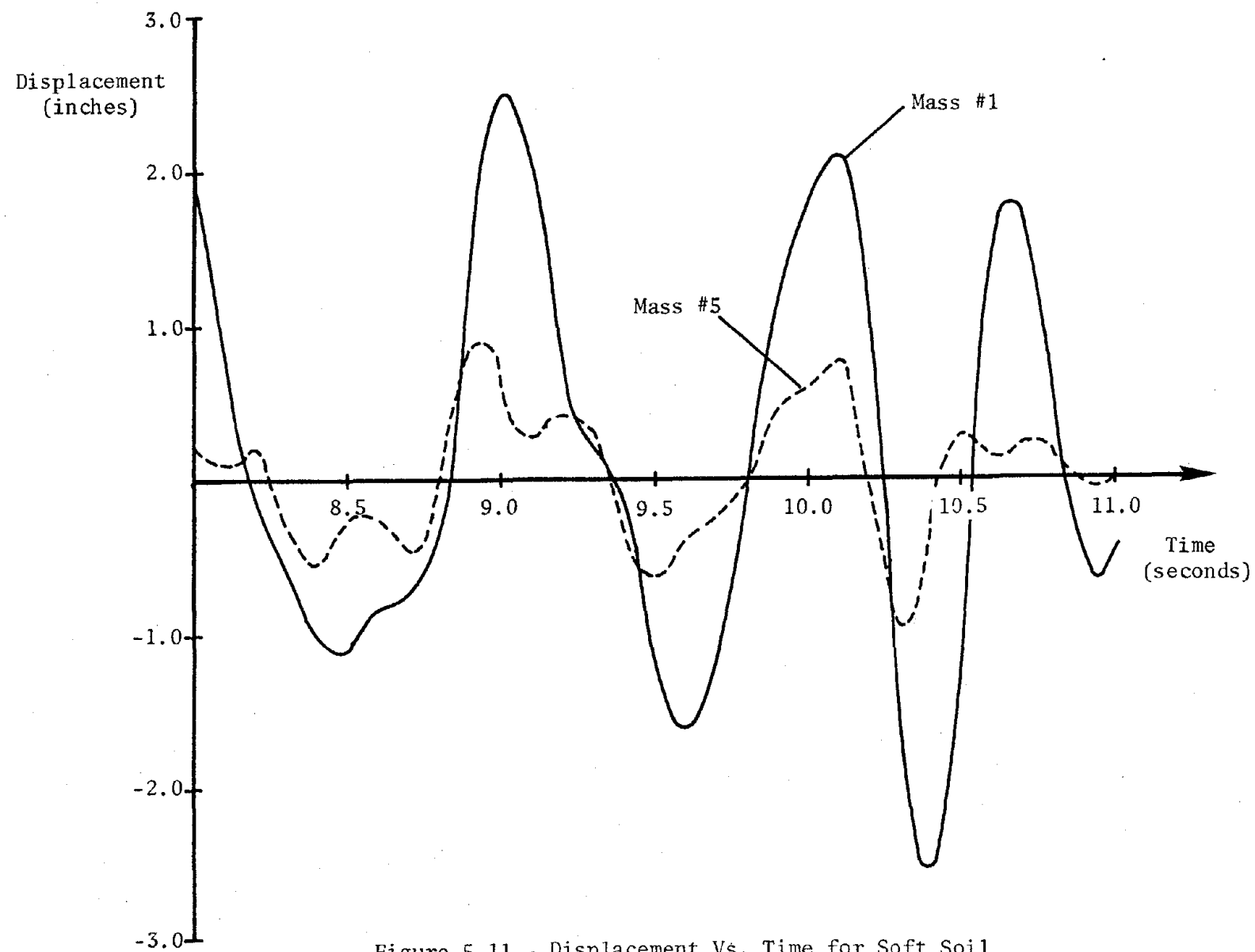
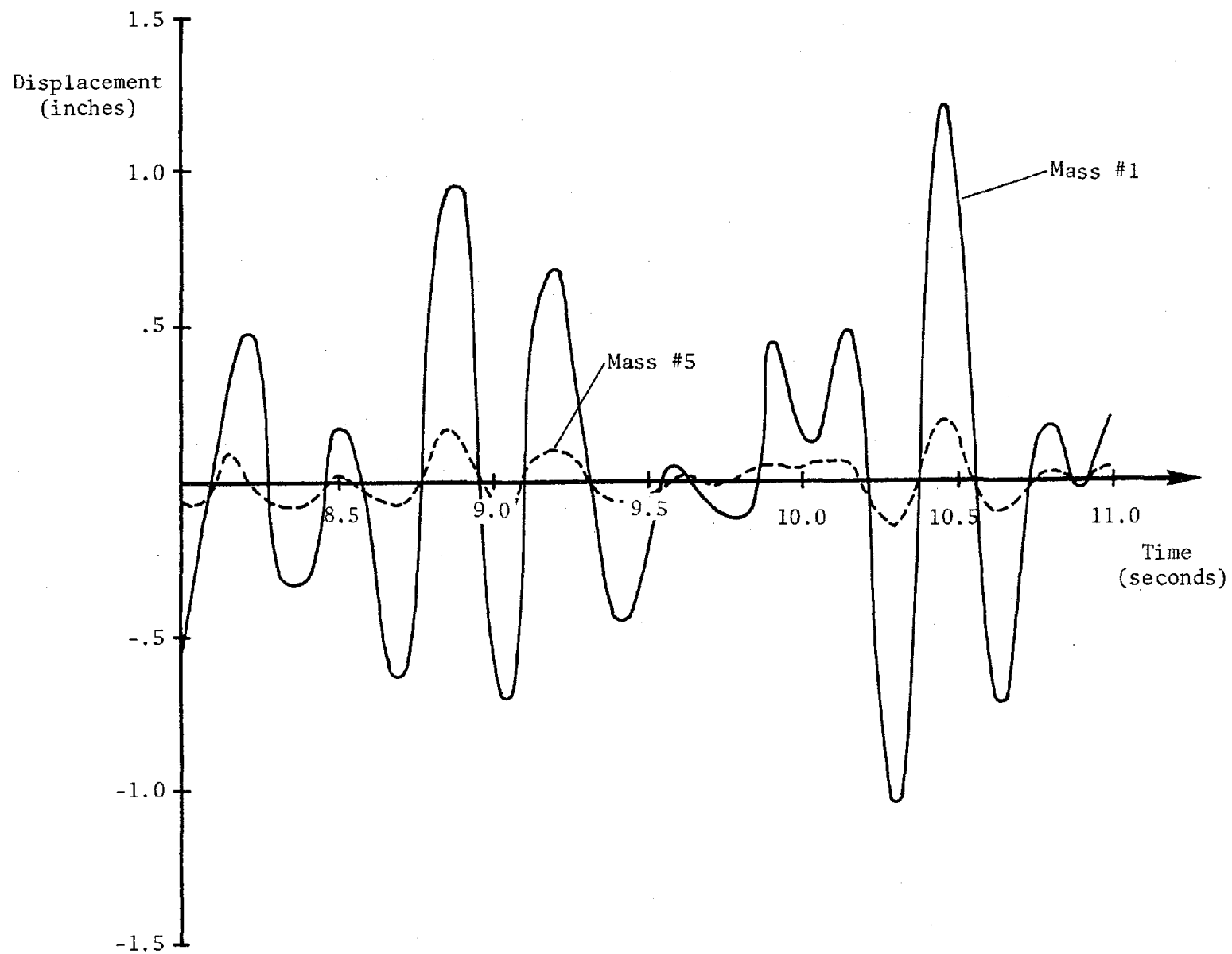Figure 5.11 - Displacement Vs. Time for Soft Soil
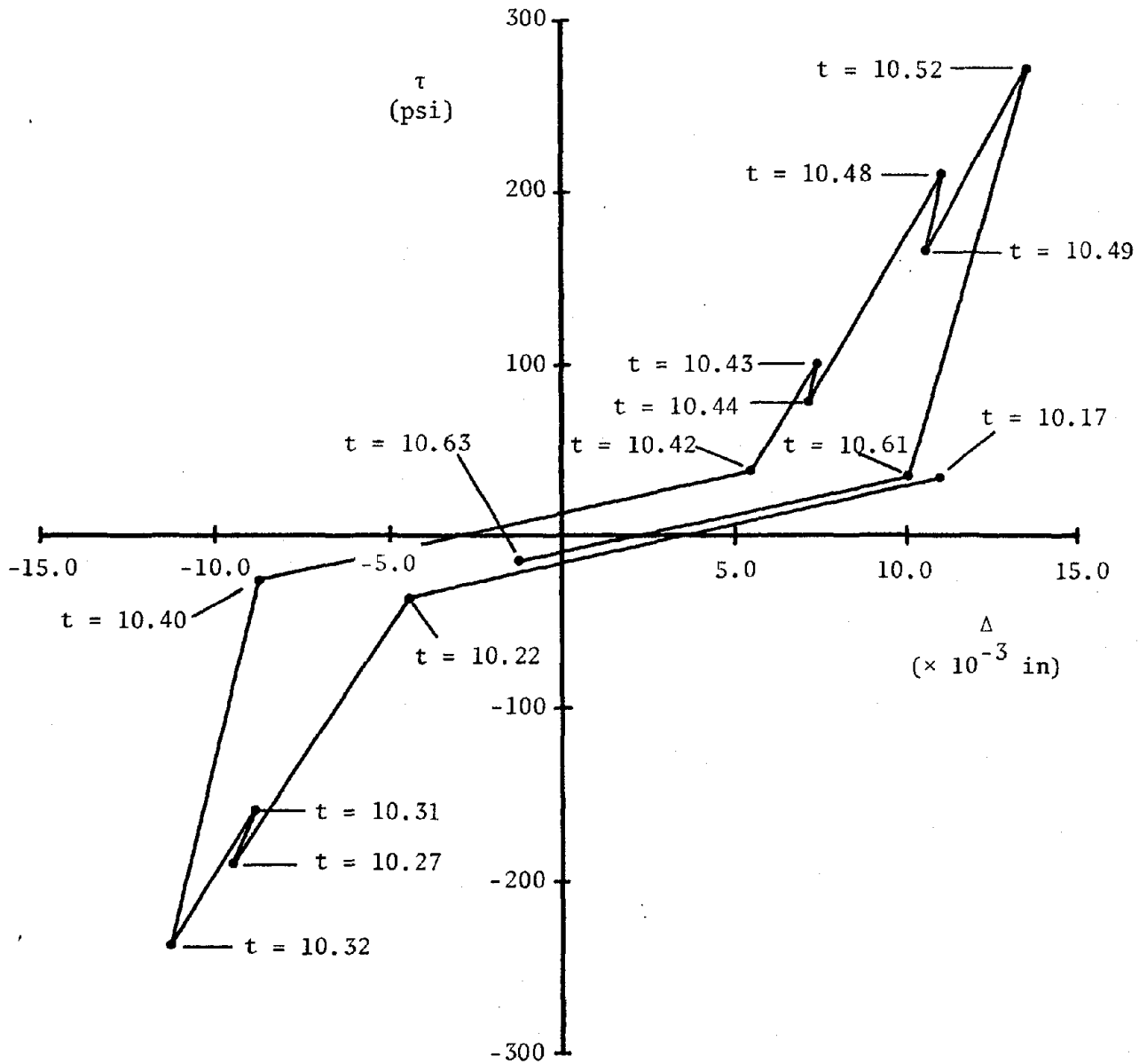
Figure 5.12 - Displacement Vs. Time for Hard Soil

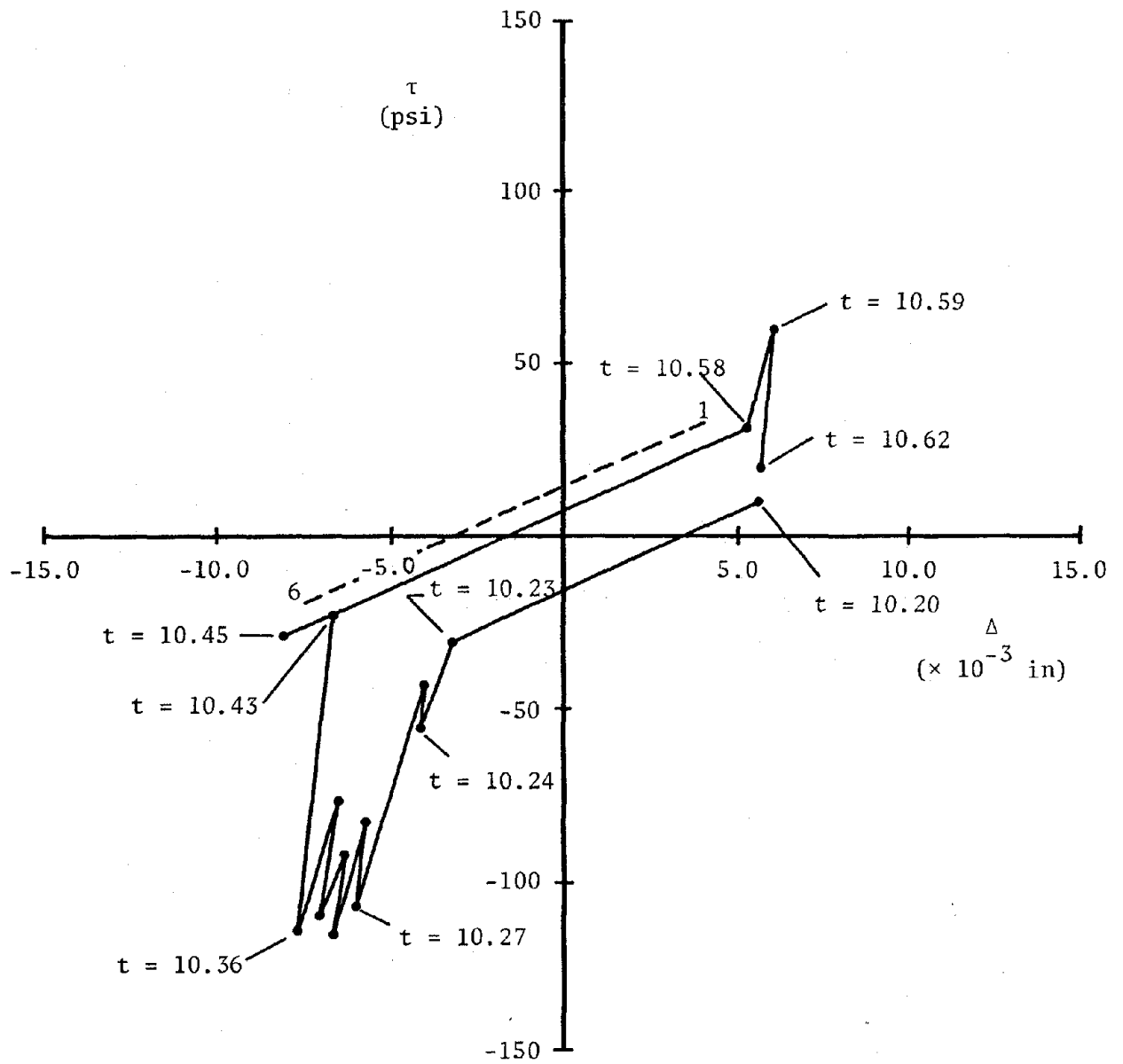Figure 5.13 - Shear Stress Vs. Crack Slip
for Medium Soil Stiffness
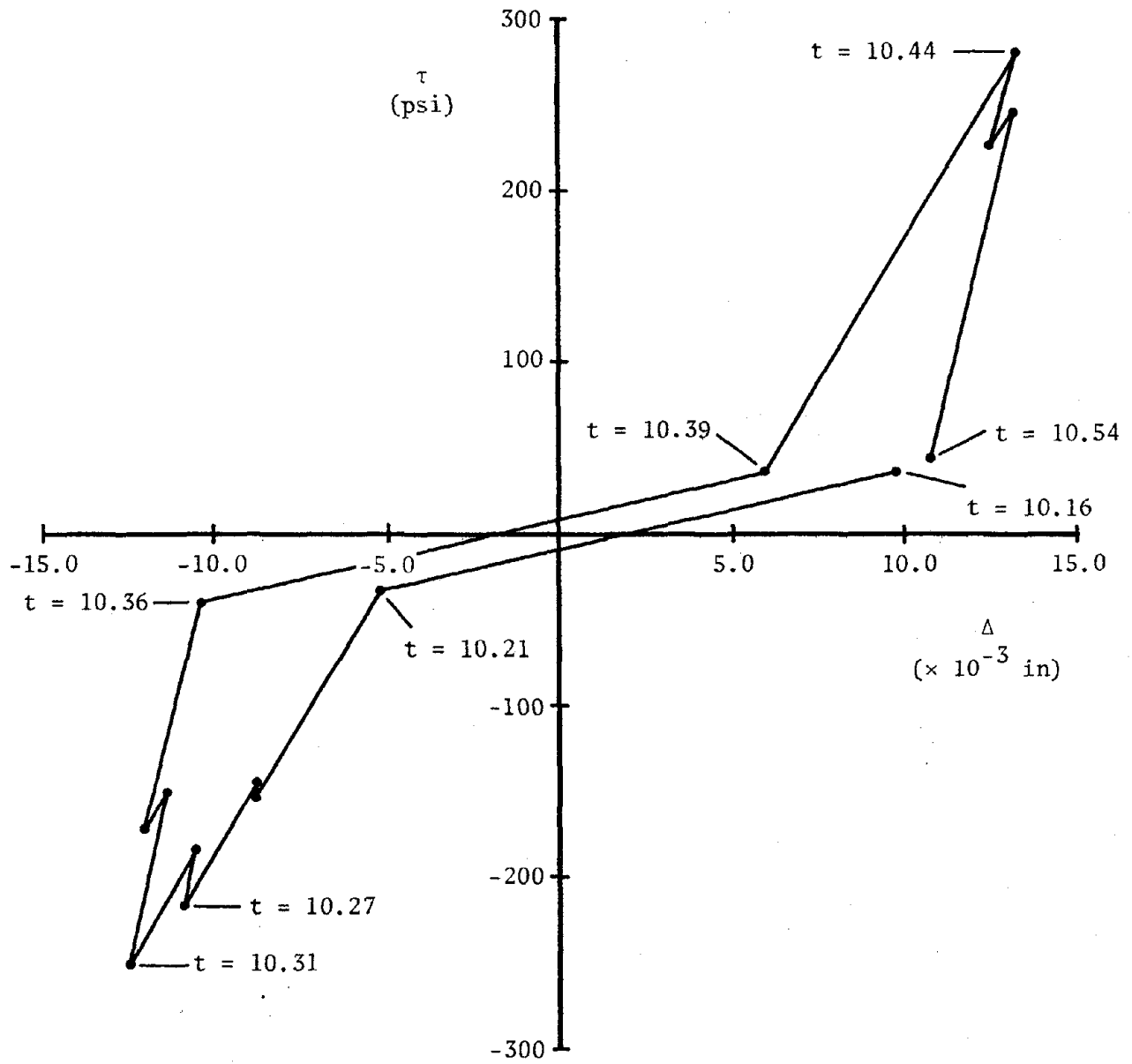
Figure 5.14 - Shear Stress Vs. Crack Slip for Soft Soil

Figure 5.15 - Shear Stress Vs. Crack Slip for Hard Soil